



## Acknowledgments

I would like to thank to O.Univ.- Prof. Dipl.-Ing. Mag. Dr. Christian R. Noe for giving me an interesting topic for my diploma thesis and enabling me to become a member of his research group which deals with blood-brain barrier.

I thank to Dipl.-Ing. Dr. Winfried Neuhaus for being my supervisor, for his great help, acquired knowledge, experience and for his friendly approach.

I thank to Mag. Katarzyna Szaszka and Mag. Andrea Deutsch for their help in laboratory and for nice collegiate relationship.

I thank to Ass. Prof., Mag.Dr, Hannelore Kopelent for her help during organizing my studies at the University of Vienna and introducing me into cultural life in Vienna.

I thank Prof. RNDr. Petr Solich, CSc. for being my Erasmus coordinator and that he had taken care of all administration before I left for Vienna.

Next, I would like to thank my supervisor at the Charles University doc. RNDr. Veronika Opletalová, Ph.D. for last corrections and adjustments.

Special thanks belong to my family, especially to my parents, Marie and Josef Lebloch, for their great support.

## Abstract

Six different substances blocking ion channels were chosen (verapamil, diltiazem, nifedipine, phenobarbital, memantine, amantadine) for the purpose of this work. All these substances are routinely used in clinical practice and it is well known that adverse effects on the central nervous system can occur during therapy with them. Therefore, both single and group transport studies were carried out to investigate and compare the transport abilities of chosen ion channel antagonists to penetrate the BBB and to find out the interference between them.

The required data for each substance used in single and group studies were determined using the Transwell BBB *in vitro* model based on EVC304 cell line. Diazepam and carboxyfluorescein were used as internal standards for normalization of permeability data.

According to the obtained data from single studies nifedipine as drug acting in periphery passes the BBB faster than internal standard diazepam (acting in CNS) and much more faster than other ion channel blockers acting in periphery, too. In clinical practice it can mean that nifedipine used for concrete clinical problem can have more CNS adverse effects in comparison to verapamil or diltiazem. The permeability data also demonstrate that verapamil, diltiazem, nifedipine and diazepam permeate through the BBB according to their lipophilicity in contrast to phenobarbital, which must be actively transported. This fact is supported by the results from group studies, where it was found that the permeability of the CNS drug phenobarbital was significantly increased by co-administration of peripherally acting Ca<sup>2+</sup>-channel blockers verapamil and diltiazem. Consequently, we have confirmed the concept that phenobarbital can be substrate of P-gP, which functionality is influenced by verapamil and diltiazem.

## Abstrakt

Pro účel této diplomové práce bylo vybráno šest různých blokátorů iontových kanálů běžně používaných v klinické praxi (verapamil, diltiazem, nifedipin, fenobarbital, memantin a amantadin). Je dobře známo, že během terapie těmito látkami se mohou vyskytnout nežádoucí účinky v centrálním nervovém systému. Proto byly provedeny jak jednotlivé, tak i skupinové transportní studie, aby bylo možno porovnat u zvolených blokátorů iontových kanálů jejich schopnost transportu přes hematoencefalickou bariéru (HEB), popřípadě zhodnotit interakce mezi nimi.

Získaná data o každé látce použité v jednotlivých a skupinových studiích byla stanovena za použití Transwell *in vitro* modelu hematoencefalické bariéry tvořeného humánní buněčnou linií ECV304. Pro normalizaci dat o prostupnosti látek přes HEB byly použity vnitřní standardy diazepam a karboxyfluorescein.

Podle dat získaných v jednotlivých studiích prostupoval nifedipin (látka účinkující na periférii) přes HEB rychleji než vnitřní standard diazepam (působící v CNS) a mnohem rychleji než ostatní blokátory iontových kanálů, jež účinkují též na periférii. V klinické praxi to může znamenat, že nifedipin použitý při léčbě konkrétního klinického problému může mít v porovnání s verapamilem nebo diltiazemem víc centrálních nežádoucích účinků. Získaná data o prostupnosti přes HEB také ukazují, že verapamil, diltiazem, nifedipin a diazepam pronikají do mozku podle lipofility, tedy rozdílně než fenobarbital, který je pravděpodobně aktivně transportován. Tento fakt je podporován výsledky ze skupinových studií, kde bylo nalezeno, že permeabilita fenobarbitalu, jakožto látky účinkující v CNS, podstatně vzrostla při transportu společně s periferně účinkujícím verapamilem a diltiazemem. Následně je zde potvrzeno, že fenobarbital je substrátem P-glykoproteinu a jeho funkce je ovlivněna verapamilem a diltiazemem.

## Prohlášení

Prohlašuji, že tato práce je mým původním autorským dílem. Veškerá literatura a další zdroje, z nichž jsem při zpracování čerpala, jsou uvedeny v seznamu použité literatury a v práci řádně citovány.

# Contents

Abbreviations.....	8
1. INTRODUCTION.....	10
1.1 The blood-brain barrier.....	10
1.2 The morphology and physiology of the blood-brain barrier.....	11
1.2.1 Endothelial cells.....	12
1.2.2 Tight junctions.....	12
1.2.2.1 The claudins.....	13
1.2.2.2 The occludins.....	14
1.2.2.3 Junctional adhesion molecules (JAMs).....	14
1.2.2.4 Cytoplasmic accessory proteins.....	15
1.2.2.5 Adherens junctions.....	16
1.2.3 Astrocytes.....	16
1.2.4 The transport systems of the blood-brain barrier.....	17
1.3 The pathology of the blood-brain barrier.....	19
1.3.1 Infectious or inflammatory processes.....	20
1.3.2 Cerebral ischemia.....	21
1.3.3 Brain tumours.....	21
1.4 Drug targeting to the brain.....	21
1.5 The role of calcium.....	23
1.5.1 Calcium signalling.....	23
1.5.2 The role of calcium in healthy brain.....	24
1.5.3 The role of calcium in neurodegeneration.....	25
1.6 Compounds of interest.....	26
1.6.1 Calcium channel blockers.....	26
1.6.2 NMDAR antagonists.....	28
1.6.3 Phenobarbital.....	29
1.7 The aim of the study.....	31
2. MATERIAL AND METHODS.....	32
2.1 Cell culture.....	35
2.2 Transport studies.....	37
2.2.1 <i>In vitro</i> models of the blood-brain barrier.....	37
2.2.2 Transwell model.....	38
2.2.2.1 Coating of inserts for the Transwell model.....	38
2.2.2.2 Cell seeding.....	39
2.2.2.3 Medium exchange in the Transwell model.....	39
2.2.3 Transport studies.....	40
2.2.4 Measurement of the Transendothelial Electrical Resistance (TEER).....	42
2.2.5 Fluorescence measurement.....	43
2.2.6 Reversed-phase high performance liquid chromatography.....	44
2.2.7 Single studies – experimental conditions.....	46
2.2.8 Group studies – experimental conditions.....	46
2.3 Calculation of permeability coefficient.....	47
3. RESULTS.....	50
3.1 Transport study of verapamil – Single study.....	51
3.2 Transport study of diltiazem – Single study.....	57
3.3 Transport study of nifedipine – Single study.....	63
3.4 Transport study of phenobarbital – Single study.....	69
3.5 Transport study of memantine – Single study.....	75
3.6 Transport study of amantadine – Single study.....	78

3.7 Transport study of diltiazem/phenobarbital – Group study.....	84
3.8 Transport study of verapamil/phenobarbital – Group study.....	92
3.9 Summary of transport study results.....	100
3.9.1 Single study.....	100
3.9.2 Group study.....	103
3.9.3 Ranking of substances according to the fastness (RatioPE <sub>cell</sub> /Diaz).....	105
3.9.3.1 Single study.....	105
3.9.3.2 Group study.....	106
3.9.4 Measurement of the TEER during transport studies.....	108
4. DISCUSSION AND CONCLUSIONS.....	109
5. SOUHRN.....	117
6. REFERENCES.....	119

## Abbreviations

ABC transporters	ATP-binding cassette transporters
AC	<i>N</i> -Acetylcysteine
ACM	Astrocytes conditioned medium
AD	Alzheimer's disease
AJ	Adherens junctions
ALS	Amyotrophic lateral sclerosis
AQP4	Aquaporin 4
BBB	Blood brain barrier
BECs	Brain endothelial cells
bFGF	Basic fibroblast growth factor
cADP	Cyclic adenosine diphosphate
CF	Carboxyfluorescein
CNS	Central nervous system
CSF	Cerebrospinal fluid
CV	Cleared volume
DIV-BBB	The dynamic in vitro model of the BBB
DPBS	Dulbecco's Phosphate Buffered Saline
EC	Effect of correction
ECs	Endothelial cells
ER	Endoplasmic reticulum
GDNF	Glial-derived neurotrophic factor
HBSS	Hank's Balanced Salt Solution
HD	Huntington's disease
IMDM	Iscove's Modified Dulbecco's Medium
InsP3	Inositol-1,4,5-trisphosphate
InsP3R	Inositol-1,4,5-trisphosphate receptors
IS	Internal standards
JAMs	Junctional adhesion molecules
LDL	Low density lipoproteins
LTD	Long-term depression
LTP	Long-term potentiation
MDRs	Multidrug Resistant Proteins
MeOH	Methanol
NCS	New born calf serum
NMDAR	<i>N</i> -methyl-D-aspartate receptor
OAPs	Orthogonal arrays of particles
OCT	Organic cation transporters
OPA	<i>o</i> -phthalaldehyde
OATP	Organic Anion Transporter Peptides
PD	Parkinson's disease
PE	Permeability coefficient
P-gP	P-glycoprotein
PIP2	Phosphatidylinositol 4,5-bisphosphate
PM	Plasma membrane
PS	Permeability slope
RMT	Receptor-mediated transcytosis
ROCC	Receptor-operated Ca <sup>2+</sup> channels

RyRs  
SCAs  
SOCCs  
SR  
TEER  
TGF- $\beta$   
TJ  
VEGF  
VOCCs  
ZO

Ryanodine receptors  
Spinocerebellar ataxias  
Store-operated Ca<sup>2+</sup> channels  
Sarcoplasmic reticulum  
Transendothelial Electrical Resistance  
Transforming growth factor- $\beta$   
Tight junctions  
Vascular endothelial growth factor  
Voltage- operated Ca<sup>2+</sup> channels  
Zonula occludens

# 1 INTRODUCTION

## 1.1 The blood-brain barrier

The central nervous system (CNS) is the most critical and sensitive system in the human body and therefore must be tightly sealed from the changeable milieu of blood by physical barriers, such as the blood-brain barrier (BBB), the blood-CSF barrier and the arachnoid barrier, to be protected from toxic and pathogenic agents in the blood. The BBB exerts the greatest control over the immediate microenvironment of brain cells. Besides its physical barrier function, BBB enables selective transport of nutrients and efflux of potentially harmful compounds and finally, due to the enzymatic activity, acts as a metabolic barrier to inactivate many neuroactive and toxic compounds. The BBB produces interstitial fluid (ISF) that provides an optimal medium for neuronal functions and helps to maintain homeostasis in brain (Engelhardt and Sorokin, 2009; Abbott et al, 2006; Hawkins and Davis, 2005).

The original concept of a barrier preventing the movement of certain materials between the blood and the adult brain is attributed to the German scientist Paul Ehrlich, who dealt with studies of dye injections administered into circulation. In 1885, Ehrlich made these experiments with aniline derivatives and observed that after parenteral injection of dyes into circulation of adult animal practically all organs were stained, except the brain and spinal cord. He thought that this difference was due to different binding affinities of the nervous system for these dyes (Ribatti et al., 2006).

However, shortly afterwards Edwin E. Goldman, an student of Ehrlich, showed that the very same dyes when injected directly into the cerebrospinal fluid readily stained nervous tissue but not any other tissue (Engelhardt and Sorokin, 2009). This supported the concept of some kind of barrier at the level of the cerebral blood vessels (Bradbury, 1993).

In 1900, Lewandowsky introduced the term “Blood-Brain Barrier”, which was assumed between blood and CNS, but only with the invention of electron microscopy in 1960s was it possible to correlate the ultrastructural localization of the blood-brain barrier with the capillary endothelial cells within the brain (Ribatti et al., 2006; Engelhardt and Sorokin, 2009)

## 1.2 The morphology and physiology of the blood-brain barrier

The blood-brain barrier is formed by cerebral microvessels. Their permeability is regulated by the capillary endothelial cells and is dependent on the complex of tight junctions. The vascular endothelium is encircled by layer of astrocyte end-feet and two basement membranes can be distinguished, an endothelial cell basement membrane and an astroglial basement membrane. Between them pericytes are distributed (Figure 1.1). All these components constitute a “neurovascular unit” that is essential for the health and correct function of the CNS (Engelhardt and Sorokin, 2009; Hawkins and Davis, 2005).

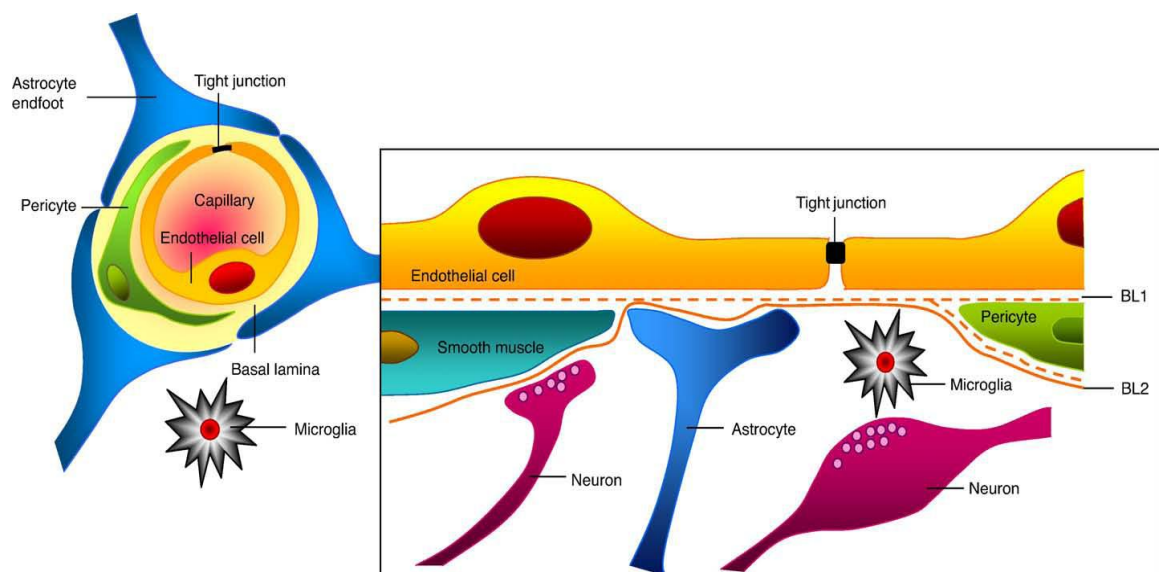


Figure 1.1 Scheme of the brain capillary

The picture shows the main components of the blood-brain barrier: a blood capillary formed by endothelial cells interconnected by tight junctions, basal lamina and pericytes, which are surrounded by astrocyte ent-feet (Abbott et. al., 2009).

The BBB is present in all brain regions, except for the circumventricular organs including area postrema, median eminence, neurohypophysis, pineal gland, subfornical organ, and lamina terminalis. Blood vessels in these areas of the brain have fenestrations that permit diffusion of blood-borne molecules across the vessel wall. These unprotected areas of the brain are regulated by autonomic nervous system and endocrine glands of the body (Ballabh et al., 2003).

### 1.2.1 Endothelial cells

BBB structure is composed of cerebral endothelial cells (ECs) forming brain and spinal cord capillaries, in association with various perivascular cells such as smooth muscle cells, pericytes, microglial cells and astrocytes.

Distinct morphologic and metabolic characteristics of the brain microvascular ECs were observed thanks to electron microscopy studies of the BBB, different to those present in peripheral tissues. The most important of these are:

- ECs are normally connected at junctional complex by tight junctions and adherent junctions
- Endothelial cytoplasm lacking fenestrations typically present in peripheral-tissue capillaries
- Fewer pinocytotic vesicles compared to peripheral ECs
- More mitochondria, suggesting important metabolic activity (Correale and Villa, 2009)

### 1.2.2 Tight junctions

BBB properties are primarily determined by endothelial junctional complexes consisting of tight junctions (TJ) and adherens junctions (AJ). The tight junctions are responsible for the severe restriction of the paracellular diffusional pathway between the endothelial cells to ions and other polar solutes, and effectively block penetration of macromolecules by this route. In contrast, small substances such as O<sub>2</sub> and CO<sub>2</sub> diffuse freely across plasma membranes along their concentration gradient. The impediment to ion movement results in the high in vivo electrical resistance of the blood–brain barrier. In comparison to human placental endothelial cells with transendothelial resistance of 22 – 52 Ω×cm<sup>2</sup>, which helps to permit rapid paracellular exchange of nutrients and waste products between the mother and fetus, or to urinary bladder epithelium with very high transepithelial resistance of 6000 – 30 000 Ω×cm<sup>2</sup> for preserving urine composition is electrical resistance of the blood-brain barrier in the range of 1500 – 2000 Ω×cm<sup>2</sup>, which is necessary for maintaining brain homeostasis (Stamatovic et. al., 2008; Ballabh et. al., 2003; Abbott et. al., 2009; Huber et. al., 2001a).

Structurally, TJs form a continuous network of parallel, interconnected, intramembrane strands of proteins linked to an actin-based cytoskeleton that allows the TJ to form a seal while remaining capable of rapid modulation and regulation (Figure 1.2). These TJs include an intricate complex of transmembrane

(claudins, occludin, and junctional adhesion molecule) and cytoplasmic (zonula occludens, cingulin, AF-6, and 7H6) proteins (Engelhardt and Sorokin, 2009; Huber et. al., 2001a).

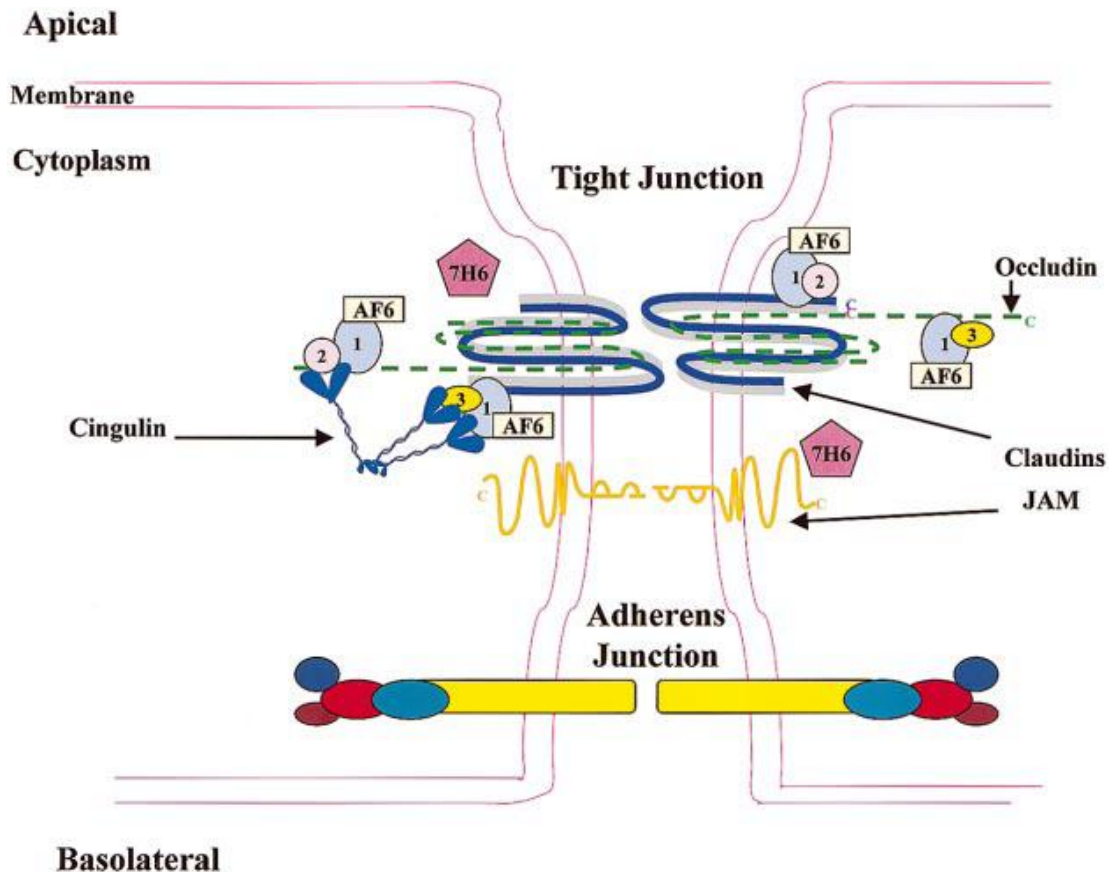


Figure 1.2 Scheme of cell-cell contacts between two endothelial cells of the BBB  
The picture shows molecular organisation of major components of TJ and AJ localized in paracellular space of the brain capillary, adapted from (Huber et. al., 2001b).

### 1.2.2.1 The claudins

Claudins are principal barrier-forming phosphoproteins that belong to the PMP22/EMP/MP20/claudin family of proteins and have four transmembrane domains. They are 20- to 24-kDa proteins, of which at least 24 have been identified in mammals. Claudins form dimers and bind homotypically to claudins on adjacent endothelial cells to form the primary seal of the TJ, from this results their function in the TJ complex, namely to limit paracellular ion movement selectively and this produces the high electrical resistance of the barrier (Stamatovic et. al., 2008; Ballabh et. al., 2003; Hawkins and Davis, 2005).

Claudin-3, -5 and -12 are localized on the BBB, whereas the presence of claudin-1 seems to vary among species, though this has not been fully clarified (Correale and Villa, 2009).

#### ***1.2.2.2 The occludin***

Occludin was identified in 1993 as the first tight junctional transmembrane protein by immunogold freeze fracture microscopy in chickens and then in mammals. It is a 65-kDa phosphoprotein with four transmembrane domains, has a short NH<sub>2</sub>-terminal cytoplasmic domain and a long COOH-terminal cytoplasmic domain, which is likely involved with the cytoskeleton via accessory proteins, such as zonula occludens ZO-1 and ZO-2 (Ballabh et. al., 2003; Wolburg and Lippoldt, 2002; Hawkins and Davis, 2005).

Presence of this regularory protein in the BBB is correlated with increased electrical resistance across the barrier and decreased paracellular permeability (Huber et. al., 2001). Multiple phosphorylation sites have been identified its serine and threonine residues, and the phosphorylation state of occludin regulates its association with both cell membrane and regulates barrier permeability. In addition, recent studies have demonstrated that occludin regulates epithelial cell differentiation and that mature cells need occludin to regulate rather than establish their barrier properties (Correale and Villa, 2009; Wolburg and Lippoldt, 2002).

#### ***1.2.2.3 Junctional adhesion molecules (JAMs)***

Junctional adhesion molecules (JAMs) belong to the immunoglobulin superfamily and are expressed in tight junctions of endothelial and epithelial cells and display different patterns of homo- and probably heterophilic adhesion. Homophilic interactions are with molecules on the opposite cell, forming JAM dimmers, however heterophilic interactions can occur between different JAM family members as well as other adhesion molecules (e.g. integrins). The JAM family consists of JAM-1, JAM-2, and JAM-3 (Stamatovic et. al., 2008; Vorbrodt and Dobrogowska, 2003). It was observed that JAM-1 and JAM-3 are expressed in the brain blood vessels but not JAM-2 (Ballabh et. al., 2003).

JAM-1, a 32-kDa protein, localizes with actin at the cell-to-cell contacts and is involved in cell-to-cell adhesion through homophilic interactions, modulates leukocyte extravasation through interendothelial junctions and plays a role in the

organization of TJs, because it was observed that JAM-1 transfection reduces paracellular permeability and promotes occludin localization at intercellular junctions (Vorbrot and Dobrogowska, 2003; Wolburg and Lippoldt, 2002).

#### ***1.2.2.4 Cytoplasmic accessory proteins***

Cytoplasmic accessory proteins associate with transmembrane components of the TJ in the cytoplasm. These members of TJ formation include zonula occludens proteins (ZO-1, ZO-2, and ZO-3), cingulin, afadin (AF6), 7H6, and several others (Ballabh et. al., 2003; Hawkins and Davis, 2005).

Zonula occludens proteins (ZO-1, ZO-2, and ZO-3) belong to a family of multidomain proteins known as the membrane-associated guanylate kinase homologs (MAGUKs), their role in signal transduction may be due in large part to the demonstrated ability of these proteins to organize protein complexes at the plasma membrane. ZO-1 was the first tight junction protein to be identified and together with ZO-2 and ZO-3 (supplementary components of ZO-1) are considered to be junctional peripheral proteins connecting all the major transmembrane barrier proteins (e.g. claudins and occludin) with actin filaments and form a critical link that stabilizes the barrier for larger solutes (Fanning et. al, 1998; Van Itallie et. al., 2009; Vorbrot and Dobrogowska, 2003). They contain three PDZ domains (PDZ1, PDZ2, and PDZ3), one SH<sub>3</sub> domain, and one guanyl kinaselike (GUK) domain. Claudins bind to the PDZ1 domain of ZO-1, ZO-2, and ZO-3 with COOH-terminal group and occludin interacts with the GUK domain on ZO-1. Finally, actin binds to COOH-terminal of ZO-1 and ZO-2 and this complex cross-links transmembrane elements and thus provides structural support to the endothelial cells (Ballabh et. al., 2003).

Cingulin is a 140 – 160-kDa protein that associates with ZOs, JAM-1, and myosin and it is hypothesized to serve as a scaffolding protein that links TJ accessory proteins to the cytoskeleton.

AF-6, a 180-kDa protein with two Ras-associating domains, regulates the cell-cell contact via interactions with ZO-1.

The function of 7H6 is not known, but in response to cellular ATP depletion, this 155-kDa protein reversibly dissociates from the TJ complex and therefore plays a role in maintenance and maturation of TJ (Hawkins and Davis, 2005; Huber et. al., 2001a; Stamatovic et. al., 2008).

### ***1.2.2.5 Adherens junctions***

The major transmembrane components of AJs are termed cadherins. These membrane glycoproteins are linked to the actin cytoskeleton via the sub-membrane plaque proteins catenins. The cadherin superfamily contains more than 40 members and can be grouped into three classes: protocadherins, desmosomal cadherins, and classical cadherins. Desmosomal cadherins represent the calcium-dependent cell adhesion molecules of desmosomes, whereas classical cadherins regulate calcium-dependent cell adhesion at the AJs and also at cell contacts, which do not have a discrete ultrastructural organization. The most important representative of classical cadherins is a vascular endothelium cadherin (VE-cadherin), known also as cadherin-5. VE-cadherin is an important determinant of microvascular integrity, and together with catenins, forms the complex that functions as an early-recognition mechanism between endothelial cells. Recent *in vitro* and *in vivo* studies show that VE-cadherin is required for endothelial integrity in quiescent vessels and in organization of new vessels (Correale and Villa, 2009; Vorbrodt and Dobrogowska, 2003).

### **1.2.3 Astrocytes**

Astrocytes are glial cells, which ensheath ninety percent of the abluminal surface of cerebral microvasculature endothelium. The close apposition of the astrocytic end-feet on the capillary walls and their close relationship with neurons predestine them to participate in nutritive and metabolic support of neurons (Correale and Villa, 2009; Carvey et al., 2009).

Astrocytes can upregulate many BBB features, leading to tighter tight junctions (physical barrier), the expression and polarized localization of transporters, including P-glycoprotein and GLUT-1 glucose carrier (transport barrier), and specialized enzyme systems (metabolic barrier) (Abbott et al, 2006). The key roles in gliovascular signalling and in regulation of brain water and electrolyte metabolism under normal and pathological conditions play the water-channel protein aquaporin-4 (AQP4) and the potassium channel K4.1, which are assembled in astrocytic end-feet membranes in regular square arrays called orthogonal arrays of particles (OAPs) (Correale and Villa, 2009; Verkman, 2002).

It is also thought that the astrocytes are able to secrete a range of chemical agents that induce the formation of tight junctions in the ECs. Several of these

glia-derived factors, including transforming growth factor- $\beta$  (TGF- $\beta$ ), glial-derived neurotrophic factor (GDNF), basic fibroblast growth factor (bFGF) and angiopoietin 1 can induce aspects of the BBB phenotype in endothelial cells *in vitro* (Abbott et al, 2006; Carvey et al., 2009).

#### **1.2.4 The transport systems of the blood brain barrier**

Whilst the lipid nature of the BBB presents no restraint to the movement of the respiratory gases, it would be anticipated to restrict the transport of hydrophilic compounds, e.g. sugars, amino acids and other metabolites, and of metallic and other ions (Bradbury, 2006).

There are 4 properties that determine the passage of substances through the BBB: size, lipid solubility, specific transporters, and electrical charge. Transcellular diffusion allows the transport of very small molecules, such as water, oxygen and carbon dioxide, and lipophilic substances, such as ethanol, heroin or chloramphenicol (Huber et. al., 2001a; Moody, 2006). The movement of water-soluble molecules or large molecular weight substances such as ions, glucose, amino acids, nucleotides, vitamins and proteins necessary for brain function is largely regulated by specific transport systems within ECs that allow entry into the brain. Various physiological transport processes are present at the BBB level (Figure 1.3). If the substance experiences a downhill concentration gradient, the action is termed facilitated diffusion. If the substance is being pumped against a concentration gradient (uphill) and energy is required, we speak about active transport (Carvey et al., 2009; Correale and Villa, 2009; Moody, 2006).

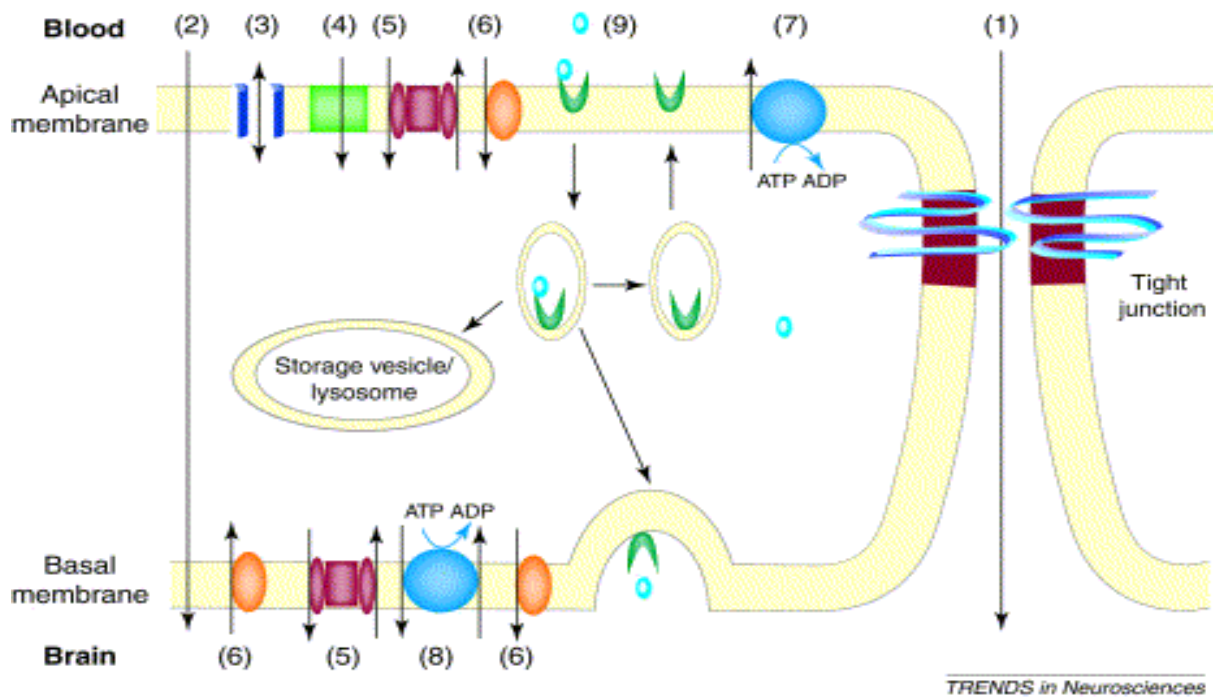


Figure 1.3 The transport systems of the BBB

The picture shows different transport systems: (1) paracellular diffusion, (2) transcellular diffusion, (3) cation channels, (4) ion symports, (5) ion antiports, (6) facilitated diffusion active transport, (7) active transport, (8) active antiport transport and (9) endocytosis (receptor-adsorptive mediated). Source (Huber et. al., 2001b).

Ion transport systems at the BBB are critical to normal brain function and are coupled to maintain electrical neutrality within the brain endothelial cells while also regulating pH.  $\text{Na}^+\text{-K}^+$  ATPase pump regulates sodium influx into the brain interstitial space in exchange for potassium. This pump maintains a high  $\text{Na}^+$  gradient at the BBB, allowing  $\text{Na}^+$  dependent transport to occur.  $\text{Na}^+\text{-H}^+$  exchanger,  $\text{Na}^+\text{-Cl}^-$  symporter,  $\text{Na}^+\text{-H}^+$  exchanger and  $\text{Cl}^-\text{-HCO}_3^-$  exchanger help to maintain electrical neutrality and play critical roles in regulating the intracellular pH of the endothelium. The  $\text{Na}^+\text{-K}^+\text{-2 Cl}^-$  cotransporter is expressed in the BBB, too. In addition, to ionic flux across the endothelial cell layer, the  $\text{K}^+$  channel at the end-feet of astrocytes release  $\text{K}^+$  into the perivascular space, where it can be subsequently transported into ECs (using the  $\text{Na}^+\text{-K}^+$  ATPase pump) and eventually out of the brain. An increase level of extracellular  $\text{K}^+$  produced by neuronal depolarization leads to further depolarization of neurons as well as glia and thus regulation of extracellular  $\text{K}^+$  is critical. Next to this, carrier-mediated transporters expressed on the endothelial cells of the BBB tend to be highly stereospecific for selective transport of small

molecules, such as hexoses, amino-acids, monocarboxylic acids, nucleosides, amines and vitamins (Carvey et al., 2009; Correale and Villa, 2009).

Receptor-mediated transcytosis (RMT) is an important process for moving large molecules, which are delivered to the brain by specific receptors. RMT requires ligand binding to a specific receptor at the luminal side of the BEC which initiates the process of endocytosis including the formation of intracellular transport vesicles that deliver the dissociated ligand to the parenchyma. These receptors include the insulin receptor, transferrin receptor for delivery of iron, LDL receptor and others (Carvey et al., 2009). In contrast to RMT, absorptive mediated endocytosis is initiated by polycationic molecules binding to negative charges on the plasma membrane. This process lacks specific targeting and may lead to widespread absorption (Correale and Villa, 2009).

Additionally, active efflux pumps are presented at the luminal membrane. The ATP-binding cassette (ABC) transporters require ATP to transport solutes across the BBB (against a concentration gradient). Included in this family of proteins are the Multidrug Resistant Proteins (MDRs), the MDR associated proteins (MRPs), and Breast Cancer Resistance protein. The first MDR protein identified was P-glycoprotein (P-gp), which is an ATP-dependent efflux pump preventing the passage of drugs and toxins across the BBB into the brain and may facilitate their transport from brain to blood (e.g. cholesterol, lipid glucocorticoid, peptide and many lipid-soluble drugs) (Carvey et al., 2009; Correale and Villa).

Next to the transport function, the BBB affects physiologic substrates as well as xenobiotics thank to CYP enzymes presented in the BBB, astrocytes and circumventricular organ (Carvey et al., 2009; Moody, 2006). For example, levo-dihydroxyphenylalanine (L-DOPA), administered for treatment of Parkinson disease, is metabolised by dopamindecarboxylase (DDC) to dopamine (Lim, 2005).

### **1.3 The pathology of the blood-brain barrier**

Under physiologic conditions the BBB is relatively impermeable, but in pathologic conditions a number of chemical mediators are released that increase BBB permeability (Ballabh et al., 2004). Barrier dysfunction can range from mild and transient tight junction opening to chronic barrier breakdown, and changes in transport systems and enzymes can also occur (Abbott et al., 2009). The BBB is abnormally breached in conditions such as hypertension, intra-arterial injections

of hyperosmolar solutions, exposure to inflammatory mediators (cytokines), activation of leukocytes, hypercapnia, and ischemia (Moody, 2006).

Acute brain injury leads to failure of high energy processes such as the Na<sup>+</sup>-K<sup>+</sup> ATPase pump, because of decreased production of ATP in neurons. The result of this process is cellular edema evoked by influx of sodium and water, which leads to anaerobic metabolism, and thus cellular acidosis, and influx of calcium with release of excitatory amino acids like glutamate. Calcium influx triggers the deleterious activation of a variety of enzymes that compromise the functional and structural integrity of the endothelial cells (Lo et al., 2001).

### **1.3.1 Infectious or inflammatory processes**

In normal brain, highly specialized cerebral endothelial cells limit entry of leukocytes and circulating substances into the brain. In contrast, inflammatory mediators, which are released during infectious processes such as bacterial meningitis, encephalitis, sepsis or pathogenesis of HIV-associated dementia, multiple sclerosis and Alzheimer disease, alter the integrity of the BBB with consequent migration of leukocytes into the brain. The CNS is ordinarily protected by astrocytes and microglia but in pathologic circumstances they can amplify inflammation and mediate cellular damage. Interaction of astrocyte, microglia, and immune system leads to an altered production of neurotoxins and neurotrophins by these cells (Ballabh et al., 2003; Moody, 2006).

During inflammation, e.g. bacterial meningitis, in brain cytokines are liberated and react with circulating white cells and the endothelium, thereby up-regulating cytokines elaborated by these endothelial cells. After that follows activation of adhesion molecules, which trap white blood cells, open the barrier, and permit the white blood cells to pass through the BBB. During this process antibiotics can enter the brain (Moody, 2006). In Alzheimer disease, microglia and astrocyte are activated by  $\beta$ -amyloid protein and related oligopeptides, leading to a cascade of events producing toxic molecules, neuronal damage, and synaptic dysfunction. On the other hand, during multiple sclerosis reactive T cells recognize and destroy myelin sheath and the underlying axons. In this case disruption of the BBB is one of the initial key steps and massive infiltration of T cells and the formation of demyelinating foci then follows (Ballabh et al., 2003).

There are lots of pathologies associated with inflammation, which conduce to loss of tightness of the BBB, e.g. uncontrolled hypertension, pain, stroke, trauma, convulsion etc. (Abbott et al., 2009; Moody, 2006).

### **1.3.2 Cerebral ischemia**

The ischemic insult of the BBB involves a loss of blood flow as well as depletion of oxygen and essential nutrients and is associated with increased microvascular permeability and disruption of tight junctions. Hypoxic reorganization of BBB TJ seems to be mediated in part by cytokines, vascular endothelial growth factor (VEGF) and nitric oxide (NO), and astrocytes appear to play a protective role. In addition, diabetes is also associated with increased vascular permeability, because of harmful effects in microvessels and a known risk factor for ischemic stroke of this disease (Ballabh et al., 2003; Hawkins and Davis, 2005).

### **1.3.3 Brain tumours**

The BBB is poorly developed in brain tumour leading to increased vascular permeability. It has been observed that in human gliomas and metastatic adenocarcinoma the interendothelial TJ were opened, because of down-regulation of claudins and redistribution of astrocyte aquaporin-4 (AQP4) and the potassium channel K4.1 (Abbott et al, 2006; Ballabh et al., 2003).

## **1.4 Drug targeting to the brain**

Today, we do not have ideal drugs for many diseases of the brain, such as Alzheimer's disease, Parkinson's disease, stroke, depression, schizophrenia, epilepsy, migraine, and others. Therefore, much effort is going towards delivery and targeting of drugs to the brain.

The ability of drugs to pass freely to the brain depends on lipophilicity and molecular weight. Not the case, the molecule of drug needs a carrier-mediated entry (either a facilitated diffusive or an energy-dependent entry) or be able to link to receptor (e.g. insulin or transferrin receptor).

Another way how to get drug to the brain is to prepare prodrugs, which involves the administration of the drug in a form that is inactive, or weakly active, but is readily able to penetrate the BBB. Ideally, the prodrug should be lipid soluble so that it easy penetrates the BBB and is converted into the active form

solely within the brain. When the active form of molecule is more polar than the prodrug, it can be effectively locked into the brain. For example morphine, the effective analgesic, does not enter the CNS readily, but when converted to heroine, lipid solubility increases and brain uptake of course too.

By modulating of the BBB, so that the paracellular route of access to the brain is either partially or completely opened, is it possible to deliver some drugs to the brain. For example, hypertonic mannitol or alkylglycerols are able to open the tight junctions between the ECs, or ultrasound and electromagnetic radiation can be employed as modulators of BBB functions.

As mentioned previously, the BBB contains several efflux pumps, such as ABC transporters, which expel lots of drugs from the brain. When we want to avoid the activity of these efflux transporters, we can use either specific inhibitors or try to design analogues of drugs with known efficacy, but without being influenced by the efflux transporters. Well known modulators of ABC transporters are verapamil, probenecid, cyclosporine A, quinidine, sulfinpyrazone and several others.

Another possibility for significant delivery of relatively large amounts of drug or agent to the CNS is to incorporate them into liposomes or nanoparticles. These relatively complex and large structures (may range up to 500 nm in diameter) can reach the brain by passive targeting similar to small molecules, because their distribution is mainly determined by physico-chemical and physiological conditions.

Because of the lack of success in targeting the brain via the vascular route, invasive methods, such as direct injection or infusion, either into brain parenchyma or intraventricularly or intrathecally into CSF, have been applied to macromolecular drugs as well as to the delivery of viral vectors, most commonly used are adeno-associated viral vectors (AAV) and lentiviral vectors (LV) . This approach may also be used to introduce a slow-release implant or a colony of stem cells into the brain. This route might be useful for a longer-term slow infusion of drugs, but will always be attended by risk of damage of brain tissue both in the place of action and along the track used for delivery of drug to the brain.

Among several other manners, which have been developed for drug targeting to the brain, belong e.g. cell-penetrating peptide vectors or delivery the olfactory epithelium and nerves (Begley, 2004; De Boer and Gaillard, 2007).

As it was mentioned before, acute brain injury increases permeability of the BBB. Therefore, it is typically assumed that all compounds can be essentially delivered through an intravascular approach and penetrate brain. Optimization of drug delivery will play a major role in determining therapeutic gain (Lo et al., 2001).

## 1.5 The role of calcium

### 1.5.1 Calcium signalling

Calcium ( $\text{Ca}^{2+}$ ) is a key signaling ion, controlling many different intracellular and extracellular processes, such as synaptic activity, gene transcription, muscle contraction, cell proliferation, cell-cell communication or adhesion (Bootman et al., 2001a; Marambaud et al., 2009). In most cells  $\text{Ca}^{2+}$  has its major signalling function when its concentration is elevated in the cytosolic compartment.

$\text{Ca}^{2+}$  concentration inside cells is regulated by “on” and “off” mechanisms depending on whether they increase or decrease cytosolic  $\text{Ca}^{2+}$ . The  $\text{Ca}^{2+}$  “on” mechanisms include channels located at the plasma membrane (PM) which regulate the supply of  $\text{Ca}^{2+}$  from the extracellular space, and channels on the endoplasmic reticulum (ER) and sarcoplasmic reticulum (SR). Whereas “off” mechanisms include  $\text{Ca}^{2+}$ ATPases on the PM and on the ER and SR which remove  $\text{Ca}^{2+}$  from the cytoplasm (e.g.  $\text{Na}^+/\text{Ca}^{2+}$  exchange). When cells are at rest, an intracellular concentration of  $\text{Ca}^{2+}$  is  $\pm 100\text{nM}$ . However, stimulation of cells, for example by depolarisation, mechanical deformation or hormonal activation, increases the cytosolic  $\text{Ca}^{2+}$  concentration to  $1\ \mu\text{M}$  or more (Bootman et al., 2001b).

Several different types of calcium entry channels are present in cells. Voltage-operated  $\text{Ca}^{2+}$  channels (VOCCs) serve as a major route for calcium entry into cells, particularly excitable cells, and are activated by depolarization of membrane potential. VOCCs are divided into two groups: high voltage-activated and low voltage-activated channels. Low voltage-activated channels are T-type and are mainly localized to the nervous system. High voltage-activated channels can further be subdivided into L-type, widely expressed in many tissues of the brain and the cardiovascular system, P/Q-type, N-type, and R-type channels, which mainly function within the CNS (Liao et al., 2009). Receptor-operated  $\text{Ca}^{2+}$  channels (ROCCs) are activated by the binding of an agonist to the extracellular domain of the channel. These types of  $\text{Ca}^{2+}$  channel are particularly prevalent

on secretory cells and at nerve terminals. Well known ROCCs include the nicotinic acetylcholine receptor and the *N*-methyl-D-aspartate receptor (NMDAR). Store-operated  $\text{Ca}^{2+}$  channels (SOCCs) are activated in response to depletion of the intracellular  $\text{Ca}^{2+}$  store, either by physiological  $\text{Ca}^{2+}$ -mobilising messengers or pharmacological agents.

$\text{Ca}^{2+}$  is released from intracellular stores by messenger-activated channels. When hormones or growth factors bind to specific receptors at the plasma membrane, it leads to the activation of phospholipase C, which catalyses the hydrolysis of phosphatidylinositol 4,5-bisphosphate (PIP<sub>2</sub>) to the intracellular messengers inositol 1,4,5-trisphosphate (InsP<sub>3</sub>) and diacylglycerol. InsP<sub>3</sub> binds to specific receptors (InsP<sub>3</sub>Rs) on the ER or SR, which changed conformation such that an integral channel is opened and  $\text{Ca}^{2+}$  is released to the cytoplasm. InsP<sub>3</sub>Rs are almost ubiquitously expressed in mammalian tissues, in contrast to ryanodine receptors (RyRs), their structurally and functionally analogues, which are largely present in excitable cell types, such as muscle and neurons and are activated by cyclic adenosine diphosphate (cADP). Both RyRs and InsP<sub>3</sub>Rs are sensitive to cytosolic  $\text{Ca}^{2+}$  concentrations and are focal points for the convergence of many different signalling pathways (Bootman et al., 2001b).

### 1.5.2 The role of calcium in healthy brain

Calcium participates in many neuronal functions. Neurons, because of their morphology and the selective distribution of  $\text{Ca}^{2+}$  channels, produce a hierarchy of calcium signals caused by synaptic input.  $\text{Ca}^{2+}$  signals within brain underlie changes in synaptic plasticity such as long-term potentiation (LTP) and long-term depression (LTD).  $\text{Ca}^{2+}$  is implicated in both stimulating and depressing the transmission of nervous signals.

Neurons express  $\text{Ca}^{2+}$ -activated  $\text{K}^{+}$  channels that hyperpolarise the plasma membrane following an action potential and promote repolarisation of the cell after an action potential and thus regulate the frequency of firing action potentials.

It is well known that local  $\text{Ca}^{2+}$  signals control the release of neurotransmitter in the active zones of pre-synaptic nerve terminals and neuroendocrine cells.

It has been well established that many neuronal cells display spontaneous  $\text{Ca}^{2+}$  signals necessary for growth, migration and differentiation and that  $\text{Ca}^{2+}$  regulates the motility and directionality of neuronal growth cones.

Additionally the plasticity of  $\text{Ca}^{2+}$  as an intracellular messenger is almost matched by the versatility of some of its effectors, which mediate many of the effects of  $\text{Ca}^{2+}$ , for example ubiquitous  $\text{Ca}^{2+}$ -binding protein calmodulin (Bootman et al., 2001a).

### 1.5.3 The role of calcium in neurodegeneration

Beside the normal function of calcium in healthy brain, calcium is involved in many facets of pathophysiology, where the calcium signaling is abnormal, including necrosis, apoptosis, and neurodegenerative disorders, such as Alzheimer's disease (AD), Parkinson's disease (PD), amyotrophic lateral sclerosis (ALS), Huntington's disease (HD) and spinocerebellar ataxias (SCAs) (Bezprozvanny and Mattson, 2008; Yu et al., 2009).

Neuronal calcium signaling undergoes significant age-dependent changes therefore the risk of neurodegenerative disorders increases with age. These changes include increased  $\text{Ca}^{2+}$  release from intracellular stores through inositol-1,4,5-trisphosphate receptors (InsP3R) and ryanodine receptors (RyRs), enhanced  $\text{Ca}^{2+}$  influx through L-type voltage-operated calcium channels (VOCCs), reduced contribution of NMDAR-mediated  $\text{Ca}^{2+}$  influx, increased slow after-hyperpolarization due to activation of  $\text{Ca}^{2+}$ -dependent  $\text{K}^+$  channels, reduced cytosolic  $\text{Ca}^{2+}$  buffering capacity and activation of calcineurin and calpains (Bezprozvanny and Mattson, 2008). All these fundamental aging processes may also contribute to the calcium dysregulation in AD, because of oxidative and metabolic stress evoked by alterations of calcium in normal aging (Yu et al., 2009).

In addition, extracellular  $\text{Ca}^{2+}$  depletion and increased intracellular level of  $\text{Ca}^{2+}$  could lead to disruption of BBB TJ. Interestingly, both abnormally high and abnormally low intracellular concentration of  $\text{Ca}^{2+}$  can disrupt the TJ via decreased expression and/or disrupted protein-protein interactions, indicating a role for intracellular stores in the regulation of TJ. Then  $\text{Ca}^{2+}$  influx or release from intracellular stores can activate any number of kinase signal cascades, which lead to the activation of transcription factors that regulate TJ protein expression (Hawkins and Davis, 2005).

## 1.6 Compounds of interest

The substances were chosen according to their ability to influence the level of calcium, and the adverse effects within CNS were important deciding factor, too, because they show that the substance is able to pass the brain. The chemical structures of chosen ion channel blockers are shown in Table 1.1 with molecular weight and log *P*.

### 1.6.1 Calcium channel blockers

Calcium antagonists were approved for the treatment of hypertension in the 1980s. Since the time their use has been extended to additional conditions such as angina pectoris, paroxysmal supraventricular tachyarrhythmias, hypertrophic cardiomyopathy, Raynaud phenomenon, pulmonary hypertension, diffuse esophageal spasm, and cerebral vasospasm. This group is heterogeneous and includes 3 main classes: phenylalkylamines (verapamil), benzothiazepines (diltiazem), and dihydropyridines (nifedipine). The first-generation drugs in each class are verapamil, diltiazem, and nifedipine, respectively. The second generation of the 1,4-dihydropyridines includes calcium antagonists with an extended-release mechanism (Grossman and Messerli, 2004).

Intracellular concentration of calcium is provided by several mechanisms: Na<sup>+</sup>/Ca<sup>2+</sup> exchange, Ca<sup>2+</sup> pump and voltage- and receptor-operated calcium channels. In myocard and vascular muscle cells are mainly L-type calcium channels, which are opened for long time, and T-type calcium channels (present in sinoatrial node) opened only for a short term. Calcium antagonists from each class differ in physico-chemical properties and binding on L-type calcium channel. Dihydropyridine derivatives have always higher selectivity to vessels than to heart. They bind to the inactive calcium channel. In contrast verapamil and diltiazem bind to the opened calcium channel and therefore they have higher effect in tissues with fast depolarization in sinoatrial (SA) and atrioventricular (AV) node (Lincová et al, 2007).

Calcium antagonists lower cytosolic free calcium concentration mainly through a reduction of transmembranous calcium influx, and are potent arteriolar vasodilators. They also reduce angiotensin II-mediated vasoconstriction and decrease angiotensin II stimulatory effect on adrenal biosynthesis and secretion of aldosterone. Thus calcium antagonists lower blood pressure mainly by reducing

peripheral vascular resistance but orthostatic hypotension is rare, because they predominantly affect arteriolar resistance vessels (Grossman and Messerli, 2004).

**Verapamil**, derivate of pheerylalkylamine, acts preferentially in myocardium, slows down sinus rhythm and conduction in transfer system. After intravenous application verapamil action starts in 5 minutes and continues up to 6 hours. Verapamil is used predominantly as antiarrhythmic agent, antihypertensive drug (retarded drug forms) and alternative to  $\beta$ -blockers in secondary prevention after heart attack and for prevention of restenosis after angioplasty. Verapamil is contra-indicated in a hard disorder of atrioventricular conduction, heart insufficiency and along with  $\beta$ -blockers or digoxin. This inhibitor of cytochrom P450, mainly CYP1A2 and CYP3A4 can influence concentration or action of drugs which are substrates of these isoenzymes (e.g. carbamazepine, cyclosporine, digoxin, quinidine, theophylline and  $\beta$ -blockers). Side effects manifest as constipation, headache, oedema, heart failure or bradycardia.

**Diltiazem** is a derivate of benzothiazepine. Its action is more close to verapamil than to nifedipine. Diltiazem has arteriodilatation action and slows down atrioventricular conduction. This drug reduces incidence of ventricular tachycardia and extrasystole. The negative inotropic action is not so expressive in comparison to verapamil, as well as side effects, but contra-indications and interaction are analogous.

**Nifedipine** is the most common dihydropyridine derivate. All dihydropyridines have only minimal effect on cardiac contractility, cardiac rate and atrioventricular conduction, and therefore do not act antiarrhythmically. Vasodilatation action of nifedipine reduces peripheral vascular resistance and this evokes mild rise of heart expenditure and increases cardiac rate. Common drug forms of nifedipine have short half-life (2-3 hours), which causes blood pressure variation and activation of regulatory mechanisms, especially increased activity of sympathetic nervous system, therefore retarded drug forms are used. Common characteristic of all dihydropyridines is hepatic transformation and for these reasons the dose has to be regulated during hepatic disorders. The interactions with other drugs that induce or inhibit cytochrom P450 are possible, too. Side effects are quite frequent and manifest as headache or peripheral oedema. The common contra-indication is heart failure and cardiogenic shock (Lincová et al, 2007).

### 1.6.2 NMDAR antagonists

Physiological NMDAR activity is essential for normal neuronal function, such as neuronal survival and maturation, neuronal migration induction of long-term potentiation (LTP), a cellular/electrophysiological correlate of learning and memory formation, formation of sensory maps and neurodegeneration.

Under normal conditions of synaptic transmission, the NMDAR-channel is gated by extracellular  $Mg^{2+}$  sitting in the channel and only activated for brief periods of time, which allows  $Ca^{2+}$  (and other cations) to move into the cell for the subsequent physiological functions. Under pathological conditions, however, overactivation of the receptor relieves the  $Mg^{2+}$  block and causes an excessive amount of  $Ca^{2+}$  influx into the nerve cell, which then triggers a variety of processes that can lead to necrosis, apoptosis, or dendritic/ synaptic damage.

Potential neuroprotective agents that block virtually all NMDA receptor activity had unacceptable clinical side-effects, but the adamantane derivative, memantine blocks preferentially excessive NMDA receptor activity without disrupting normal activity (Chen and Lipton, 2006).

**Memantine** was first synthesized in the 1960s, and was found in the 1989 to inhibit NMDARs with an  $IC_{50}$  of approximately 1 mM, which corresponds well with its therapeutic concentration range. Memantine works by blocking the channel of NMDAR and is classified as an 'open channel blocker' because it can enter the channel and block current flow only after channel opening. This NMDAR antagonist has clinical utility in many nervous system diseases, of which the most prominent currently is AD, a disease characterized by deficits in glutamatergic neurotransmission. However, memantine might have far broader therapeutic utility, and is effective in the treatment of other dementias and neurodegenerative diseases, including Parkinson's and Huntington's disease (Johnson and Kotermanski, 2006).

Memantine is a derivative of amantadine, an anti-influenza agent and has a three-ring (adamantane) structure with a bridgehead amine ( $-NH_2$ ) that under physiological conditions carries a positive charge ( $-NH_3^+$ ) (Chen and Lipton, 2006).

**Amantadine** is a stable derivative of adamantane, which affects the replication of three antigenic subtypes of influenza A (H1N1, H2N2, H3N2). Amantadine blocks a channel protein in the viral coat that permits influx of protons; thus, "uncoating" is prevented. Moreover, amantadine inhibits viral maturation.

The drug is also used prophylactically and, if possible, must be taken before the outbreak of symptoms.

Amantadine is mild antagonist of the glutamate/NMDAR subtype, ultimately leading to a diminished release of acetylcholine and probably increases release of dopamine and decreases its re-uptake. This substance is used for treatment of mild parkinsonian manifestations but it can not be used in the long term, because its dopaminergic action is lost after 6 months at the latest. The side effects are nausea, dizziness, insomnia and incidence of others such as depression, damage of coordination, fuzziness, anxiety and dryness in mouth (Lincová et al, 2007; Lüllmann et al., 2000).

### **1.6.3 Phenobarbital**

Phenobarbital is the oldest drug in treatment of epilepsy (1911). It is effective in tonic-clonic convulsions and partial seizures. Phenobarbital inhibits the release of glutamate and so indirectly influences NMDAR, which is connected with a ligand-gated ion channel that, upon stimulation with glutamate, permits entry of both  $\text{Na}^+$  and  $\text{Ca}^{2+}$  ions into the cell. Phenobarbital augments activation of the  $\text{GABA}_A$  receptor connected with chloride channel by physiologically released amounts of GABA, chloride influx into the neurons is increased and membrane hyperpolarization of postsynaptic neuronal cells follows, thus the transmission of epileptic activity impend. Among adverse effects of phenobarbital belongs sedation, difficulty in concentrating and slowing of drive. Moreover, cutaneous, hematological, and hepatic changes may necessitate a change in medication. Phenobarbital may lead to osteomalacia or megaloblastic anemia. Last not least phenobarbital induces hepatic enzymes responsible for drug biotransformation. Combinations between anticonvulsants or with other drugs may result in clinically important interactions (Kwan and Brodie, 2004; Lincová et al, 2007; Lüllmann et al., 2000).

Substance	Chemical structure	Mr (g/mol)	Log <i>P</i>
verapamil		422.62	3.899±0.51
diltiazem		372.49	3.634±0.94
nifedipine		344.33	2.966±0.58
phenobarbital		232.24	1.668±0.26
memantine		179.31	3.177±0.27
amantadine		151.25	2.218±0.24

Table 1.1 An overview of ion channel blockers used in the transport studies. It is featured their molecular structure, molecular weight and log *P*. Log *P* values were adopted from <http://scifinder.cas.org>, accessed on 18<sup>th</sup> of February 2010. The chemical structures were drawn in program ChemDraw and molecular weights were calculated by this program, too.

## 1.7 Aim of the study

As it was mentioned before, 6 different substances blocking ion channels were chosen (verapamil, diltiazem, nifedipine, phenobarbital, memantine, amantadine) for purpose of this work. All these substances are routinely used in clinical practice and it is well known that adverse effects on the central nervous system can occur during therapy with them. Therefore, the first intention of this thesis was to investigate and compare the transport abilities of chosen calcium channel antagonists to penetrate across the BBB.

It is not rare that especially elderly people suffer from several concurrent chronic conditions (multimorbidity), e.g. heart diseases or memory problems, and they can easily take a number of medicaments. In this case the problem of interference between drugs is very actual, and it is necessary to know how the clinical potential of each substance can be influenced. In sequence, one substance which is preferentially used for treatment of CNS disorders (phenobarbital) was chosen and then was observed if its ability to reach CNS is influenced by different substances commonly used in treatment of heart diseases (verapamil and diltiazem).

## 2 MATERIALS AND METHODS

### Cell culture and transport studies

- ECV 304 Cell line European Collection of Animal Cell Cultures (ECACC, Wildshire, UK)
- T0665 holo-Transferrin human, A2942 Amphotericin B, H8264 HBSS, G9391 Gelatin from bovine skin, Type B, Sigma-Aldrich Handles GmbH, Vienna, Austria
- 21765-029 Ham's F12, 21980-032 IMDM, 25030 L(+)-glutamine, 26010-074 NCS, 15630-049 HEPES buffer, 15400 10x Trypsin/EDTA, 15140 Penicilin/Streptomycin, 25080 7.5% (v/v) bicarbonate Gibco BRL Life Technologies, now invitrogen L.T., Vienna, Austria
- H15-002 DPBS buffer PAA Laboratories GmbH, Pashing, Austria
- 51550 Heparin Sodium salt from porcine intestinal mucosa Fluka BioChemica, Buchs, Switzerland
- 150703 Collagen bovine MP Biomedicals, Inc., Solon, Ohio
- Falcon Tissue Culture Plate Falcon Cell Culture Insert Becton Dickinson Austria GesmbH, Schwechat, Austria
- Sterilin disposable pipettes; 10ml, 25ml Berlworld Scientific ldt, Stone, Staffordshire, STO5A, UK
- CellStar sterile PP-test tubes; 15ml, 50ml Greiner Bio-One GmbH, Germany
- Eppendorf Reasearch pipettes Eppendorf AG, Hamburg, germany
- Millipore Millicell Electrical Resistance System (ERS) Millipore, Vienna, Austria
- Thoma, counting chamber Superior Marienfeld, Germany

## Substances

- 94837 Verapamil hydrochloride Fluka BioChemica, Buchs, Switzerland
- D2521 (+)-cis-Diltiazem hydrochloride Sigma-Aldrich Handles GmbH, Vienna, Austria
- N7636 Nifedipine Sigma-Aldrich Handles GmbH, Vienna, Austria
- Phenobarbital Received from Mr. Möllner (AGES PharmMed, Vienna, Austria)
- 298080010 1,3-Dimethyl-5-aminoadamantane hydrochloride (Memantine) Acros organics, New Jersey, USA
- 151670050 1-Adamantamine hydrochloride (Amantadine) Acros organics, New Jersey, USA
- Diazepam Received from Dr. Maierhofer (AGES PharmMed, Vienna, Austria)
- 21877 5(6)- Carboxyfluorescein Fluka BioChemica, Buchs, Switzerland

## Other chemicals

- 1.11452.0005  $\sigma$ -Phtalaldehyde (OPA) Merc, Darmstadt, Germany
- 01039 *N*-Acetyl-L-cystein (AC) Fluka BioChemica, Buchs, Switzerland
- 6308 di-Natriumtetraborat Merc, Darmstadt, Germany
- 1.06007.2500 Methanol Merc, Darmstadt, Germany
- 1648 HPLC grade Acetonitrile Fisher Scientific UK Limited, Loughborough, UK
- 4873 Potassium dihydrogen phosphate Merc, Darmstadt, Germany
- 295700025 Phosphoric acid 85% Acros organics, New Jersey, USA
- 1.05104.1000 di-Potassium hydrogen phosphate Merc, Darmstadt, Germany

## HPLC

- DDV-20A5/Prominence Degaser Shimadzu
- SIL-20AC/Prominence Auto sampler Shimadzu
- CTO-20AC/Prominence Column Oven Shimadzu
- SPD-20A/Prominence UV detector Shimadzu
- RID-10A/Shimadzu Refractive Index Detector Shimadzu
- CMB-20A/Prominence Communications Bus Module Shimadzu
- 28105-154030 BDS Hypersil C18 Column, 150 x 4 mm, 5µm particle size Thermo Scientific
- 28105-014001 BDS Hypersil C18 5UM Pre-column, 10 x 4mm, Drop-in Guards 4/PK Thermo Scientific
- 70201 Crimp vials N11-1 HP, pack of 100, clear, capacity 1,5 ml Macherey – Nagel, Düren, Germany
- 70231 Crimb caps N11 TB/oA, pack of 100 Macherey – Nagel, Düren, Germany

## 2.1 Cell culture

The cell culture work was performed in sterile conditions it means that all operations were done in the laminar flow cabinet and everything what we wanted to place in the laminar flow cabined had to be cleaned with 70% (v/v) ethanol. Sterile tools were used, such as sterile disposable pipettes or sterile PP-test tubes not to contaminate growing cell line or stock bottle with medium or another solution. After work the laminar flow cabinet was closed and sterilized with ultraviolet radiation.

For the experiments ECV304 cell line was used. These cells originated from umbilical vein endothelial cells by spontaneous transformation and we obtained them from European Collection of Animal Cell Cultures (Takahashi et al., 1990). The layer of the ECV304 under light microscope is shown in the Figure 2.1.

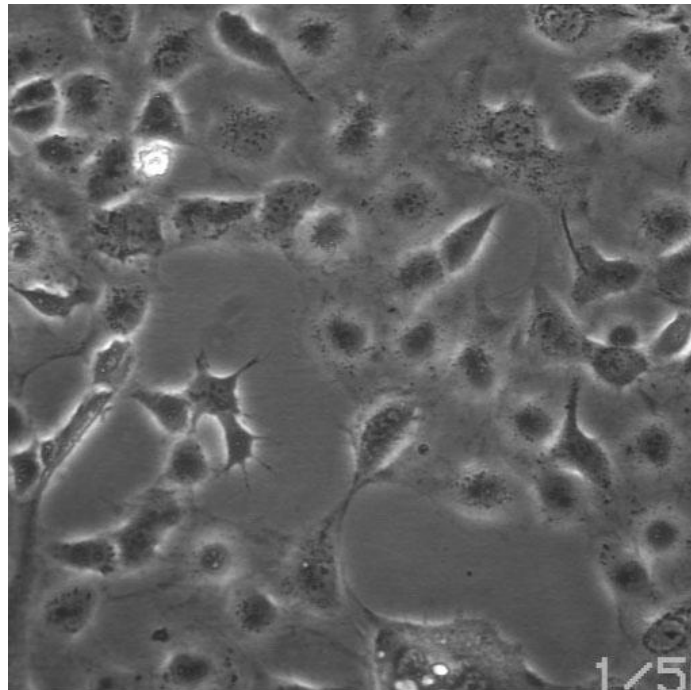


Figure 2.1 Typical morphology of the ECV304 cell line, adopted from <http://www.ub.es/biocel/wbc/recursos/coleccionphc.htm>, accessed on 11.1.2010.

The cell culture work was started by coating of a new sterile T25 flask with 2ml of 1% sterile gelatin solution. The whole surface area had to be covered equally and incubated 30 minutes at the room temperature. After incubation the gelatine solution was removed and the ECV304 cells were seeded on the flask. The cells were incubated at 37 °C, 5% CO<sub>2</sub>, and 96% humidity. These conditions were optimal for the growing of the cells.

For cell feeding the growth medium (PBMEC minus Fib medium) was used, it was for the first time changed the day after seeding and then every second day. The composition of medium with exact volumes of all solutions is described in the Table 2.1 Before changing of the medium, the stock bottle with medium had to be pre-warmed to 37 °C at least for 30 minutes in a warming chamber to avoid a temperature shock of cells. The old medium was removed from the flask and was replaced with 5 ml of fresh growth medium. The flask was labeled and placed back to the incubator. Before every medium change the cells were checked under the light microscope and if the cell layer was confluent, the cells could be split.

<b>PBMEC minus Fib medium</b>	<b>For 500 ml</b>
Ham's F12	103.75 ml
IMDM	103.75 ml
200 mM L-glutamine	17.50 ml
10mg/ml Transferrin	250.00 µl
1000U/ml Heparin	250.00 µl
NCS (Newborn Calf Serum)	19.00 ml
10 000U/ml Penicilin; 10 mg/ml Streptomycin	5.00 ml
ACM-C6 (astrocyt conditioned medium)	250 ml
250 µg/ml Amphotericin B	500.00 µl

Table 2.1 List of exact volumes of different components of the PBMEC minus Fib medium.

Sterile PBS, Trypsin/EDTA solution and growth medium were used for splitting of the cells. First of all them were pre-warmed to 37 °C in a warming chamber and placed in the laminar flow cabinet together with the flask. The old growth medium was removed from the flask and cells were washed with 2 ml PBS twice. Then 2 ml of Trypsin/EDTA solution were added for 30 seconds. Exact volumes of different components of the Trypsin/EDTA solution are listed in the Table 2.2 After removing of Trypsin/EDTA solution cells were detached from the growth surface by knocking the flask on a table. After that the surface of the flask was washed in 9 point process with 5 ml of new growth medium. The cell suspension was homogenized, transferred into a test tube and used for preparing a new flask and for seeding on transwell model. For preparing a new flask the required volume of the cell suspension was transferred into a new T25 flask, which was coated by gelatin before, usually in the ratio of one to ten (0,5 ml of cell suspension and 4,5 ml of growth medium). In the end the flask was

labeled with the name of the cell line, passage, date and my word caps, and placed into the incubator.

<b>Trypsin/EDTA solution</b>	<b>For 200 ml</b>
10× Trypsin/EDTA solution	20.00 ml
10x HBSS	20.00 ml
Sterile DPBS	154.00 ml
1M Hepes	2.00 ml
7,5% (v/v) bicarbonate	2.00 ml
10 000U/ml Penicilin; 10 mg/ml Streptomycin	2.00 ml

Table 2.2 Composition of Trypsin/EDTA solution with exact volumes of all solutions.

If the cells had to be stored for a short period, maximum 4 months, they could be frozen at -80 °C. After removing growth medium from the flask 2 ml of cryo-medium were added and the flask was incubated for 15 minutes at 4°C in a fridge (Table 2.3). After that the flask was given into a freezer (-80 °C).

When the frozen cells were needed again, they were taken out of the freezer and put into the incubator (37 °C), where they thaw slowly until the medium was removable. Then the cryo-medium was removed and 5ml of fresh pre-warmed growth medium were added. The cells were split next day.

<b>Cryo-medium</b>	<b>For 1.50 ml</b>
NCS	1.395 ml
DMSO 7% (v/v)	105 µl

Table 2.3 Composition of Cryo-medium

## 2.2 Transport studies

### 2.2.1 *In vitro* models of the blood brain barrier

BBB models are systems which reproduce the physiological, anatomical and functional characteristics of the BBB. These models were invented to enable prediction of the penetration of drugs across the BBB, to understand pathology of various neurological diseases or to enable pre-screening and optimization of new drug and gene delivery formulations. There are large quantitative and qualitative differences between various models. Today, three basic *in vitro* models are

available: the *in silico* models, the Transwell model and the dynamic *in vitro* model of the BBB (DIV-BBB) (Cucullo et al., 2005).

### 2.2.2 Transwell model

The Transwell model consists of a porous membrane insert placed in a plate, which divides it to two compartments, an upper and lower. The upper compartment serves as a donor compartment imitating lumen of brain microvessel and the lower as an acceptor compartment representing the brain. This model is characterized by side-by-side diffusion system, thanks to porous semipermeable membrane with cell cultivation immersed in growth media. The advantages of this model are simplicity, easy applicability, the ability to perform multiple experiments at the same time, inexpensiveness and time-unpretentiousness (Cucullo et al., 2005).

For purposes of this thesis 6-well plate and inserts with membrane surface of 4.2 cm<sup>2</sup> and pore size 1 μm, which does not allow migration of the cells through the insert, were used (Figure 2.2).

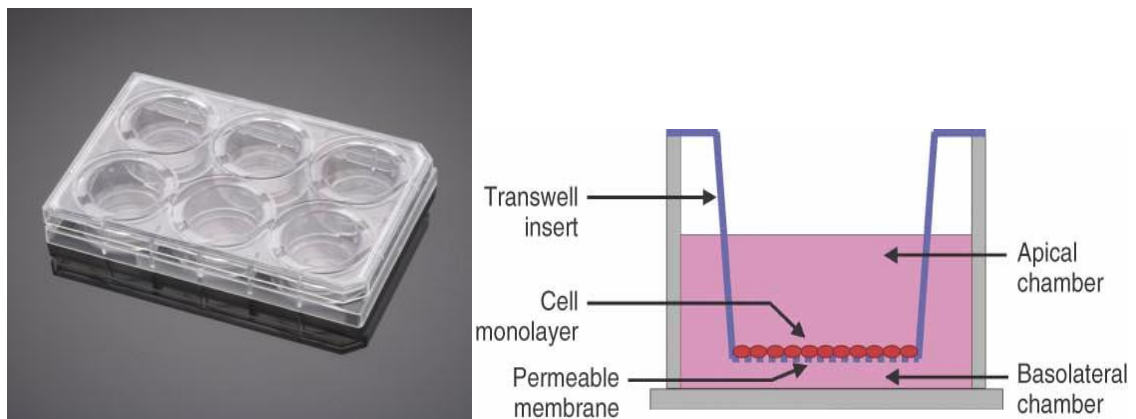


Figure 2.2 Left picture shows a typical 6-well Transwell apparatus. Source: <http://www.bdbiosciences.com/ptProduct.jsp?prodId=363075>, accessed on 12.1.2010.

Right picture presents a schematic diffusion chamber of a Transwell model. Source: <http://media.wiley.com/wires/WNAN/WNAN53/mfig003.jpg>, accessed on 11.1.2010.

#### 2.2.2.1 Coating of inserts for the Transwell model

At first, the 6-well plate and the inserts were placed into the laminar flow cabinet. The 6-well plate was taken out of the packing and the inserts were transferred into the 6-well plate using tweezers that were sterilized in a flame before. The tweezers were sterilized again after replacing of 2 or 3 inserts. When all inserts were placed in the plate, every insert was coated with 150 μl

of 0.14 mg/ml sterile collagen solution and the plate was shaken gently to cover the whole surface of the inserts. Then the 6-well plate was put in the incubator (37 °C, 5% CO<sub>2</sub>, and 96% humidity) for 1 hour. After incubation the supernatant of collagen solution was removed from every insert, and the plate could be used for seeding the cells.

#### ***2.2.2.2 Cell seeding***

The cells used for the seeding were obtained from cell cultivation during cell splitting (as mentioned before). The cells were seeded at the density of 50 000 cells/cm<sup>2</sup> and exact amount of cells given onto inserts had to be calculated. Therefore 40 µl of cell suspension were added into a Thoma chamber slide, made up two chambers, and cells were counted under the light microscope. The obtained number of cells (the average of both chambers) was multiplied by 10<sup>4</sup> to know which amount of cells per milliliter we have. This number was then divided by amount of cells/ml necessary for seeding of inserts. With this operation we obtained the factor, which was used for counting the amount of cell suspension needed for preparation of suspension for seeding of the inserts, only by dividing an amount of needed suspension by a factor.

The 6-well plate was filled with 3 ml of pre-warmed growth medium per well and 2 ml of the same medium were added into three inserts used as a blind control. Residuary three inserts were seeded with prepared cell suspension, 2 ml per insert, too. Every insert was positioned to the center of the well, the plate was labeled and placed into the incubator (37 °C, 5% CO<sub>2</sub>, and 96% humidity).

#### ***2.2.2.3 Medium exchange in the Transwell model***

The cells in Transwell model had to grow for 14 days to become tight enough for transport studies. For the cells survival a regular exchange of growth medium is necessary, it means that for the first time the medium was changed the next day after the seeding of the cells, and then every second day. Before every medium exchange the cell growth was observed in the microscope.

The plate was placed into a laminar flow cabinet. The inserts with the cells were emptied quickly and directly to a waste bottle and placed into an empty sterile plate intended for medium exchange. For manipulation with insert tweezers sterilized in the flame were used. After removing and replacing all inserts containing cells the medium was removed from the wells. Every empty well was

then filled with 3 ml of pre-warmed growth medium, and the inserts were placed back, using tweezers again. Finally, 2 ml of medium were added per insert. Every insert was positioned to the center of well and the plate was placed back into the incubator. Every time the medium was exchanged only in wells with cells. In the blind control wells the medium was changed for the first time 14 days after seeding, before starting the experiment.

### 2.2.3 Transport studies

After 14 day's the cell layer was tight enough and usable for transport study. This was checked by measuring TEER values. (Procedure of TEER measurement is described in section 2.6). Initially, the growth medium in the Transwell model was changed for the fresh one in all 6 inserts and the plate was incubated for 1 hour at room temperature, detection of TEER followed. After that all insets were emptied, transferred into new plate pre-filled with 3 ml of pre-warmed HBSS per well and 2 ml of HBSS were pipetted to every insert. This new plate was incubated at 37 °C for 30 minutes and then the TEER was measured immediately. Both plates (with medium and with HBSS) were stored in the incubator (37 °C) during transport study.

In the meantime, the substance solution containing 100 µl of test substance, 100 µl of diazepam and 5 µl of carboxyfluorescein in HBSS was prepared and placed to the incubator. Test substances were either dissolved in methanol or in water (Table 2.4). Diazepam dissolved in methanol and carboxyfluorescein dissolved in water were used as internal standards to minimize the influence of variability of cell layer. Diazepam with its high lipophilicity can pass the BBB easily via passive diffusion in contrast to carboxyfluorescein which is much more hydrophilic and goes through the BBB via paracellular route.

<b>Substance and its concentration in the subsatance solution</b>	<b>Solvent</b>	<b>Concentration of stock solution</b>
verapamil – 100 µM	methanol	10 mM
diltiazem – 100 µM	methanol	10 mM
nifedipine – 100 µM	methanol	10 mM
phenobarbital – 100 µM	methanol	10 mM
amantadine – 100 µM	water	10 mM
memantine – 100 µM	water	1 mM

Table 2.4 shows concentrations of each substance in the substance solution and concentrations of used stock solutions.

For the transport study C6 medium is usually used, but we could not work with it, because our group of substances contained memantine and amantadine, which had to be analyzed by derivatization of their amino-groups. (Derivatization of memantine and amantadine is mentioned in section 2.8). C6 medium contains amino-groups, too, and with using of this medium we would not be able to analyze them. Therefore the HBSS solution, which mimics the composition of C6 medium, was used in our experiment.

In the meantime 6 non-sterile plates were filled with HBSS solution (3ml/well) and placed into incubator for at least 1 hour. After determination of TEER values the plate with inserts was taken out a laminar flow cabinet and inserts were emptied into waste container. The 6 plates were taken out of the incubator (after 1 hour), labeled and the inserts were transferred to the first position of plates, it means that every plate contained 1 insert. The transport study started with filling of the first insert with substance solution and the interval of 30 seconds was kept between filling each insert. For this experiment the time intervals of 5, 10, 15, 20, 30 and 60 minutes was kept. With every time interval the inserts were transferred to the next well using tweezers. It was very important to follow up the exact time and write down every time variance. The whole experiment was made in the incubator, where every plate was placed immediately after filling the insert with substance solution. After finishing of the transport study, the samples from supernatant, wells, substance solution and pure HBSS solution were collected to eppendorf vial, which were labeled and stored in a fridge (4 °C). All samples were intended for fluorescence measurement and HPLC analysis.

Finally, empty inserts from transport study were transferred to the plate with HBSS stored in incubator before, loaded with 2 ml of HBSS per insert and incubated for at least 30 minutes by 37 °C. Then TEER was detected immediately. Inserts were transferred into the plate with growth medium and then incubation for at least 1 hour at room temperature and measurement of TEER followed.

## 2.2.4 Measurement of the Transendothelial Electrical Resistance (TEER)

Measurement of the TEER is the most straightforward method to assess the tightness and integrity of the Transwell model (Deli et al., 2005). TEER was measured using Millipore Milli-Cell Electrical Resistance system (ERS) (Figure 2.3). This apparatus consist of two electrodes, one longer and one shorter, which were normally stored in 70% (v/v) ethanol.



Figure 2.3 This picture shows Millipore Milli-Cell ERS voltmeter, adopted from <http://www.fishersci.com/wps/portal/APPLICATION?store=Scientific&segment=scientificStandard>, accessed on.12.1.2010.

Before each measurement the electrodes were equilibrated by replacing them into a test tube with the same solution used in 6-well plate intended for determination of the TEER (HBSS or growth medium) for at least 30 minutes. The electrical resistance is temperature dependent, therefore the used solutions had to be incubated to desired temperature. During measurement the longer electrode was inserted to the well and shorter to the insert. It was very important to place the longer electrode exactly between outer wall of insert and inner wall of the well, because every wrong position influenced the measured values as well as touching of the metal part of the electrode by hand (Figure 2.4). After measuring of three wells with cells, the TEER values were written down, the electrode was put in the test tube with ethanol for approximately 10 seconds and then back

to the used solution. The measurement of the three blank inserts followed. TEER values of the cell layer were calculated by following formula:

$$\text{TEER } [\Omega \times \text{cm}^2] = (\text{TEER}_{\text{cell}} - \text{average TEER}_{\text{blank}}) \times \text{surface area (4.2 cm}^2)$$

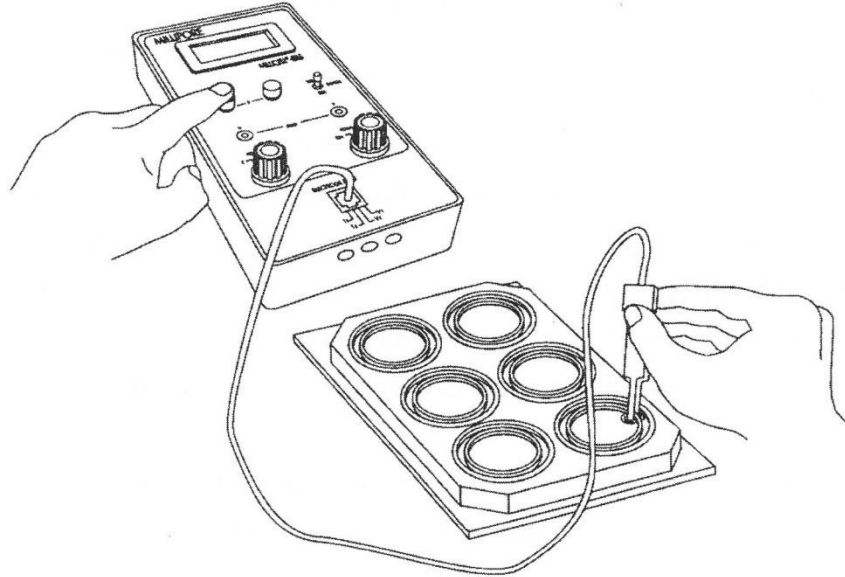


Figure 2.4 The picture illustrates the TEER measurement, including correct position of the electrode.

### 2.2.5 Fluorescence measurement

The fluorescence was usually measured next day after transport study. The collected samples were taken out of a fridge and incubated at room temperature for at least 30 minutes. After that each sample was pipetted three times in amount of 100  $\mu\text{l}$  into the fluorescence plate and fluorescence was measured by a microplate reader (BMG, excitation: 485 nm, emission: 520-535 nm). The obtained data were used for calculation of the clearance and permeability of CF.

### 2.2.6 Reversed-phase high performance liquid chromatography (RP-HPLC)

Transport studies were accomplished across the BBB in vitro model based on cell line ECV304 with following ion channel blockers verapamil, diltiazem, nifedipine, phenobarbital, memantine and amantadine. Amounts of permeated substances were quantified by HPLC to generate cleared volume (CV) (section 2.3, Eq.1). Before starting the HPLC analysis, the injection needle was washed by a mixture 60:40 of acetonitril and water. All eluents used for HPLC had to be sterile and degassed, whereof was achieved with sterile filtration and ultrasonic degassing for at least 20 minutes. For our experiment potassium phosphate buffer mixed with methanol (MeOH) was used as eluent, but different values of pH of potassium phosphate buffer and various ratios of buffer:MeOH had to be used because of heterogeneity of analyzed substances (Table 2.5). All used methods were found in literature and tested before the measurement (sometimes they were a little bit optimized). Every sample was measured three times and obtained peak areas were integrated and used for the calculation of the permeability coefficient.

Before analysis, memantine and amantadine had to be derivatized with *o*-phthalaldehyde (OPA) solution (1mg/ml) and with *N*-acetylcysteine (AC) solution (2,5mg/ml), both prepared in 0.1 M borax buffer, pH 10 (Higashi and Fujii, 2005). The borax buffer was prepared by dissolving of 3.81 g dinatriumtetraborat in 100 ml water. Then 50 mg OPA were dissolved in 50 ml of 0,1 M borax buffer, pH 10, and 125 mg of AC were dissolved in 50 ml of 0,1 M borax buffer, pH 10. Both had to be prepared freshly before labeling. The samples for HPLC were prepared by mixing 250  $\mu$ l of each sample obtained from the transport study plus 500  $\mu$ l of OPA solution plus 500  $\mu$ l of AC solution and immediately measured on the same day.

Substance	Buffer/ MeOH [v/v]	Buffer pH	Flow rate [ml/min]	Time [min]	t [°C]	Detection [nm]	Retention time [min]	
							Subst.	Diaz.
<b>verapamil</b> <sup>1</sup>	40/60	2.5	1.0	10	25	UV-254	3.1	6.6
<b>diltiazem</b> <sup>2</sup>	45/55	4.8	1.0	13	25	UV-254	6.5	10.8
<b>nifedipine</b> <sup>3</sup>	45/55	4.8	1.0	13	25	UV-254	6.0	10.5
<b>phenobarbital</b> <sup>4</sup>	50/50	2.5	1.0	14	25	UV-254	3.0	11.6
<b>memantine</b> <sup>5</sup>	30/70	7.0	1.0	10	25	UV-320	8.5	3.3
<b>amantadine</b> <sup>5</sup>	35/65	7.0	1.0	10	25	UV-320	7.5	4.5
<b>diltiazem/ phenobarbital</b>	45/55	4.8	1.0	12	25	UV-254	6.4	10.2
							2.4	
<b>verapamil/ phenobarbital</b>	45/55	4.8	1.0	12	25	UV-254	4.9	10.2
							2.4	

Table 2.5 Different conditions used for HPLC analysis obtained from literature and optimized for our conditions. Source: (<sup>1</sup>Chen and Lee, 1996; <sup>2</sup>Li et al., 2003; <sup>3</sup>Zendelovska et al., 2006; <sup>4</sup>Franeta et al., 2002; <sup>5</sup>Shuangjin et al., 2007).

### 2.2.7 Single studies – experimental conditions

Transport study	Fluorescence measurement	HPLC analysis	ECV passage	Substance solution - composition
12.11.2009	18.11.2009	25.11.2009	204	100 µM <b>verapamil</b>
				100 µM diazepam
				5 µM CF
				in HBSS
19.11.2009	23.11.2009	19.1.2010	205	100 µM <b>memantine</b>
				100 µM diazepam
				5 µM CF
				in HBSS
26.11.2009	27.11.2009	29.1.2010	206	100 µM <b>amantadine</b>
				100 µM diazepam
				5 µM CF
				in HBSS
10.12.2009	11.12.2009	15.12.2010	208	100 µM <b>phenobarbital</b>
				100 µM diazepam
				5 µM CF
				in HBSS
17.12.2009	18.12.2009	5.1.2010	209	100 µM <b>nifedipine</b>
				100 µM diazepam
				5 µM CF
				in HBSS
22.12.2009	22.12.2009	11.1.2010	210	100 µM <b>diltiazem</b>
				100 µM diazepam
				5 µM CF
				in HBSS

Table 2.6 shows the basic information about implementation of the single transport studies.

### 2.2.8 Group studies – experimental conditions

Transport study	Fluorescence measurement	HPLC analysis	ECV passage	Substance solution - composition
21.1.2010	22.1.2010	26.1.2010	212	100 µM <b>diltiazem</b>
				100 µM <b>phenobarbital</b>
				100 µM diazepam
				5 µM CF
				in HBSS
26.1.2010	26.1.2010	27.1.2010	213	100 µM <b>verapamil</b>
				100 µM <b>phenobarbital</b>
				100 µM diazepam
				5 µM CF
				in HBSS

Table 2.6 shows the basic information about implementation of the group transport studies.

### 2.3 Calculation of the permeability coefficient

When every sample from transport study was analyzed three times using HPLC and all peaks were integrated. The average values of peak areas of each sample were calculated and used to generate cleared volume (CV) values by equation 1:

$$CV[\mu\text{l}] = (C_{Bn} \times V_B) / C_A \quad \text{Eq. 1}$$

Where  $C_{Bn}$  is the substance concentration in the basolateral chamber (well) and  $C_A$  refers to the concentration in the apical compartment (insert).  $V_B$  is the volume in the well (3 ml = 3000  $\mu\text{l}$ ). For our calculation  $C_B$  was replaced with the peak area for a certain time point and  $C_A$  with the peak area of the stock solution (Neuhaus et al., 2006).

The inserts were transferred during transport study from one well into the next. For calculation of clearance values for several time points equation 2 was used:

$$CV[\mu\text{l}] = (C_{Bn} \times (V_B / C_A - \sum C_{Bn-1} \times 1.5)) \quad \text{Eq. 2}$$

Since the amount of the test compound in the apical insert decreases over time under conditions of unidirectional flux, the  $C_A$  value for each time point (each well) has to be corrected. Thus, the summed up total amount of substance found in each basolateral compartment before the actual one ( $\sum C_{Bn-1}$ ) is related to the apical volume and subtracted from  $C_A$ . Number 1.5 represents ration between the corresponding volumes of the compartments (well/insert; 3 ml/2 ml) (Neuhaus et al., 2006).

The permeability slope (PS) values were obtained from the graph, where slope of cleared volume vs. time was determined by linear regression analysis by using Microsoft Excel program. The reciprocal values of the average of permeability coefficients without cell layer ( $PS_{\text{control}}$ ) and with cell layer ( $PS_{\text{all}}$ ) were used for calculation of reciprocal values of permeability coefficient of cell monolayer only ( $PS_{\text{cell}}$ ) by equation 3 (Neuhaus et al., 2006):

$$1/ PS_{\text{cell}} = 1/PS_{\text{all}} - 1/PS_{\text{control}} \quad \text{Eq. 3}$$

$PS_{\text{cell}}$  value was used for calculation of the permeability coefficient (PE) according to equation 4:

$$\text{PE}[\text{cm}/\text{min}] = \text{PS}_{\text{cell}}/(1000 \times 4.2) \quad \text{Eq. 4}$$

Where 4.2 corresponds to a surface area of the insert [cm<sup>2</sup>] and 1000 is a factor derived from PS unit [μl/min] as follows equation 5 (Vaněček, 2007):

$$(\mu\text{l} / \text{min})/4.2 \text{ cm}^2 = (\text{mm}^3 / \text{min})/4.2 \text{ cm}^2 = [\text{cm}^3 / (1000 \times \text{min})]/4.2 \text{ cm}^2 = \text{Eq. 5}$$

$$\text{cm}/[\text{min} \times (1000 \times 4.2)]$$

The PE value in [cm/min] could be easily converted to the PE value in [μm/min] by multiplying with 10000.

Effect of correction (EC) was also calculated from equation 6 to illustrate if the collagen-coated membrane influences the transport or if the cell monolayer is the main barrier for a distinct transport route. An effect of correction of approximately 100% means that the cell monolayer is the major limiting barrier for the transport and the underlying matrix, as well as the membrane support have no significant influence on the resulting permeability coefficient. The effect of correction represents the fraction of PE<sub>cell</sub> divided by PE<sub>all</sub> and multiplied with 100 to get results in [%] (Neuhaus et al., 2006).

$$\text{EC} = (\text{PE}_{\text{cell}}/\text{PE}_{\text{all}}) \times 100 \quad \text{Eq. 6}$$

To minimalise the variation evoked either by the collagen coated membrane or by the cell monolayer, the permeation coefficients were expressed as ratio normalized to the internal standards (IS) – diazepam (Diaz) and carboxyfluorescein (CF). The ratios show how much slower or faster the substance (Subst) permeates in comparison to internal standard (IS) (Novakova, 2009). The ratios were calculated for cell layer only (PE<sub>cell</sub>) from equation 7 and for membrane with cell layer (PE<sub>all</sub>) from equation 8:

$$\text{PE}_{\text{cell}} \text{ Ratio Subst/IS} = \text{PE}_{\text{cell-Subst}}/\text{PE}_{\text{cell-IS}} \quad \text{Eq. 7}$$

$$\text{PE}_{\text{all}} \text{ Ratio Subst/IS} = \text{PE}_{\text{all-Subst}}/\text{PE}_{\text{all-IS}} \quad \text{Eq. 8}$$

The ratio between two internal standards was derived from equation 9 and 10:

$$\text{PE}_{\text{cell}} \text{ Ratio IS}_{\text{Diaz}}/\text{IS}_{\text{CF}} = \text{PE}_{\text{cell-Diaz}}/\text{PE}_{\text{cell-CF}} \quad \text{Eq. 9}$$

$$\text{PE}_{\text{all}} \text{ Ratio IS}_{\text{Diaz}}/\text{IS}_{\text{CF}} = \text{PE}_{\text{all-Diaz}}/\text{PE}_{\text{all-CF}} \quad \text{Eq. 10}$$

Finally, the recovery of drugs [%] after transport study was calculated. The summation of amount of substance in each well, and in insert were compared to the amount of substance in substance solution (100%) according to equation 11:

$$\text{Recovery [\%]} = C_{\text{sum}} \times 100 / C_{\text{STL}} \quad \text{Eq. 11}$$

Where  $C_{\text{sum}}$  means summation of amount of substance in each well and in insert after transport study and  $C_{\text{STL}}$  refers to amount of substance in substance solution.

### 3 RESULTS

**The single transport studies** were accomplished across the BBB in vitro model based on cell line ECV304 with following channel blockers: verapamil, diltiazem, nifedipine, phenobarbital, memantine and amantadine. Amounts of permeated substances were quantified by HPLC to generate cleared volume (CV) (section 2.3, Eq.1). Results are presented as diagrams of cleared volume vs. time (where CA, CB, CC represent three inserts with cell monolayer and BA, BB, BC represent the three blank inserts). The average permeability slope values ( $PS_{\text{control}}$ ,  $PS_{\text{all}}$ ) for each substance were obtained and  $PS_{\text{cell}}$  were calculated (section 2.3, Eq.3) using Microsoft Excel. The average permeability coefficient ( $PE_{\text{cell}}$ ) for cell layer was calculated (section 2.3, Eq. 4) and converted to units [ $\mu\text{m}/\text{min}$ ] (section 2.3, Eq.5).  $PE_{\text{all}}$  was also determined to enable to generate the effect of correction (section 2.3, Eq.3). All values were calculated for time intervals 5-140 min. and 0-5 min. (only during transport study of verapamil some mistake occurred and time intervals had to be changed to 8-140 min. and 0-8 min.).

**The group transport studies** were designed to find out the interference between chosen ion channel antagonists. Therefore two group studies were made: the transport study of diltiazem/phenobarbital and the transport study of verapamil/phenobarbital, where an antiepileptic agent phenobarbital as representative drug used in therapy, because of its acting within the CNS, was chosen to see if the fastness of phenobarbital to cross the BBB is influenced by verapamil or diltiazem, whose represent the drugs acting in periphery (with effect on heart and blood vessels). For these experiments the same materials and methods as in the single transport studies were used.

### 3.1 Transport study of verapamil – Single study

Transport study of verapamil was accomplished across the BBB *in vitro* model based on cell line ECV304. Amounts of permeated substance were quantified by HPLC. In the time interval 8-140 the average permeability slope values for verapamil were:  $PS_{\text{control}} = 7.25 \mu\text{l}/\text{min}$ ,  $PS_{\text{all}} = 3.36 \mu\text{l}/\text{min}$  and calculated  $PS_{\text{cell}} = 6.27 \mu\text{l}/\text{min}$ . The average permeability coefficient ( $PE_{\text{cell}}$ ) for cell layer was  $15.05 \pm 2.36 \mu\text{m}/\text{min}$ .  $PE_{\text{all}}$  amounted to  $7.97 \pm 0.66 \mu\text{m}/\text{min}$ . The effect of correction reached to 187.18 %. All values were calculated using equations from section 2.3. In this experiment the second control value (slope=4.33) was excluded due to an mistake after 15 minutes during the transport study.

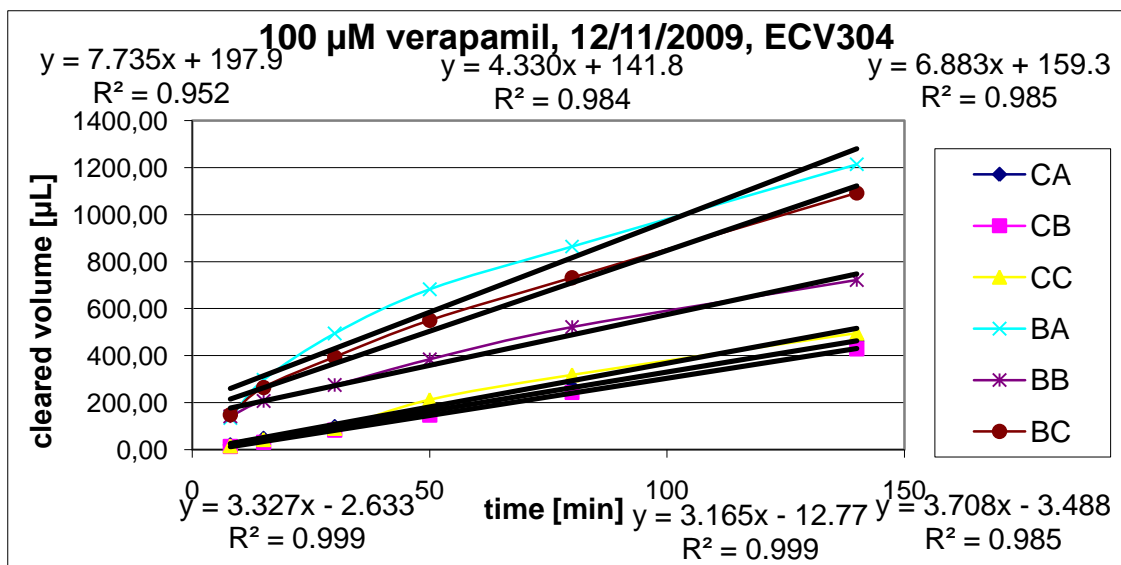


Figure 3.1 Dependence of cleared volume on the time interval 8-140 minutes for verapamil.

	$PS_{\text{Control}}$	$PS_{\text{all}}$	$1/PS_{\text{cell}}$	$PS_{\text{cell}}$	$PE_{\text{cell}}$ [cm/min]	$PE_{\text{cell}}$ [ $\mu\text{m}/\text{min}$ ]
Cell1	7.25	3.29	0.17	6.03	0.0014	14.35
Cell2	7.25	3.13	0.18	5.51	0.0013	13.11
Cell3	7.25	3.67	0.13	7.43	0.0018	17.68
<b>Average</b>	<b>7.25</b>	<b>3.36</b>	<b>0.16</b>	<b>6.27</b>	<b>0.0015</b>	<b>15.05</b>
SD						2.36

Table 3.1 Determination of permeability coefficient of verapamil for time interval 8-140 minutes for cell layer only.

	$PS_{\text{all}}$	$1/PS_{\text{cell}}$	$PS_{\text{cell}}$	$PE_{\text{cell}}$ [cm/min]	$PE_{\text{cell}}$ [ $\mu\text{m}/\text{min}$ ]
Cell1	3.29	0.30	3.29	0.0008	7.83
Cell2	3.13	0.32	3.13	0.0007	7.45
Cell3	3.67	0.27	3.67	0.0009	8.73
<b>Average</b>	<b>3.36</b>	<b>0.30</b>	<b>3.35</b>	<b>0.0008</b>	<b>7.97</b>
SD					0.66

Table 3.2 Determination of permeability coefficient of verapamil for time interval 8-140 minutes.

In the time interval 0-8 the average permeability slope values for verapamil were:  $PS_{\text{control}} = 28.28 \mu\text{l}/\text{min}$ ,  $PS_{\text{all}} = 3.36 \mu\text{l}/\text{min}$  and  $PS_{\text{cell}} = 3.81 \mu\text{l}/\text{min}$ .  $PE_{\text{cell}}$  was  $9.12 \pm 2.09 \mu\text{m}/\text{min}$ .  $PE_{\text{all}}$  amounted to  $8.00 \pm 1.62 \mu\text{m}/\text{min}$ . EC reached to 113.55%. All values were calculated using equations from section 2.3.

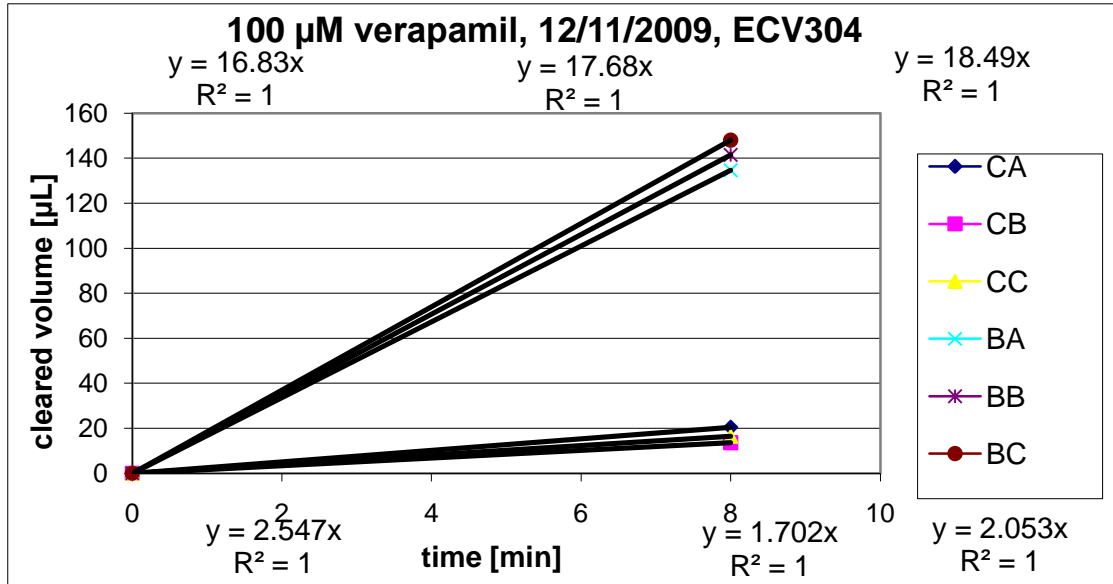


Figure 3.2 Dependence of cleared volume on the time interval 0-8 minutes for verapamil.

	$PS_{\text{Control}}$	$PS_{\text{all}}$	$1/PS_{\text{cell}}$	$PS_{\text{cell}}$	$PE_{\text{cell}} [\text{cm}/\text{min}]$	$PE_{\text{cell}} [\mu\text{m}/\text{min}]$
Cell1	28.28	4.08	0.21	4.76	0.0011	11.34
Cell2	28.28	2.72	0.33	3.01	0.0007	7.18
Cell3	28.28	3.29	0.27	3.72	0.0009	8.85
<b>Average</b>	<b>28.28</b>	<b>3.36</b>	<b>0.26</b>	<b>3.81</b>	<b>0.0009</b>	<b>9.12</b>
SD						2.09

Table3.3 Determination of permeability coefficient of verapamil for time interval 0-8 minutes for cell layer only.

	$PS_{\text{all}}$	$1/PS_{\text{cell}}$	$PS_{\text{cell}}$	$PE_{\text{cell}} [\text{cm}/\text{min}]$	$PE_{\text{cell}} [\mu\text{m}/\text{min}]$
Cell1	4.08	0.25	4.08	0.0010	9.70
Cell2	2.72	0.37	2.72	0.0006	6.49
Cell3	3.29	0.30	3.29	0.0008	7.82
<b>Average</b>	<b>3.36</b>	<b>0.31</b>	<b>3.27</b>	<b>0.0008</b>	<b>8.00</b>
SD					1.62

Table3.4 Determination of permeability coefficient of verapamil for time interval 0-8 minutes membrane of insert with cells.

## Internal standard diazepam in the transport study of verapamil

The permeability of diazepam as a function of time was determined using the same principles as for verapamil described above.

In the time interval 8-140 the average permeability slope values for diazepam were:  $PS_{\text{control}} = 9.94 \mu\text{l}/\text{min}$ ,  $PS_{\text{all}} = 6.01 \mu\text{l}/\text{min}$  and  $PS_{\text{cell}} = 15.21 \mu\text{l}/\text{min}$ .  $PE_{\text{cell}}$  was  $36.31 \pm 2.94 \mu\text{m}/\text{min}$ .  $PE_{\text{all}}$  amounted to  $14.31 \pm 0.46 \mu\text{m}/\text{min}$ . EC reached to 253.40%. All values were calculated using equations from section 2.3.

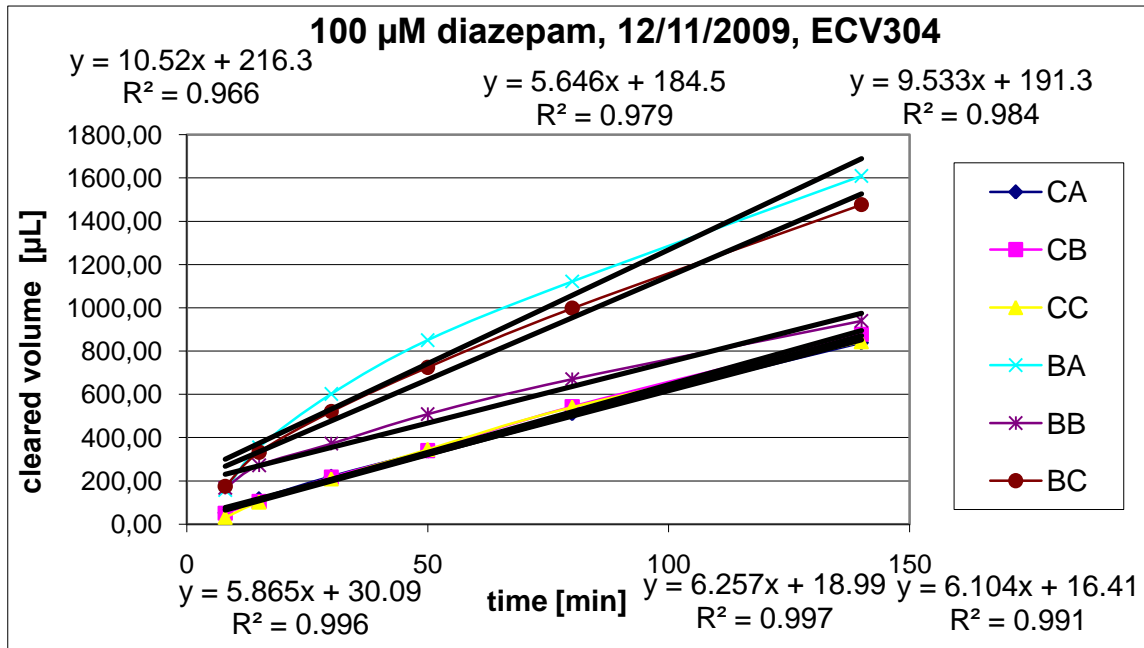


Figure 3.3 Dependence of cleared volume on the time interval 8-140 minutes for internal standard diazepam.

	$PS_{\text{Control}}$	$PS_{\text{all}}$	$1/PS_{\text{cell}}$	$PS_{\text{cell}}$	$PE_{\text{cell}} [\text{cm}/\text{min}]$	$PE_{\text{cell}} [\mu\text{m}/\text{min}]$
Cell1	9.94	5.80	0.07	13.94	0.0033	33.20
Cell2	9.94	6.19	0.06	16.40	0.0039	39.05
Cell3	9.94	6.04	0.06	15.40	0.0037	36.68
<b>Average</b>	<b>9.94</b>	<b>6.01</b>	<b>0.07</b>	<b>15.21</b>	<b>0.0036</b>	<b>36.31</b>
SD						2.94

Table 3.5 Determination of permeability coefficient of diazepam for time interval 8-140 minutes for cell layer only.

	$PS_{\text{all}}$	$1/PS_{\text{cell}}$	$PS_{\text{cell}}$	$PE_{\text{cell}} [\text{cm}/\text{min}]$	$PE_{\text{cell}} [\mu\text{m}/\text{min}]$
Cell1	5.80	0.17	5.80	0.0014	13.82
Cell2	6.19	0.16	6.19	0.0015	14.74
Cell3	6.04	0.17	6.04	0.0014	14.39
<b>Average</b>	<b>6.01</b>	<b>0.17</b>	<b>6.01</b>	<b>0.0014</b>	<b>14.31</b>
SD					0.46

Table 3.6 Determination of permeability coefficient of diazepam for time interval 8-140 minutes.

In the time interval 0-8 the average permeability slope values for diazepam were:  $PS_{\text{control}} = 33.37 \mu\text{l}/\text{min}$ ,  $PS_{\text{all}} = 8.95 \mu\text{l}/\text{min}$  and  $PS_{\text{cell}} = 12.22 \mu\text{l}/\text{min}$ .  $PE_{\text{cell}}$  was  $29.73 \pm 9.89 \mu\text{m}/\text{min}$ .  $PE_{\text{all}}$  amounted to  $21.30 \pm 5.55 \mu\text{m}/\text{min}$ . EC reached to 137.41%. All values were calculated using equations from section 2.3.

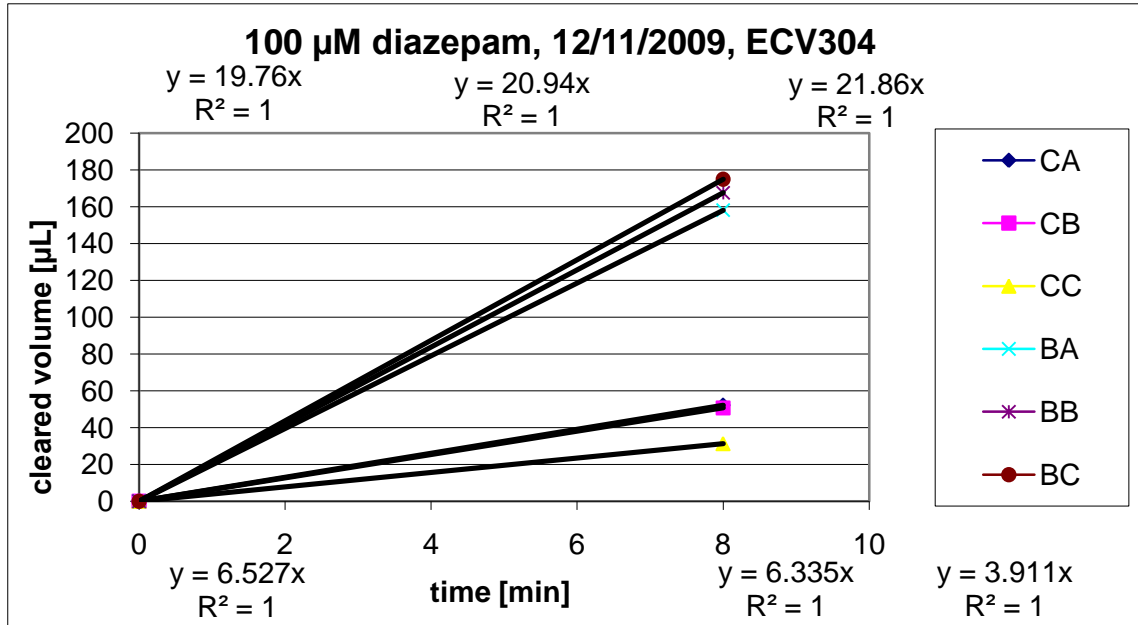


Figure 3.4 Dependence of cleared volume on the time interval 0-8 minutes for internal standard diazepam.

	$PS_{\text{Control}}$	$PS_{\text{all}}$	$1/PS_{\text{cell}}$	$PS_{\text{cell}}$	$PE_{\text{cell}} [\text{cm}/\text{min}]$	$PE_{\text{cell}} [\mu\text{m}/\text{min}]$
Cell1	33.37	10.44	0.07	15.20	0.0036	36.19
Cell2	33.37	10.14	0.07	14.56	0.0035	34.66
Cell3	33.37	6.26	0.13	7.70	0.0018	18.34
<b>Average</b>	<b>33.37</b>	<b>8.95</b>	<b>0.08</b>	<b>12.22</b>	<b>0.0029</b>	<b>29.73</b>
SD						9.89

Table3.7 Determination of permeability coefficient of diazepam for time interval 0-8 minutes for cell layer only.

	$PS_{\text{all}}$	$1/PS_{\text{cell}}$	$PS_{\text{cell}}$	$PE_{\text{cell}} [\text{cm}/\text{min}]$	$PE_{\text{cell}} [\mu\text{m}/\text{min}]$
Cell1	10.44	0.10	10.44	0.0025	24.87
Cell2	10.14	0.10	10.14	0.0024	24.13
Cell3	6.26	0.16	6.26	0.0015	14.90
<b>Average</b>	<b>8.95</b>	<b>0.12</b>	<b>8.47</b>	<b>0.0020</b>	<b>21.30</b>
SD					5.55

Table3.8 Determination of permeability coefficient of diazepam for time interval 0-8 minutes membrane of insert with cells.

## Internal standard carboxyfluorescein in the transport study of verapamil

The permeability of carboxyfluorescein as a function of time was determined using the same principles as for verapamil described above.

In the time interval 8-140 the average permeability slope values for carboxyfluorescein were:  $PS_{\text{control}} = 10.48 \mu\text{l}/\text{min}$ ,  $PS_{\text{all}} = 2.90 \mu\text{l}/\text{min}$  and  $PS_{\text{cell}} = 4.01 \mu\text{l}/\text{min}$ .  $PE_{\text{cell}}$  was  $9.59 \pm 1.39 \mu\text{m}/\text{min}$ .  $PE_{\text{all}}$  amounted to  $6.91 \pm 0.71 \mu\text{m}/\text{min}$ . EC reached to 138.49%. All values were calculated using equations from section 2.3.

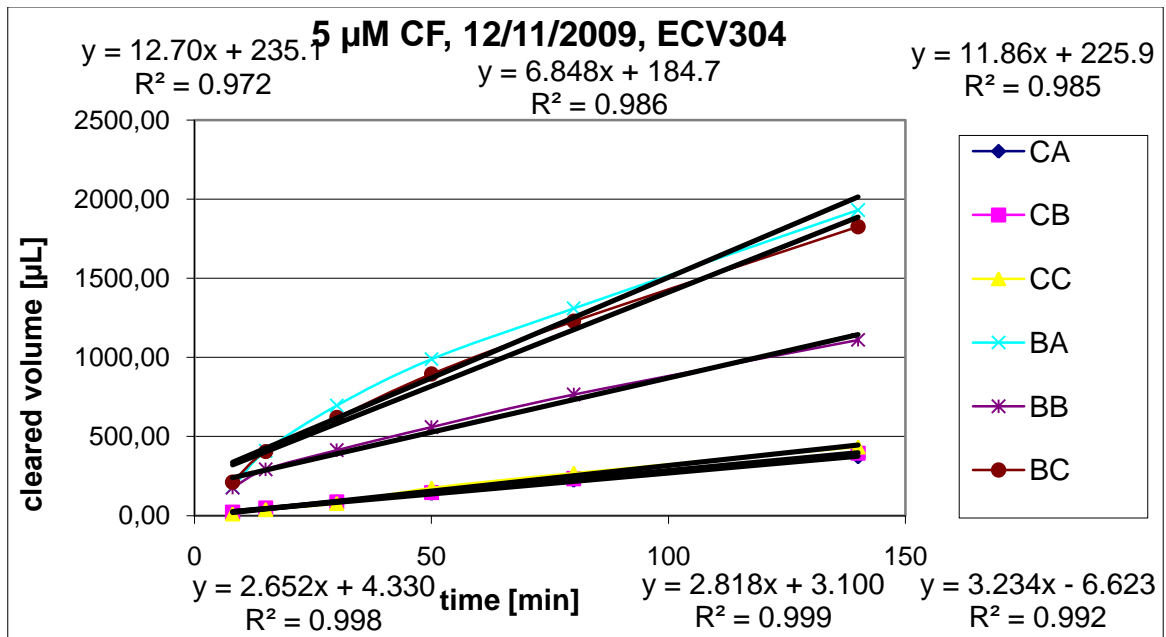


Figure 3.5 Dependence of cleared volume on the time interval 8-140 minutes for internal standard carboxyfluorescein.

	$PS_{\text{Control}}$	$PS_{\text{all}}$	$1/PS_{\text{cell}}$	$PS_{\text{cell}}$	$PE_{\text{cell}} [\text{cm}/\text{min}]$	$PE_{\text{cell}} [\mu\text{m}/\text{min}]$
Cell1	10.47	2.65	0.28	3.55	0.0008	8.46
Cell2	10.47	2.82	0.26	3.86	0.0009	9.18
Cell3	10.47	3.23	0.21	4.68	0.0011	11.14
<b>Average</b>	<b>10.47</b>	<b>2.90</b>	<b>0.25</b>	<b>4.01</b>	<b>0.0010</b>	<b>9.59</b>
SD						1.39

Table3.9 Determination of permeability coefficient of carboxyfluorescein for time interval 8-140 minutes for cell layer only.

	$PS_{\text{all}}$	$1/PS_{\text{cell}}$	$PS_{\text{cell}}$	$PE_{\text{cell}} [\text{cm}/\text{min}]$	$PE_{\text{cell}} [\mu\text{m}/\text{min}]$
Cell1	2.65	0.38	2.65	0.0006	6.32
Cell2	2.82	0.35	2.82	0.0007	6.71
Cell3	3.23	0.31	3.23	0.0008	7.70
<b>Average</b>	<b>2.90</b>	<b>0.35</b>	<b>2.88</b>	<b>0.0007</b>	<b>6.91</b>
SD					0.71

Table3.10 Determination of permeability coefficient of carboxyfluorescein for time interval 8-140 minutes membrane of insert with cells.

In the time interval 0-8 the average permeability slope values for carboxyfluorescein were:  $PS_{\text{control}} = 23.65 \mu\text{l}/\text{min}$ ,  $PS_{\text{all}} = 2.15 \mu\text{l}/\text{min}$  and  $PS_{\text{cell}} = 2.36 \mu\text{l}/\text{min}$ .  $PE_{\text{cell}}$  was  $5.65 \pm 1.78 \mu\text{m}/\text{min}$ .  $PE_{\text{all}}$  amounted to  $5.11 \pm 1.49 \mu\text{m}/\text{min}$ . EC reached to 110.04%. All values were calculated using equations from section 2.3.

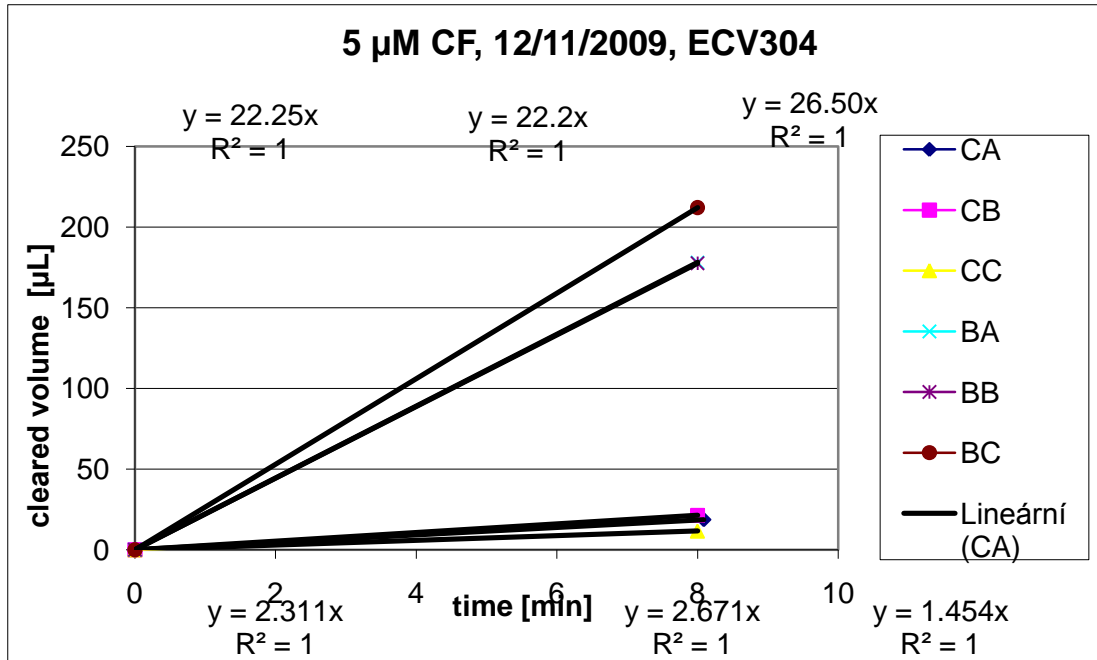


Figure 3.6 Dependence of cleared volume on the time interval 0-8 minutes for internal standard carboxyfluorescein.

	$PS_{\text{Control}}$	$PS_{\text{all}}$	$1/PS_{\text{cell}}$	$PS_{\text{cell}}$	$PE_{\text{cell}} [\text{cm}/\text{min}]$	$PE_{\text{cell}} [\mu\text{m}/\text{min}]$
Cell1	23.65	2.31	0.39	2.56	0.0006	6.10
Cell2	23.65	2.67	0.33	3.01	0.0007	7.17
Cell3	23.65	1.45	0.65	1.55	0.0004	3.69
<b>Average</b>	<b>23.65</b>	<b>2.15</b>	<b>0.42</b>	<b>2.36</b>	<b>0.0006</b>	<b>5.65</b>
SD						1.78

Table3.11 Determination of permeability coefficient of carboxyfluorescein for time interval 0-8 minutes for cell layer only.

	$PS_{\text{all}}$	$1/PS_{\text{cell}}$	$PS_{\text{cell}}$	$PE_{\text{cell}} [\text{cm}/\text{min}]$	$PE_{\text{cell}} [\mu\text{m}/\text{min}]$
Cell1	2.31	0.43	2.31	0.0006	5.50
Cell2	2.67	0.37	2.67	0.0006	6.36
Cell3	1.45	0.69	1.45	0.0003	3.46
<b>Average</b>	<b>2.15</b>	<b>0.50</b>	<b>2.01</b>	<b>0.0005</b>	<b>5.11</b>
SD					1.49

Table3.12 Determination of permeability coefficient of carboxyfluorescein for time interval 0-8 minutes for membrane of insert with cells.

### 3.2 Transport study of diltiazem – Single study

Transport study of diltiazem was accomplished across the BBB in vitro model based on cell line ECV304. Amounts of permeated substance were quantified by HPLC. In the time interval 5-140 the average permeability slope values for diltiazem were:  $PS_{\text{control}}= 8.93 \mu\text{l}/\text{min}$ ,  $PS_{\text{all}}= 3.61 \mu\text{l}/\text{min}$  and  $PS_{\text{cell}}= 6.06 \mu\text{l}/\text{min}$ . The average permeability coefficient ( $PE_{\text{cell}}$ ) for cell layer was  $14.46 \pm 1.43 \mu\text{m}/\text{min}$ .  $PE_{\text{all}}$  amounted to  $8.59 \pm 0.50 \mu\text{m}/\text{min}$ . EC reached to 168.02%. All values were calculated using equations from section 2.3.

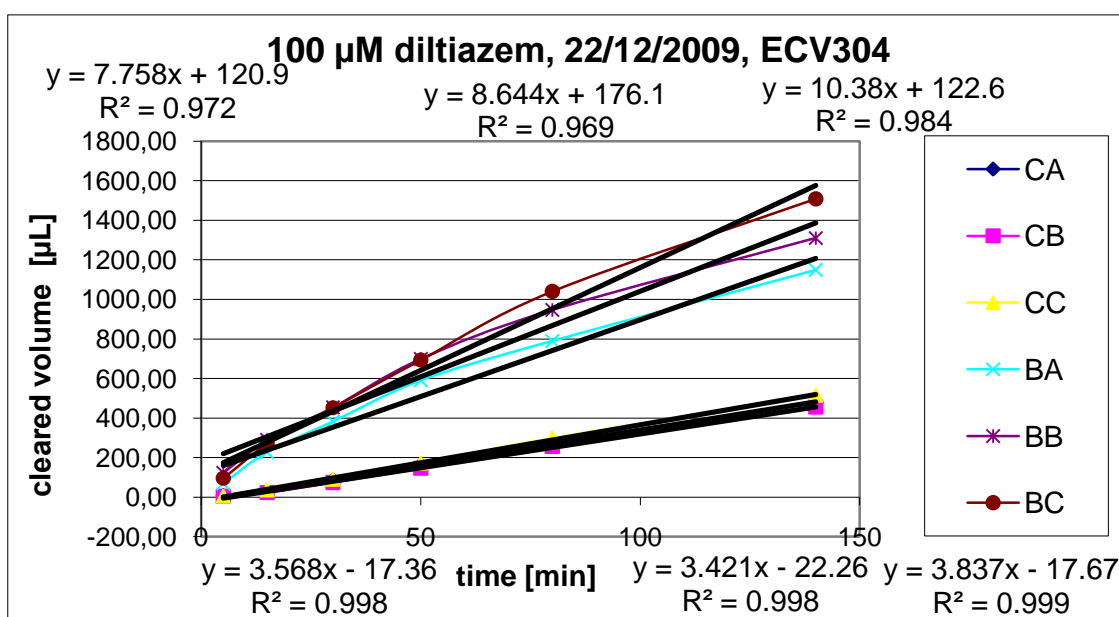


Figure 3.7 Dependence of cleared volume on the time interval 5-140 minutes for diltiazem.

	$PS_{\text{Control}}$	$PS_{\text{all}}$	$1/PS_{\text{cell}}$	$PS_{\text{cell}}$	$PE_{\text{cell}} [\text{cm}/\text{min}]$	$PE_{\text{cell}} [\mu\text{m}/\text{min}]$
Cell1	8.93	3.57	0.17	5.94	0.0014	14.15
Cell2	8.93	3.42	0.18	5.55	0.0013	13.20
Cell3	8.93	3.84	0.15	6.73	0.0016	16.02
<b>Average</b>	<b>8.93</b>	<b>3.61</b>	<b>0.17</b>	<b>6.06</b>	<b>0.0014</b>	<b>14.46</b>
SD						1.43

Table 3.13 Determination of permeability coefficient of diltiazem for time interval 5-140 minutes for cell layer only.

	$PS_{\text{all}}$	$1/PS_{\text{cell}}$	$PS_{\text{cell}}$	$PE_{\text{cell}} [\text{cm}/\text{min}]$	$PE_{\text{cell}} [\mu\text{m}/\text{min}]$
Cell1	3.57	0.28	3.57	0.0008	8.50
Cell2	3.42	0.29	3.42	0.0008	8.15
Cell3	3.84	0.26	3.84	0.0009	9.14
<b>Average</b>	<b>3.61</b>	<b>0.28</b>	<b>3.60</b>	<b>0.0009</b>	<b>8.59</b>
SD					0.50

Table 3.14 Determination of permeability coefficient of diltiazem for time interval 5-140 minutes for membrane of insert with cells.

In the time interval 0-5 average permeability slope values for diltiazem were:  $PS_{\text{control}} = 19.25 \mu\text{l}/\text{min}$ ,  $PS_{\text{all}} = 1.19 \mu\text{l}/\text{min}$  and  $PS_{\text{cell}} = 1.27 \mu\text{l}/\text{min}$ .  $PE_{\text{cell}}$  was  $3.02 \pm 0.62 \mu\text{m}/\text{min}$ .  $PE_{\text{all}}$  amounted to  $2.83 \pm 0.55 \mu\text{m}/\text{min}$ . EC reached to 106.59%. All values were calculated using equations from section 2.3.

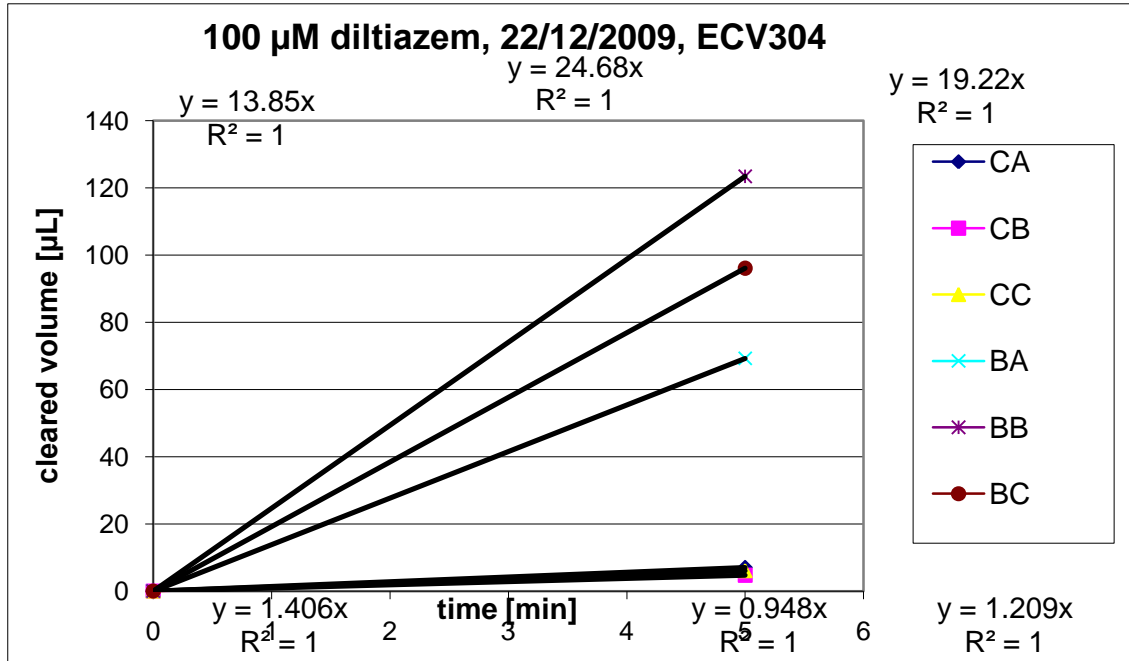


Figure 3.8 Dependence of cleared volume on the time interval 0-5 minutes for diltiazem.

	$PS_{\text{Control}}$	$PS_{\text{all}}$	$1/PS_{\text{cell}}$	$PS_{\text{cell}}$	$PE_{\text{cell}}$ [cm/min]	$PE_{\text{cell}}$ [µm/min]
Cell1	19.25	1.41	0.66	1.52	0.0004	3.61
Cell2	19.25	0.95	1.00	1.00	0.0002	2.37
Cell3	19.25	1.21	0.78	1.29	0.0003	3.07
<b>Average</b>	<b>19.25</b>	<b>1.19</b>	<b>0.79</b>	<b>1.27</b>	<b>0.0003</b>	<b>3.02</b>
SD						0.62

Table 3.15 Determination of permeability coefficient of diltiazem for time interval 0-5 minutes for cell layer only.

	$PS_{\text{all}}$	$1/PS_{\text{cell}}$	$PS_{\text{cell}}$	$PE_{\text{cell}}$ [cm/min]	$PE_{\text{cell}}$ [µm/min]
Cell1	1.41	0.71	1.41	0.0003	3.35
Cell2	0.95	1.05	0.95	0.0002	2.26
Cell3	1.21	0.83	1.21	0.0003	2.88
<b>Average</b>	<b>1.19</b>	<b>0.86</b>	<b>1.16</b>	<b>0.0003</b>	<b>2.83</b>
SD					0.55

Table 3.16 Determination of permeability coefficient of diltiazem for time interval 0-5 minutes for membrane of insert with cells.

## Internal standard diazepam in the transport study of diltiazem

The permeability of diazepam as a function of time was determined using the same principles as for diltiazem described above.

In the time interval 5-140 average permeability slope values for diazepam were:  $PS_{\text{control}} = 11.01 \mu\text{l}/\text{min}$ ,  $PS_{\text{all}} = 6.03 \mu\text{l}/\text{min}$  and  $PS_{\text{cell}} = 13.33 \mu\text{l}/\text{min}$ .  $PE_{\text{cell}}$  was  $31.80 \pm 2.49 \mu\text{m}/\text{min}$ .  $PE_{\text{all}}$  amounted to  $14.36 \pm 0.52 \mu\text{m}/\text{min}$ . EC reached to 221.28%. All values were calculated using equations from section 2.3.

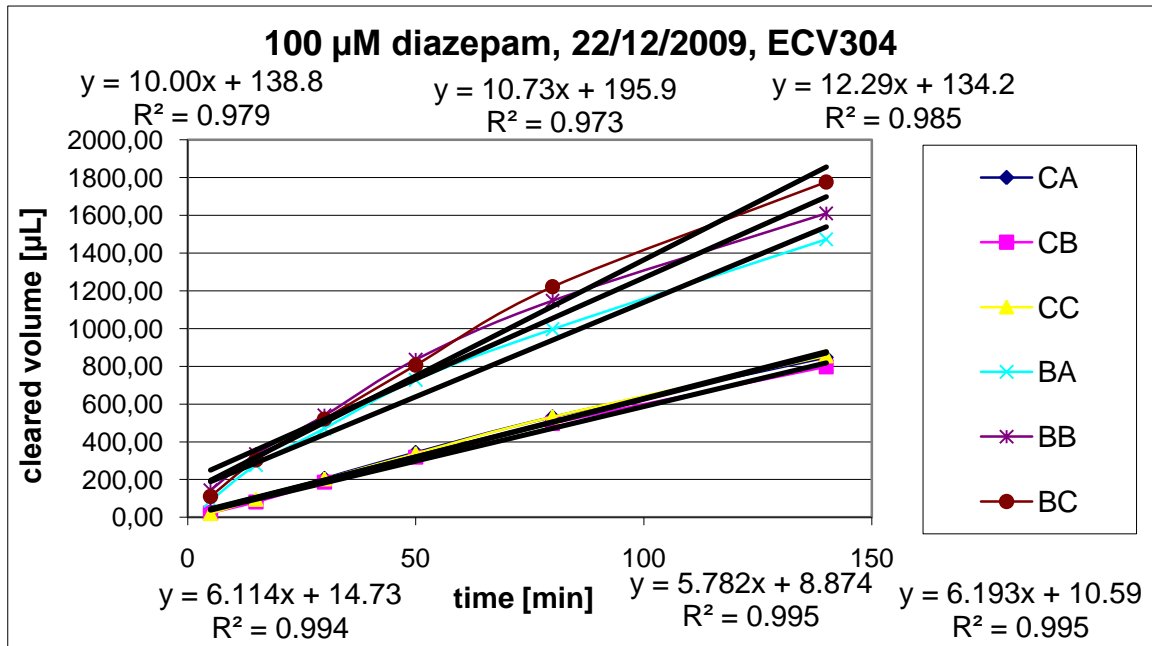


Figure 3.9 Dependence of cleared volume on the time interval 5-140 minutes for internal standard diazepam.

	$PS_{\text{Control}}$	$PS_{\text{all}}$	$1/PS_{\text{cell}}$	$PS_{\text{cell}}$	$PE_{\text{cell}} [\text{cm}/\text{min}]$	$PE_{\text{cell}} [\mu\text{m}/\text{min}]$
Cell1	11.01	6.11	0.07	13.74	0.0033	32.72
Cell2	11.01	5.78	0.08	12.17	0.0029	28.98
Cell3	11.01	6.19	0.07	14.15	0.0034	33.70
<b>Average</b>	<b>11.01</b>	<b>6.03</b>	<b>0.08</b>	<b>13.33</b>	<b>0.0032</b>	<b>31.80</b>
SD						2.49

Table 3.17 Determination of permeability coefficient of diazepam for time interval 5-140 minutes for cell layer only.

	$PS_{\text{all}}$	$1/PS_{\text{cell}}$	$PS_{\text{cell}}$	$PE_{\text{cell}} [\text{cm}/\text{min}]$	$PE_{\text{cell}} [\mu\text{m}/\text{min}]$
Cell1	6.11	0.16	6.11	0.0015	14.56
Cell2	5.78	0.17	5.78	0.0014	13.77
Cell3	6.19	0.16	6.19	0.0015	14.75
<b>Average</b>	<b>6.03</b>	<b>0.17</b>	<b>6.02</b>	<b>0.0014</b>	<b>14.36</b>
SD					0.52

Table 3.18 Determination of permeability coefficient of diazepam for time interval 5-140 minutes for membrane of insert with cells.

In the time interval 0-5 average permeability slope values for diazepam were:  $PS_{\text{control}} = 22.84 \mu\text{l}/\text{min}$ ,  $PS_{\text{all}} = 4.89 \mu\text{l}/\text{min}$  and  $PS_{\text{cell}} = 6.21 \mu\text{l}/\text{min}$ .  $PE_{\text{cell}}$  was  $14.97 \pm 4.33 \mu\text{m}/\text{min}$ .  $PE_{\text{all}}$  amounted to  $11.63 \pm 2.60 \mu\text{m}/\text{min}$ . EC reached to 127.54%. All values were calculated using equations from section 2.3.

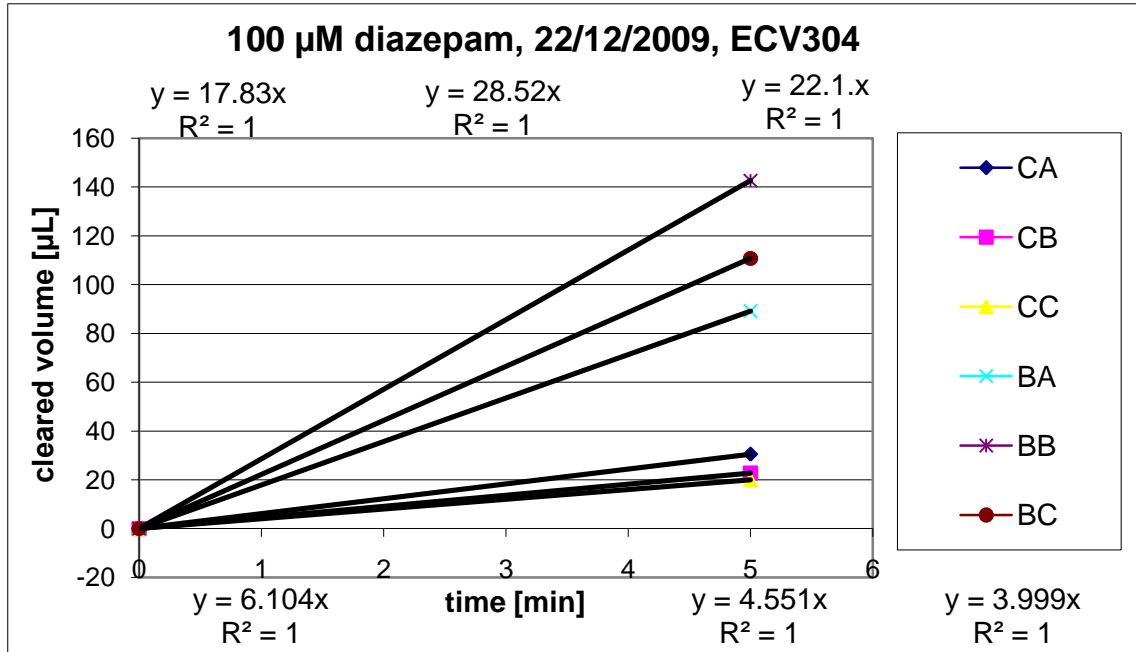


Figure 3.10 Dependence of cleared volume on the time interval 0-5 minutes for internal standard diazepam.

	$PS_{\text{Control}}$	$PS_{\text{all}}$	$1/PS_{\text{cell}}$	$PS_{\text{cell}}$	$PE_{\text{cell}} [\text{cm}/\text{min}]$	$PE_{\text{cell}} [\mu\text{m}/\text{min}]$
Cell1	22.84	6.10	0.12	8.33	0.0020	19.84
Cell2	22.84	4.55	0.18	5.68	0.0014	13.53
Cell3	22.84	4.00	0.21	4.85	0.0012	11.55
<b>Average</b>	<b>22.84</b>	<b>4.89</b>	<b>0.16</b>	<b>6.21</b>	<b>0.0015</b>	<b>14.97</b>
SD						4.33

Table 3.19 Determination of permeability coefficient of diazepam for time interval 0-5 minutes for cell layer only.

	$PS_{\text{all}}$	$1/PS_{\text{cell}}$	$PS_{\text{cell}}$	$PE_{\text{cell}} [\text{cm}/\text{min}]$	$PE_{\text{cell}} [\mu\text{m}/\text{min}]$
Cell1	6.10	0.16	6.10	0.0015	14.53
Cell2	4.55	0.22	4.55	0.0011	10.84
Cell3	4.00	0.25	4.00	0.0010	9.52
<b>Average</b>	<b>4.89</b>	<b>0.21</b>	<b>4.74</b>	<b>0.0011</b>	<b>11.63</b>
SD					2.60

Table 3.20 Determination of permeability coefficient of diazepam for time interval 0-5 minutes for membrane of insert with cells.

### *Internal standard carboxyfluorescein in the transport study of diltiazem*

The permeability of carboxyfluorescein as a function of time was determined using the same principles as for diltiazem described above.

Time interval 5-140:  $PS_{\text{control}} = 1.97 \mu\text{l}/\text{min}$ ,  $PS_{\text{all}} = 2.77 \mu\text{l}/\text{min}$  and  $PS_{\text{cell}} = 3.61 \mu\text{l}/\text{min}$ .  $PE_{\text{cell}} = 8.65 \pm 1.99 \mu\text{m}/\text{min}$ .  $PE_{\text{all}} = 6.60 \pm 1.16 \mu\text{m}/\text{min}$ .  $EC = 130.36\%$ . All values were calculated using equations from section 2.3.

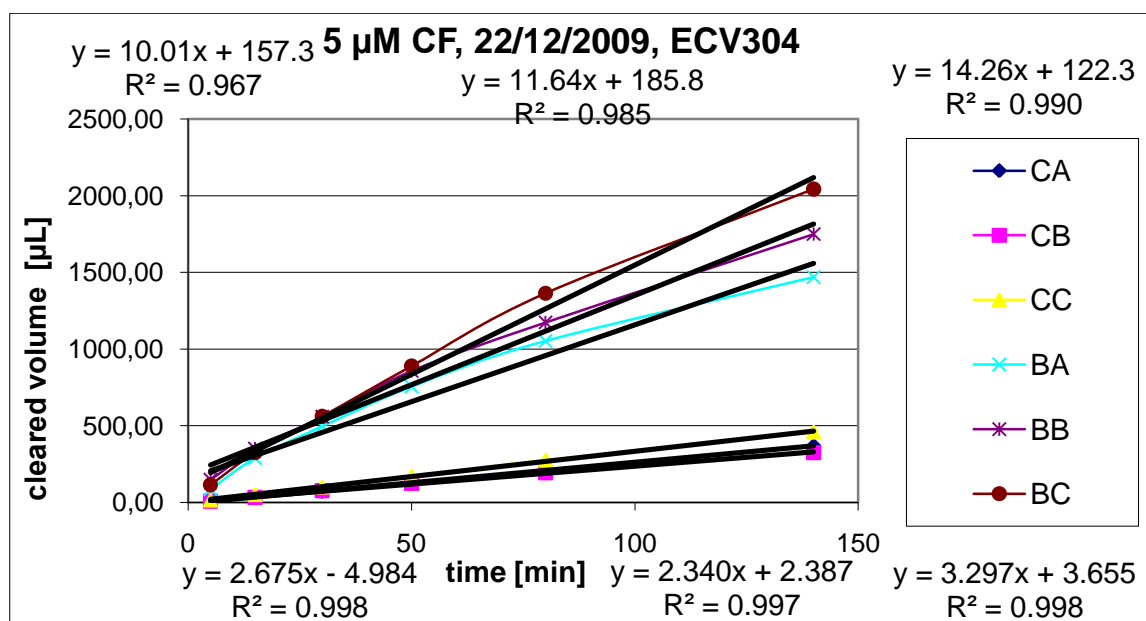


Figure 3.11 Dependence of cleared volume on the time interval 5-140 minutes for internal standard carboxyfluorescein.

	$PS_{\text{Control}}$	$PS_{\text{all}}$	$1/PS_{\text{cell}}$	$PS_{\text{cell}}$	$PE_{\text{cell}} [\text{cm}/\text{min}]$	$PE_{\text{cell}} [\mu\text{m}/\text{min}]$
Cell1	11.97	2.68	0.29	3.45	0.0008	8.20
Cell2	11.97	2.34	0.34	2.91	0.0007	6.93
Cell3	11.97	3.30	0.22	4.55	0.0011	10.83
<b>Average</b>	<b>11.97</b>	<b>2.77</b>	<b>0.28</b>	<b>3.61</b>	<b>0.0009</b>	<b>8.65</b>
SD						1.99

Table 3.21 Determination of permeability coefficient of carboxyfluorescein for time interval 5-140 minutes for cell layer only.

	$PS_{\text{all}}$	$1/PS_{\text{cell}}$	$PS_{\text{cell}}$	$PE_{\text{cell}} [\text{cm}/\text{min}]$	$PE_{\text{cell}} [\mu\text{m}/\text{min}]$
Cell1	2.68	0.37	2.68	0.0006	6.37
Cell2	2.34	0.43	2.34	0.0006	5.57
Cell3	3.30	0.30	3.30	0.0008	7.85
<b>Average</b>	<b>2.77</b>	<b>0.37</b>	<b>2.72</b>	<b>0.0006</b>	<b>6.60</b>
SD					1.16

Table 3.22 Determination of permeability coefficient of carboxyfluorescein for time interval 5-140 minutes for membrane of insert with cells.

In the time interval 0-5 average permeability slope values for carboxyfluorescein were:  $PS_{\text{control}} = 23.37 \mu\text{l}/\text{min}$ ,  $PS_{\text{all}} = 2.66 \mu\text{l}/\text{min}$  and  $PS_{\text{cell}} = 3.00 \mu\text{l}/\text{min}$ .  $PE_{\text{cell}}$  was  $7.22 \pm 2.65 \mu\text{m}/\text{min}$ .  $PE_{\text{all}}$  amounted to  $6.33 \pm 2.13 \mu\text{m}/\text{min}$ . EC reached to 112.96%. All values were calculated using equations from section 2.3.

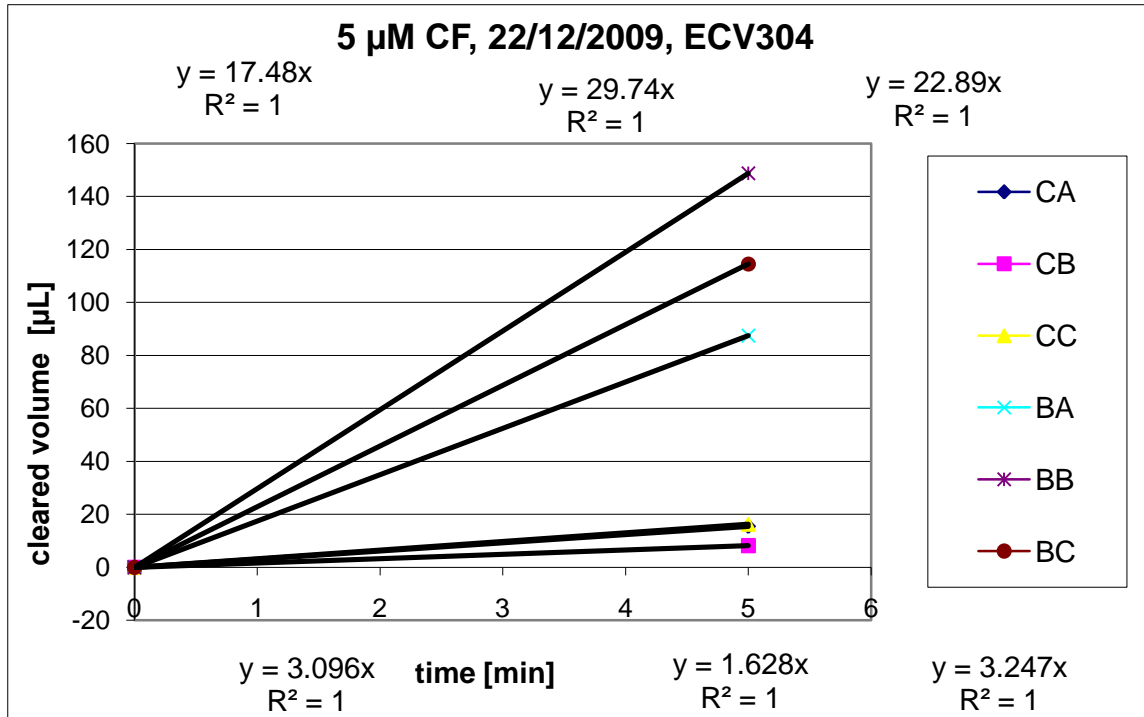


Figure 3.12 Dependence of cleared volume on the time interval 0-5 minutes for internal standard carboxyfluorescein.

	$PS_{\text{Control}}$	$PS_{\text{all}}$	$1/PS_{\text{cell}}$	$PS_{\text{cell}}$	$PE_{\text{cell}} [\text{cm}/\text{min}]$	$PE_{\text{cell}} [\mu\text{m}/\text{min}]$
Cell1	23.37	3.10	0.28	3.57	0.0008	8.50
Cell2	23.37	1.63	0.57	1.75	0.0004	4.17
Cell3	23.37	3.25	0.27	3.77	0.0009	8.98
<b>Average</b>	<b>23.37</b>	<b>2.66</b>	<b>0.33</b>	<b>3.00</b>	<b>0.0007</b>	<b>7.22</b>
SD						2.65

Table 3.23 Determination of permeability coefficient of carboxyfluorescein for time interval 0-5 minutes for cell layer only.

	$PS_{\text{all}}$	$1/PS_{\text{cell}}$	$PS_{\text{cell}}$	$PE_{\text{cell}} [\text{cm}/\text{min}]$	$PE_{\text{cell}} [\mu\text{m}/\text{min}]$
Cell1	3.10	0.32	3.10	0.0007	7.37
Cell2	1.63	0.61	1.63	0.0004	3.88
Cell3	3.25	0.31	3.25	0.0008	7.73
<b>Average</b>	<b>2.66</b>	<b>0.41</b>	<b>2.41</b>	<b>0.0006</b>	<b>6.33</b>
SD					2.13

Table 3.24 Determination of permeability coefficient of carboxyfluorescein for time interval 0-5 minutes for membrane of insert with cells.

### 3.3 Transport study of nifedipine – Single study

Transport study of nifedipine was accomplished across the BBB in vitro model based on cell line ECV304. Amounts of permeated substance were quantified by HPLC. In the time interval 5-140 average permeability slope values for nifedipine were:  $PS_{\text{control}} = 46.05 \mu\text{l}/\text{min}$ ,  $PS_{\text{all}} = 11.76 \mu\text{l}/\text{min}$  and  $PS_{\text{cell}} = 5.79 \mu\text{l}/\text{min}$ . The  $PE_{\text{cell}}$  was  $37.60 \pm 1.52 \mu\text{m}/\text{min}$ .  $PE_{\text{all}}$  amounted to  $27.99 \pm 0.84 \mu\text{m}/\text{min}$ . EC reached to 134.30%. All values were calculated using equations from section 2.3. In this transport study we had problems with analysis, because molecule of nifedipine is unstable and therefore we found lots of peaks. First only peaks of nifedipine and then all peaks of disintegrated nifedipine were integrated and permeability coefficients were calculated. When we compared both permeability coefficients, they were quit similar and therefore we decided to choose only peaks of nifedipine for further calculation.

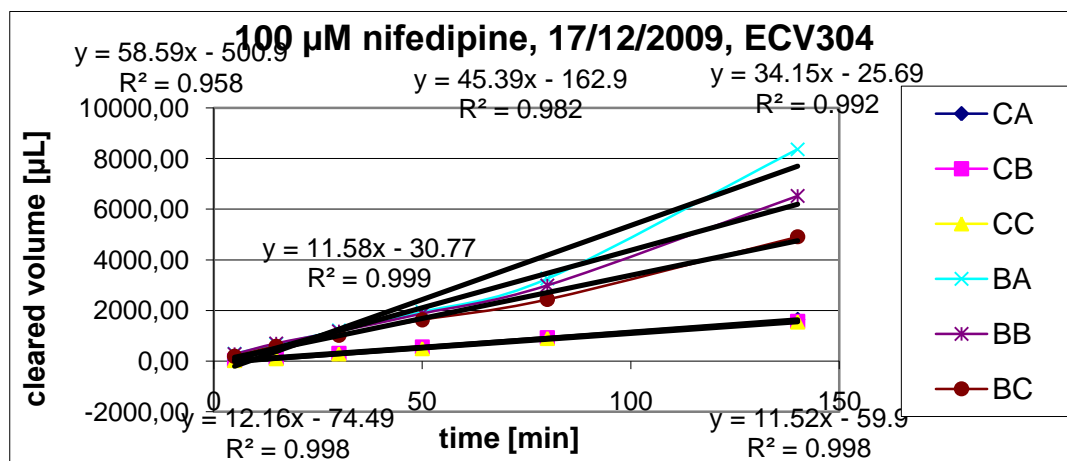


Figure 3.13 Dependence of cleared volume on the time interval 5-140 minutes for nifedipine.

	$PS_{\text{Control}}$	$PS_{\text{all}}$	$1/PS_{\text{cell}}$	$PS_{\text{cell}}$	$PE_{\text{cell}} [\text{cm}/\text{min}]$	$PE_{\text{cell}} [\mu\text{m}/\text{min}]$
Cell1	46.05	12.16	0.06	16.53	0.0039	39.35
Cell2	46.05	11.58	0.06	15.48	0.0037	36.85
Cell3	46.05	11.53	0.07	15.37	0.0037	36.61
<b>Average</b>	<b>46.05</b>	<b>11.76</b>	<b>0.06</b>	<b>15.79</b>	<b>0.0038</b>	<b>37.60</b>
SD						1.52

Table 3.25 Determination of permeability coefficient of nifedipine for time interval 5-140 minutes for cell layer only.

	$PS_{\text{all}}$	$1/PS_{\text{cell}}$	$PS_{\text{cell}}$	$PE_{\text{cell}} [\text{cm}/\text{min}]$	$PE_{\text{cell}} [\mu\text{m}/\text{min}]$
Cell1	12.16	0.08	12.16	0.0029	28.95
Cell2	11.58	0.09	11.58	0.0028	27.58
Cell3	11.53	0.09	11.53	0.0027	27.44
<b>Average</b>	<b>11.76</b>	<b>0.09</b>	<b>11.75</b>	<b>0.0028</b>	<b>27.99</b>
SD					0.84

Table 3.26 Determination of permeability coefficient of Nifedipine for time interval 5-140 minutes for membrane of insert with cells.

In the time interval 0-5 average permeability slope values for nifedipine were:  $PS_{\text{control}} = 50.54 \mu\text{l}/\text{min}$ ,  $PS_{\text{all}} = 5.09 \mu\text{l}/\text{min}$  and  $PS_{\text{cell}} = 5.67 \mu\text{l}/\text{min}$ .  $PE_{\text{cell}}$  was  $13.53 \pm 2.81 \mu\text{m}/\text{min}$ .  $PE_{\text{all}}$  amounted to  $12.13 \pm 2.29 \mu\text{m}/\text{min}$ . EC reached to 111.24%. All values were calculated using equations from section 2.3.

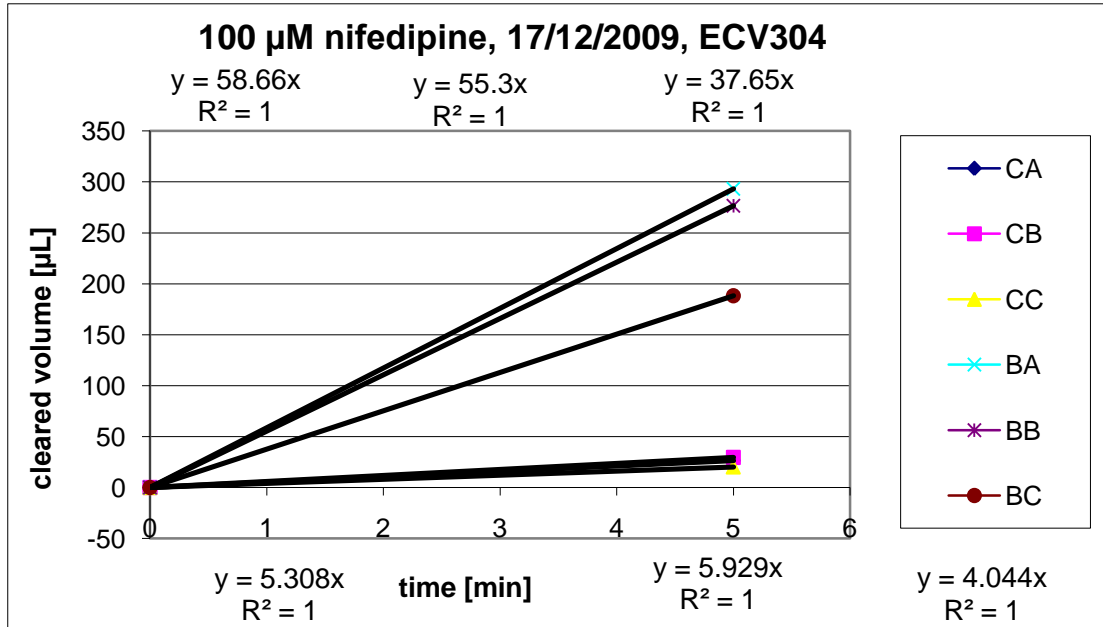


Figure 3.14 Dependence of cleared volume on the time interval 0-5 minutes for nifedipine.

	$PS_{\text{Control}}$	$PS_{\text{all}}$	$1/PS_{\text{cell}}$	$PS_{\text{cell}}$	$PE_{\text{cell}} [\text{cm}/\text{min}]$	$PE_{\text{cell}} [\mu\text{m}/\text{min}]$
Cell1	50.54	5.31	0.17	5.93	0.0014	14.12
Cell2	50.54	5.93	0.15	6.72	0.0016	16.00
Cell3	50.54	4.04	0.23	4.40	0.0010	10.47
<b>Average</b>	<b>50.54</b>	<b>5.09</b>	<b>0.18</b>	<b>5.67</b>	<b>0.0013</b>	<b>13.53</b>
SD						2.81

Table 3.27 Determination of permeability coefficient of nifedipine for time interval 0-5 minutes for cell layer only.

	$PS_{\text{all}}$	$1/PS_{\text{cell}}$	$PS_{\text{cell}}$	$PE_{\text{cell}} [\text{cm}/\text{min}]$	$PE_{\text{cell}} [\mu\text{m}/\text{min}]$
Cell1	5.31	0.19	5.31	0.0013	12.64
Cell2	5.93	0.17	5.93	0.0014	14.12
Cell3	4.04	0.25	4.04	0.0010	9.63
<b>Average</b>	<b>5.09</b>	<b>0.20</b>	<b>4.96</b>	<b>0.0012</b>	<b>12.13</b>
SD					2.29

Table 3.28 Determination of permeability coefficient of nifedipine for time interval 0-5 minutes for membrane of insert with cells.

## Internal standard diazepam in the transport study of nifedipine

The permeability of diazepam as a function of time was determined using the same principles as for nifedipine described above.

In the time interval 5-140 average permeability slope values for diazepam were:  $PS_{\text{control}} = 9.36 \mu\text{l}/\text{min}$ ,  $PS_{\text{all}} = 5.18 \mu\text{l}/\text{min}$  and  $PS_{\text{cell}} = 11.63 \mu\text{l}/\text{min}$ .  $PE_{\text{cell}}$  was  $27.75 \pm 2.04 \mu\text{m}/\text{min}$ .  $PE_{\text{all}}$  amounted to  $12.34 \pm 0.40 \mu\text{m}/\text{min}$ . EC reached to 224.56%. All values were calculated using equations from section 2.3.

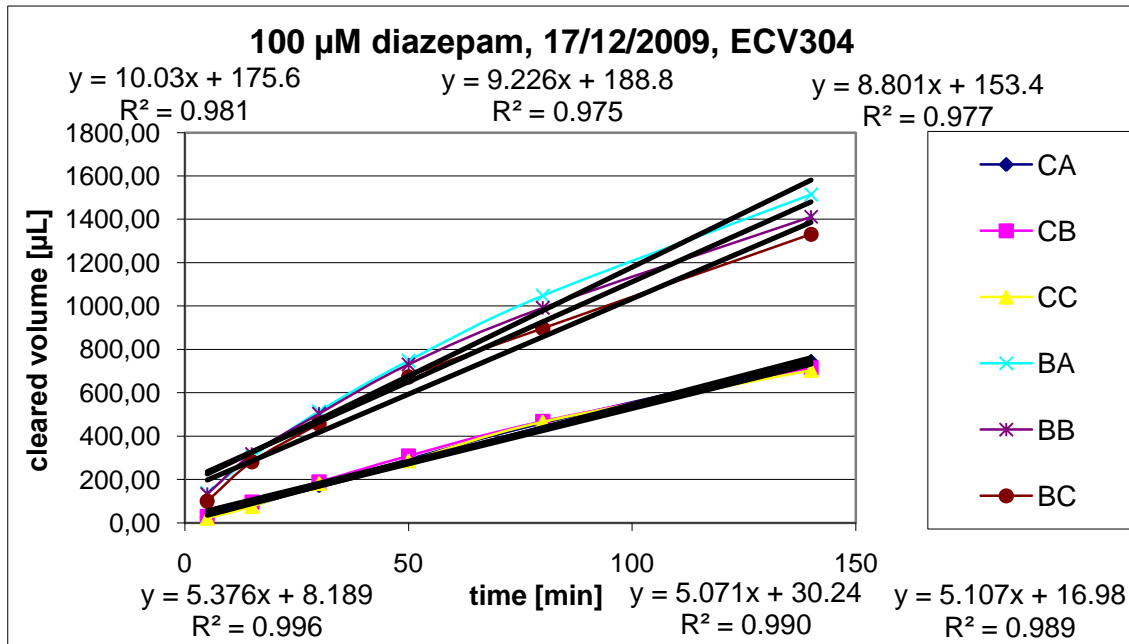


Figure 3.15 Dependence of cleared volume on the time interval 5-140 minutes for internal standard diazepam.

	$PS_{\text{Control}}$	$PS_{\text{all}}$	$1/PS_{\text{cell}}$	$PS_{\text{cell}}$	$PE_{\text{cell}}$ [cm/min]	$PE_{\text{cell}}$ [ $\mu\text{m}/\text{min}$ ]
Cell1	9.36	5.38	0.08	12.64	0.0030	30.09
Cell2	9.36	5.07	0.09	11.07	0.0026	26.37
Cell3	9.36	5.11	0.09	11.25	0.0027	26.78
<b>Average</b>	<b>9.36</b>	<b>5.18</b>	<b>0.09</b>	<b>11.63</b>	<b>0.0028</b>	<b>27.75</b>
SD						2.04

Table 3.29 Determination of permeability coefficient of diazepam for time interval 5-140 minutes for cell layer only.

	$PS_{\text{all}}$	$1/PS_{\text{cell}}$	$PS_{\text{cell}}$	$PE_{\text{cell}}$ [cm/min]	$PE_{\text{cell}}$ [ $\mu\text{m}/\text{min}$ ]
Cell1	5.38	0.19	5.38	0.0013	12.80
Cell2	5.07	0.20	5.07	0.0012	12.07
Cell3	5.11	0.20	5.11	0.0012	12.16
<b>Average</b>	<b>5.18</b>	<b>0.19</b>	<b>5.18</b>	<b>0.0012</b>	<b>12.34</b>
SD					0.40

Table 3.30 Determination of permeability coefficient of diazepam for time interval 5-140 minutes for membrane of insert with cells.

In the time interval 0-5 average permeability slope values for diazepam were:  $PS_{\text{control}} = 24.64 \mu\text{l}/\text{min}$ ,  $PS_{\text{all}} = 4.96 \mu\text{l}/\text{min}$  and  $PS_{\text{cell}} = 6.20 \mu\text{l}/\text{min}$ .  $PE_{\text{cell}}$  was  $14.85 \pm 2.98 \mu\text{m}/\text{min}$ .  $PE_{\text{all}}$  amounted to  $11.80 \pm 1.86 \mu\text{m}/\text{min}$ . EC reached to 125.31%. All values were calculated using equations from section 2.3.

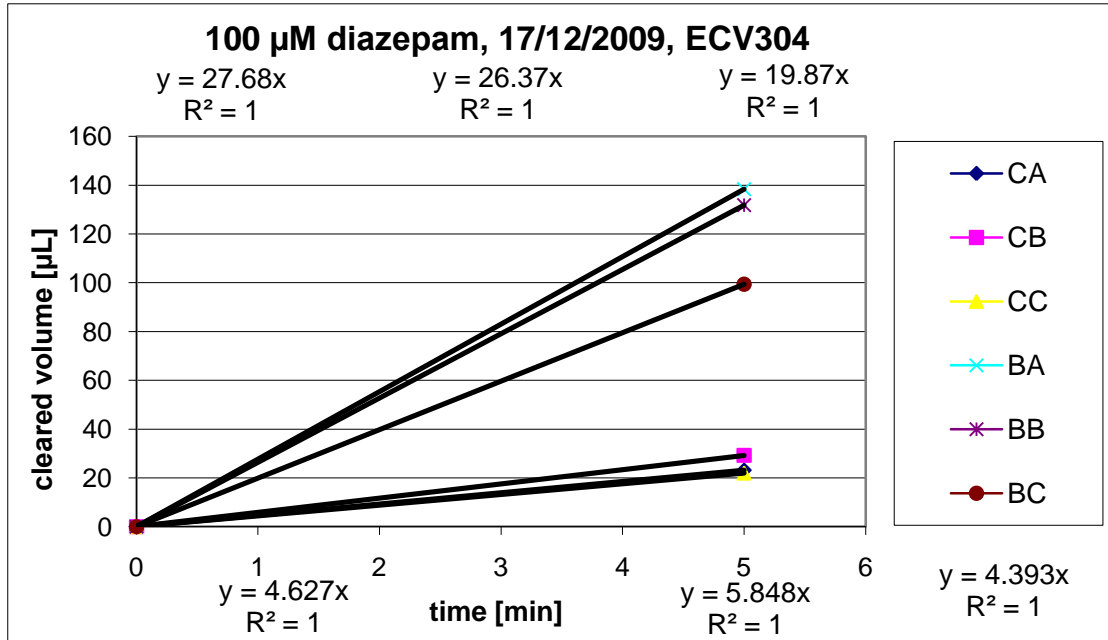


Figure 3.16 Dependence of cleared volume on the time interval 0-5 minutes for internal standard diazepam.

	$PS_{\text{Control}}$	$PS_{\text{all}}$	$1/PS_{\text{cell}}$	$PS_{\text{cell}}$	$PE_{\text{cell}} [\text{cm}/\text{min}]$	$PE_{\text{cell}} [\mu\text{m}/\text{min}]$
Cell1	24.64	4.63	0.18	5.70	0.0014	13.57
Cell2	24.64	5.85	0.13	7.67	0.0018	18.26
Cell3	24.64	4.39	0.19	5.35	0.0013	12.73
<b>Average</b>	<b>24.64</b>	<b>4.96</b>	<b>0.16</b>	<b>6.20</b>	<b>0.0015</b>	<b>14.85</b>
SD						2.98

Table 3.31 Determination of permeability coefficient of diazepam for time interval 0-5 minutes for cell layer only.

	$PS_{\text{all}}$	$1/PS_{\text{cell}}$	$PS_{\text{cell}}$	$PE_{\text{cell}} [\text{cm}/\text{min}]$	$PE_{\text{cell}} [\mu\text{m}/\text{min}]$
Cell1	4.63	0.22	4.63	0.0011	11.02
Cell2	5.85	0.17	5.85	0.0014	13.92
Cell3	4.39	0.23	4.39	0.0010	10.46
<b>Average</b>	<b>4.96</b>	<b>0.20</b>	<b>4.88</b>	<b>0.0012</b>	<b>11.80</b>
SD					1.86

Table 3.32 Determination of permeability coefficient of diazepam for time interval 0-5 minutes for membrane of insert with cells.

## Internal standard carboxyfluorescein in the transport study of nifedipine

The permeability of carboxyfluorescein as a function of time was determined using the same principles as for nifedipine described above.

In the time interval 5-140 average permeability slope values for carboxyfluorescein were:  $PS_{\text{control}} = 9.98 \mu\text{l}/\text{min}$ ,  $PS_{\text{all}} = 2.37 \mu\text{l}/\text{min}$  and  $PS_{\text{cell}} = 3.10 \mu\text{l}/\text{min}$ .  $PE_{\text{cell}}$  was  $7.38 \pm 0.16 \mu\text{m}/\text{min}$ .  $PE_{\text{all}}$  amounted to  $5.63 \pm 0.11 \mu\text{m}/\text{min}$ . EC reached to 131.04%. All values were calculated using equations from section 2.3.

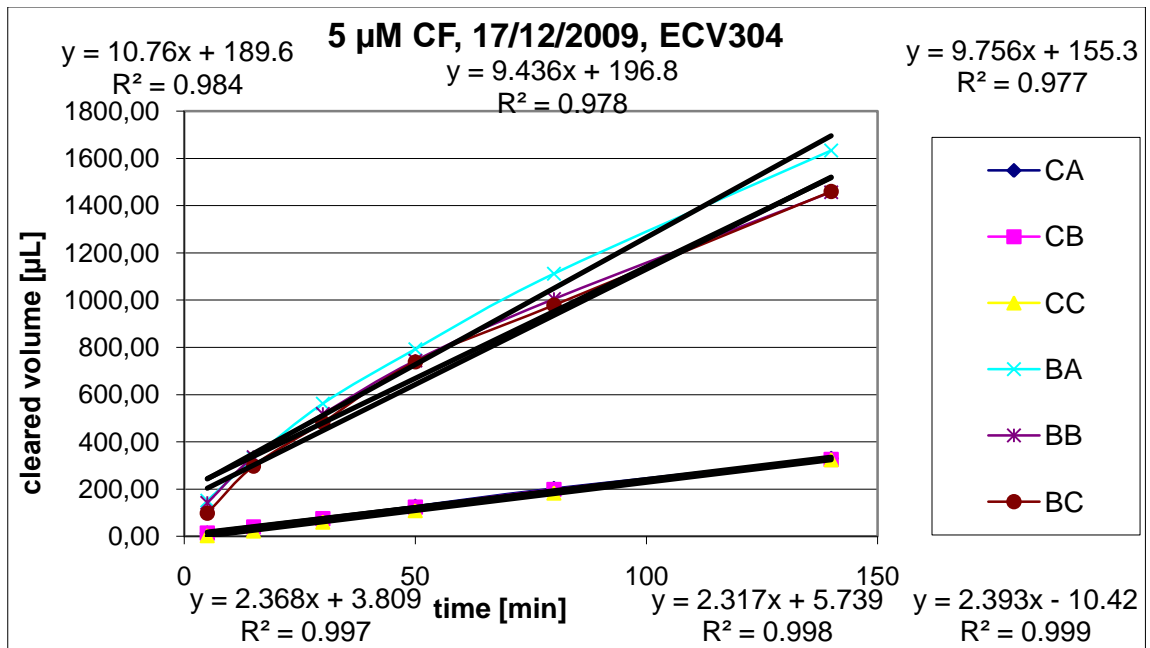


Figure 3.17 Dependence of cleared volume on the time interval 5-140 minutes for internal standard carboxyfluorescein.

	$PS_{\text{Control}}$	$PS_{\text{all}}$	$1/PS_{\text{cell}}$	$PS_{\text{cell}}$	$PE_{\text{cell}}$ [cm/min]	$PE_{\text{cell}}$ [ $\mu\text{m}/\text{min}$ ]
Cell1	9.98	2.37	0.32	3.11	0.0007	7.39
Cell2	9.98	2.32	0.33	3.02	0.0007	7.19
Cell3	9.98	2.41	0.31	3.18	0.0008	7.56
<b>Average</b>	<b>9.98</b>	<b>2.37</b>	<b>0.32</b>	<b>3.10</b>	<b>0.0007</b>	<b>7.38</b>
SD						0.16

Table 3.33 Determination of permeability coefficient of carboxyfluorescein for time interval 5-140 minutes for cell layer only.

	$PS_{\text{all}}$	$1/PS_{\text{cell}}$	$PS_{\text{cell}}$	$PE_{\text{cell}}$ [cm/min]	$PE_{\text{cell}}$ [ $\mu\text{m}/\text{min}$ ]
Cell1	2.37	0.42	2.37	0.0006	5.64
Cell2	2.32	0.43	2.32	0.0006	5.52
Cell3	2.41	0.42	2.41	0.0006	5.74
<b>Average</b>	<b>2.37</b>	<b>0.42</b>	<b>2.36</b>	<b>0.0006</b>	<b>5.63</b>
SD					0.11

Table 3.34 Determination of permeability coefficient of carboxyfluorescein for time interval 5-140 minutes for membrane of insert with cells.

In the time interval 0-5 average permeability slope values for carboxyfluorescein were:  $PS_{\text{control}} = 26.05 \mu\text{l}/\text{min}$ ,  $PS_{\text{all}} = 2.89 \mu\text{l}/\text{min}$  and  $PS_{\text{cell}} = 3.24 \mu\text{l}/\text{min}$ .  $PE_{\text{cell}}$  was  $7.73 \pm 0.59 \mu\text{m}/\text{min}$ .  $PE_{\text{all}}$  amounted to  $6.87 \pm 0.47 \mu\text{m}/\text{min}$ . EC reached to 112.46%. All values were calculated using equations from section 2.3.

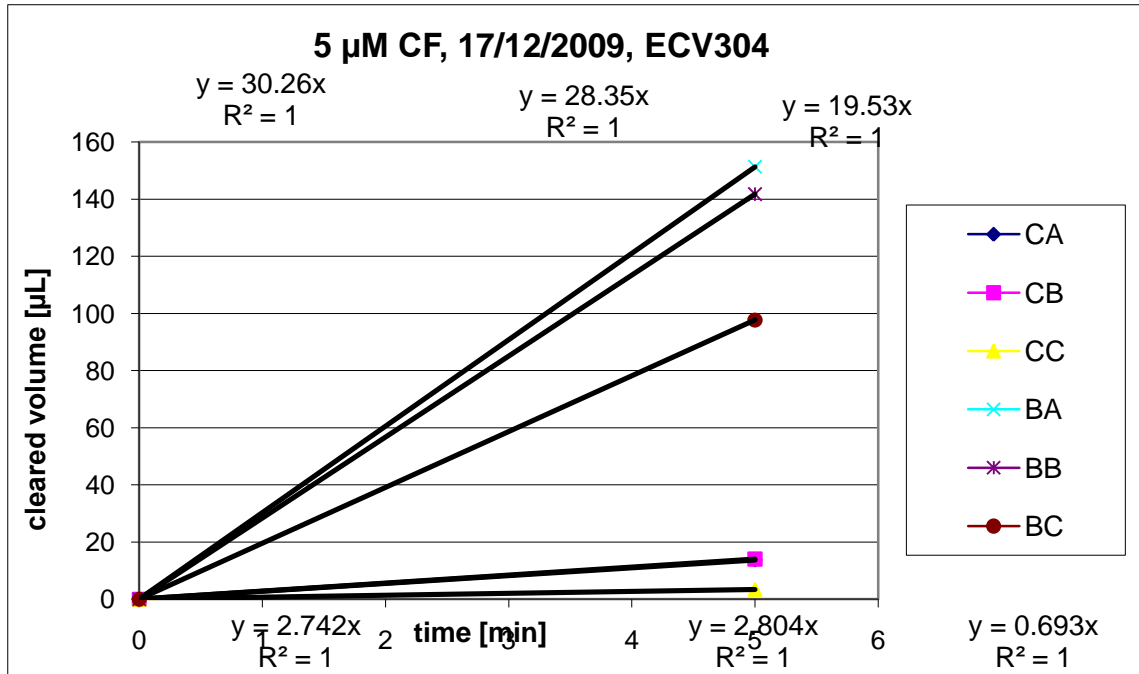


Figure 3.18 Dependence of clearance on the time interval 0-5 minutes for internal standard carboxyfluorescein.

	$PS_{\text{Control}}$	$PS_{\text{all}}$	$1/PS_{\text{cell}}$	$PS_{\text{cell}}$	$PE_{\text{cell}} [\text{cm}/\text{min}]$	$PE_{\text{cell}} [\mu\text{m}/\text{min}]$
Cell1	26.05	2.74	0.33	3.07	0.0007	7.30
Cell2	26.05	2.80	0.32	3.14	0.0007	7.48
Cell3	26.05	3.11	0.28	3.53	0.0008	8.41
<b>Average</b>	<b>26.05</b>	<b>2.89</b>	<b>0.31</b>	<b>3.24</b>	<b>0.0008</b>	<b>7.73</b>
SD						0.59

Table 3.35 Determination of permeability coefficient of carboxyfluorescein for time interval 0-5 minutes for cell layer only.

	$PS_{\text{all}}$	$1/PS_{\text{cell}}$	$PS_{\text{cell}}$	$PE_{\text{cell}} [\text{cm}/\text{min}]$	$PE_{\text{cell}} [\mu\text{m}/\text{min}]$
Cell1	2.74	0.36	2.74	0.0007	6.53
Cell2	2.80	0.36	2.80	0.0007	6.68
Cell3	3.11	0.32	3.11	0.0007	7.40
<b>Average</b>	<b>2.89</b>	<b>0.35</b>	<b>2.88</b>	<b>0.0007</b>	<b>6.87</b>
SD					0.47

Table 3.36 Determination of permeability coefficient of carboxyfluorescein for time interval 0-5 minutes for membrane of insert with cells.

### 3.4 Transport study of phenobarbital – Single study

Transport study of phenobarbital was accomplished across the BBB *in vitro* model based on cell line ECV304. Amounts of permeated substance were quantified by HPLC. In the time interval 5-140 average permeability slope values for phenobarbital were:  $PS_{control} = 11.34 \mu\text{l}/\text{min}$ ,  $PS_{all} = 4.74 \mu\text{l}/\text{min}$  and  $PS_{cell} = 8.13 \mu\text{l}/\text{min}$ . The average permeability coefficient ( $PE_{cell}$ ) for cell layer was  $19.38 \pm 0.98 \mu\text{m}/\text{min}$ .  $PE_{all}$  amounted to  $11.28 \pm 0.34 \mu\text{m}/\text{min}$ . EC reached to 171.76%. All values were calculated using equations from section 2.3.

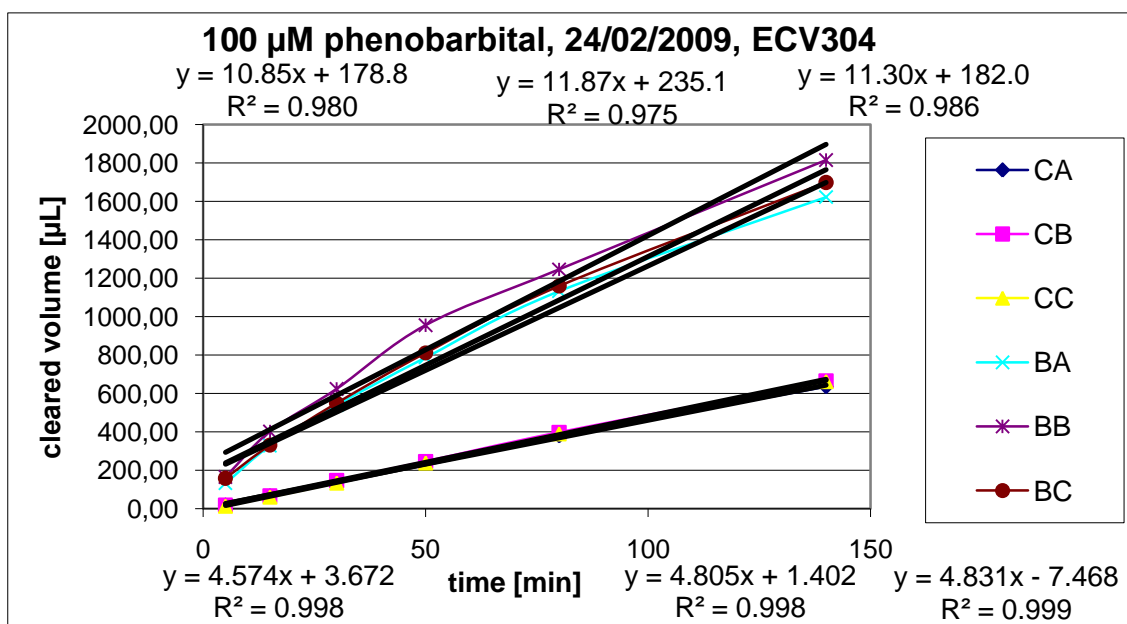


Figure 3.19 Dependence of cleared volume on the time interval 5-140 minutes for phenobarbital.

	$PS_{control}$	$PS_{all}$	$1/PS_{cell}$	$PS_{cell}$	$PE_{cell}$ [cm/min]	$PE_{cell}$ [ $\mu\text{m}/\text{min}$ ]
Cell1	11.34	4.57	0.13	7.67	0.0018	18.25
Cell2	11.34	4.81	0.12	8.34	0.0020	19.85
Cell3	11.34	4.83	0.12	8.42	0.0020	20.04
<b>Average</b>	<b>11.34</b>	<b>4.74</b>	<b>0.12</b>	<b>8.13</b>	<b>0.0019</b>	<b>19.38</b>
SD						0.98

Table 3.37 Determination of permeability coefficient of phenobarbital for time interval 5-140 minutes for cell layer only.

	$PS_{all}$	$1/PS_{cell}$	$PS_{cell}$	$PE_{cell}$ [cm/min]	$PE_{cell}$ [ $\mu\text{m}/\text{min}$ ]
Cell1	4.57	0.22	4.57	0.0011	10.89
Cell2	4.81	0.21	4.81	0.0011	11.44
Cell3	4.83	0.21	4.83	0.0012	11.50
<b>Average</b>	<b>4.74</b>	<b>0.21</b>	<b>4.73</b>	<b>0.0011</b>	<b>11.28</b>
SD					0.34

Table 3.38 Determination of permeability coefficient of phenobarbital for time interval 5-140 minutes for membrane of insert with cells.

In the time interval 0-5 average permeability slope values for phenobarbital were:  $PS_{\text{control}} = 30.44 \mu\text{l}/\text{min}$ ,  $PS_{\text{all}} = 3.56 \mu\text{l}/\text{min}$  and  $PS_{\text{cell}} = 4.03 \mu\text{l}/\text{min}$ .  $PE_{\text{cell}}$  was  $9.62 \pm 1.84 \mu\text{m}/\text{min}$ .  $PE_{\text{all}}$  amounted to  $8.47 \pm 1.45 \mu\text{m}/\text{min}$ . EC reached to 113.27%. All values were calculated using equations from section 2.3.

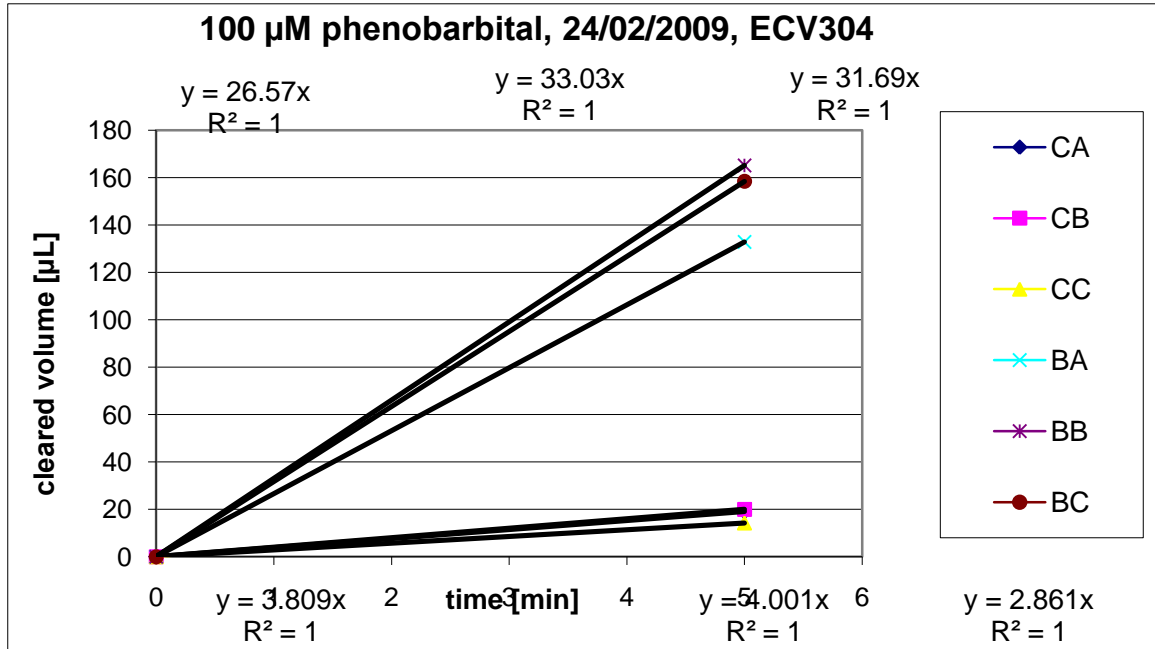


Figure 3.20 Dependence of cleared volume on the time interval 0-5 minutes for phenobarbital.

	$PS_{\text{Control}}$	$PS_{\text{all}}$	$1/PS_{\text{cell}}$	$PS_{\text{cell}}$	$PE_{\text{cell}} [\text{cm}/\text{min}]$	$PE_{\text{cell}} [\mu\text{m}/\text{min}]$
Cell1	30.44	3.81	0.23	4.35	0.0010	10.37
Cell2	30.44	4.00	0.22	4.61	0.0011	10.97
Cell3	30.44	2.86	0.32	3.16	0.0008	7.52
<b>Average</b>	<b>30.44</b>	<b>3.56</b>	<b>0.25</b>	<b>4.03</b>	<b>0.0010</b>	<b>9.62</b>
SD						1.84

Table 3.39 Determination of permeability coefficient of phenobarbital for time interval 0-5 minutes for cell layer only.

	$PS_{\text{all}}$	$1/PS_{\text{cell}}$	$PS_{\text{cell}}$	$PE_{\text{cell}} [\text{cm}/\text{min}]$	$PE_{\text{cell}} [\mu\text{m}/\text{min}]$
Cell1	3.81	0.26	3.81	0.0009	9.07
Cell2	4.00	0.25	4.00	0.0010	9.53
Cell3	2.86	0.35	2.86	0.0007	6.81
<b>Average</b>	<b>3.56</b>	<b>0.29</b>	<b>3.48</b>	<b>0.0008</b>	<b>8.47</b>
SD					1.45

Table 3.40 Determination of permeability coefficient of phenobarbital for time interval 0-5 minutes for membrane of insert with cells.

## Internal standard diazepam in the transport study of phenobarbital

The permeability of diazepam as a function of time was determined using the same principles as for phenobarbital described above.

In the time interval 5-140 average permeability slope values for diazepam were:  $PS_{\text{control}} = 10.58 \mu\text{l}/\text{min}$ ,  $PS_{\text{all}} = 5.81 \mu\text{l}/\text{min}$  and  $PS_{\text{cell}} = 12.92 \mu\text{l}/\text{min}$ .  $PE_{\text{cell}}$  was  $31.00 \pm 4.62 \mu\text{m}/\text{min}$ .  $PE_{\text{all}}$  amounted to  $13.84 \pm 0.91 \mu\text{m}/\text{min}$ . EC reached to 223.12%. All values were calculated using equations from section 2.3.

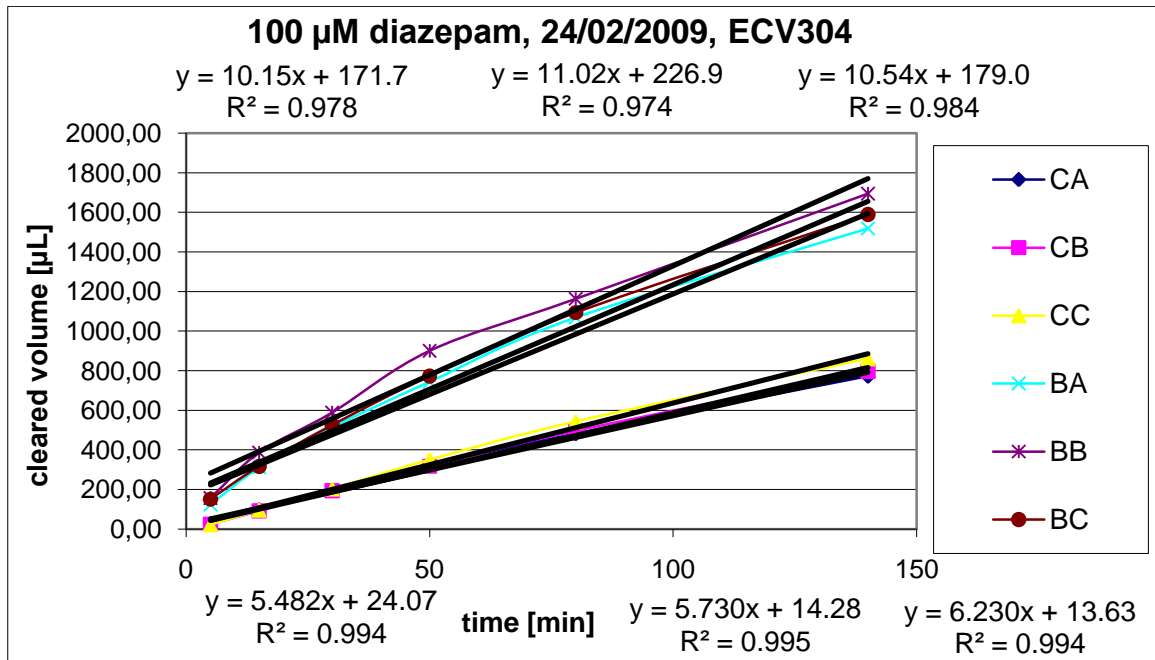


Figure 3.21 Dependence of cleared volume on the time interval 5-140 minutes for internal standard diazepam.

	$PS_{\text{Control}}$	$PS_{\text{all}}$	$1/PS_{\text{cell}}$	$PS_{\text{cell}}$	$PE_{\text{cell}} [\text{cm}/\text{min}]$	$PE_{\text{cell}} [\mu\text{m}/\text{min}]$
Cell1	10.58	5.48	0.09	11.39	0.0027	27.11
Cell2	10.58	5.73	0.08	12.51	0.0030	29.79
Cell3	10.58	6.23	0.07	15.16	0.0036	36.10
<b>Average</b>	<b>10.58</b>	<b>5.81</b>	<b>0.08</b>	<b>12.92</b>	<b>0.0031</b>	<b>31.00</b>
SD						4.62

Table 3.41 Determination of permeability coefficient of diazepam for time interval 5-140 minutes for cell layer only.

	$PS_{\text{all}}$	$1/PS_{\text{cell}}$	$PS_{\text{cell}}$	$PE_{\text{cell}} [\text{cm}/\text{min}]$	$PE_{\text{cell}} [\mu\text{m}/\text{min}]$
Cell1	5.48	0.18	5.48	0.0013	13.05
Cell2	5.73	0.17	5.73	0.0014	13.64
Cell3	6.23	0.16	6.23	0.0015	14.83
<b>Average</b>	<b>5.81</b>	<b>0.17</b>	<b>5.80</b>	<b>0.0014</b>	<b>13.84</b>
SD					0.91

Table 3.42 Determination of permeability coefficient of diazepam for time interval 5-140 minutes for membrane of insert with cells.

In the time interval 0-5 average permeability slope values for diazepam were:  $PS_{\text{control}} = 28.73 \mu\text{l}/\text{min}$ ,  $PS_{\text{all}} = 4.86 \mu\text{l}/\text{min}$  and  $PS_{\text{cell}} = 5.85 \mu\text{l}/\text{min}$ .  $PE_{\text{cell}}$  was  $13.95 \pm 1.70 \mu\text{m}/\text{min}$ .  $PE_{\text{all}}$  amounted to  $11.57 \pm 1.16 \mu\text{m}/\text{min}$ . EC reached to 120.40%. All values were calculated using equations from section 2.3.

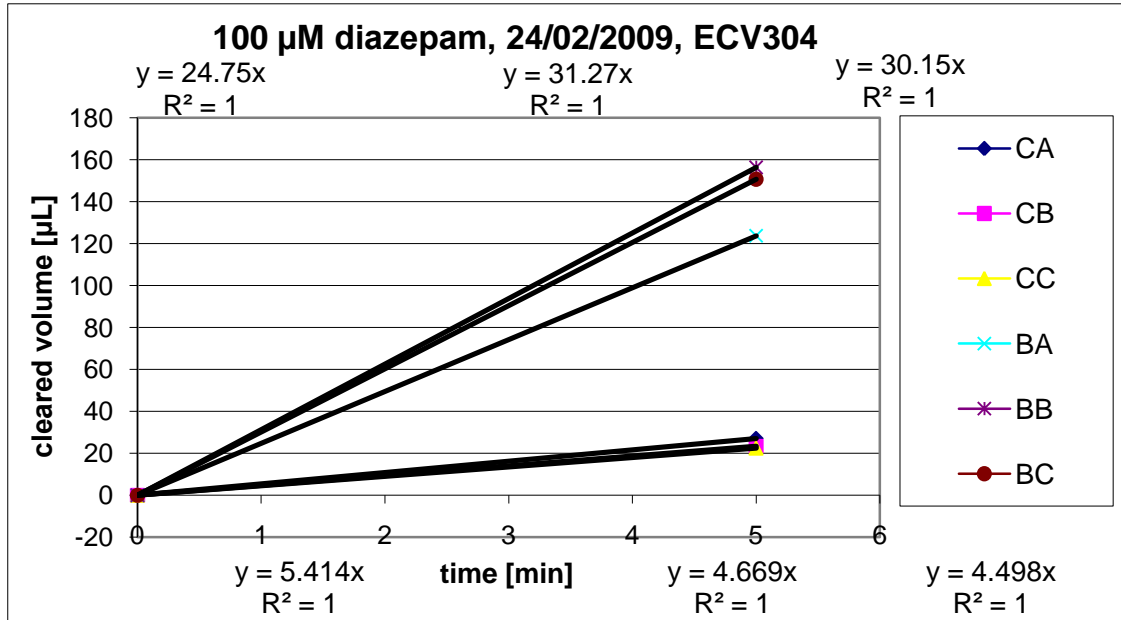


Figure 3.22 Dependence of clearance on the time interval 0-5 minutes for internal standard diazepam.

	$PS_{\text{Control}}$	$PS_{\text{all}}$	$1/PS_{\text{cell}}$	$PS_{\text{cell}}$	$PE_{\text{cell}} [\text{cm}/\text{min}]$	$PE_{\text{cell}} [\mu\text{m}/\text{min}]$
Cell1	28.73	5.41	0.15	6.67	0.0016	15.88
Cell2	28.73	4.67	0.18	5.58	0.0013	13.27
Cell3	28.73	4.50	0.19	5.33	0.0013	12.70
<b>Average</b>	<b>28.73</b>	<b>4.86</b>	<b>0.17</b>	<b>5.85</b>	<b>0.0014</b>	<b>13.95</b>
SD						1.70

Table 3.43 Determination of permeability coefficient of diazepam for time interval 0-5 minutes for cell layer only.

	$PS_{\text{all}}$	$1/PS_{\text{cell}}$	$PS_{\text{cell}}$	$PE_{\text{cell}} [\text{cm}/\text{min}]$	$PE_{\text{cell}} [\mu\text{m}/\text{min}]$
Cell1	5.41	0.18	5.41	0.0013	12.89
Cell2	4.67	0.21	4.67	0.0011	11.12
Cell3	4.50	0.22	4.50	0.0011	10.71
<b>Average</b>	<b>4.86</b>	<b>0.21</b>	<b>4.83</b>	<b>0.0011</b>	<b>11.57</b>
SD					1.16

Table 3.44 Determination of permeability coefficient of diazepam for time interval 0-5 minutes for membrane of insert with cells.

## Internal standard carboxyfluorescein in the transport study of phenobarbital

The permeability of carboxyfluorescein as a function of time was determined using the same principles as for phenobarbital described above.

In the time interval 5-140 average permeability slope values for carboxyfluorescein were:  $PS_{\text{control}} = 10.60 \mu\text{l}/\text{min}$ ,  $PS_{\text{all}} = 2.22 \mu\text{l}/\text{min}$  and  $PS_{\text{cell}} = 2.81 \mu\text{l}/\text{min}$ .  $PE_{\text{cell}}$  was  $6.70 \pm 0.61 \mu\text{m}/\text{min}$ .  $PE_{\text{all}}$  amounted to  $5.29 \pm 0.38 \mu\text{m}/\text{min}$ . EC reached to 126.52%. All values were calculated using equations from section 2.3.

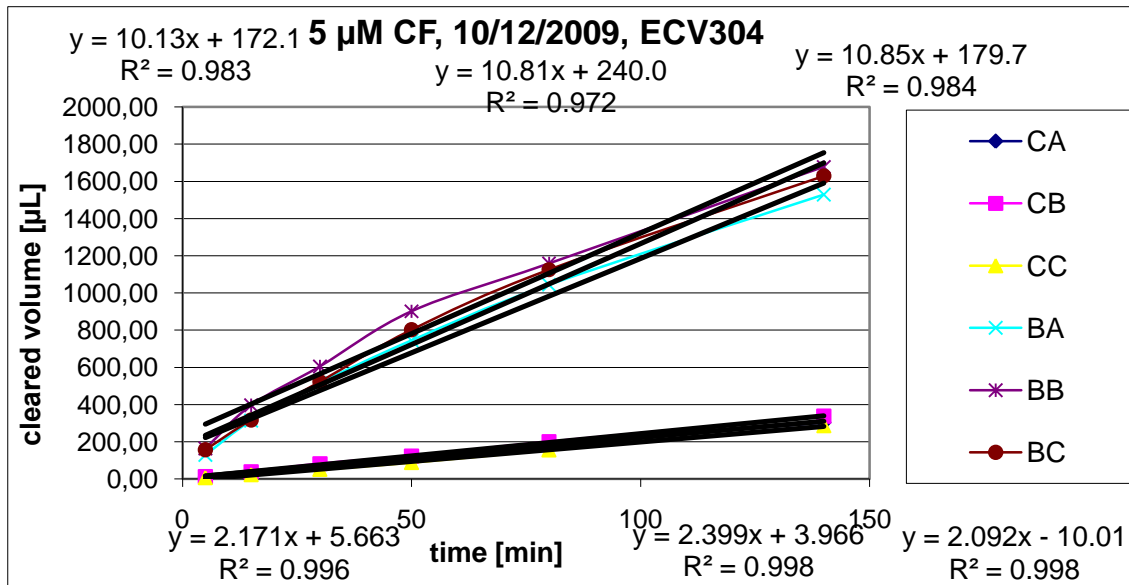


Figure 3.23 Dependence of cleared volume on the time interval 5-140 minutes for internal standard carboxyfluorescein.

	$PS_{\text{Control}}$	$PS_{\text{all}}$	$1/PS_{\text{cell}}$	$PS_{\text{cell}}$	$PE_{\text{cell}} [\text{cm}/\text{min}]$	$PE_{\text{cell}} [\mu\text{m}/\text{min}]$
Cell1	10.60	2.17	0.37	2.73	0.0007	6.50
Cell2	10.60	2.40	0.32	3.10	0.0007	7.38
Cell3	10.60	2.09	0.38	2.61	0.0006	6.21
<b>Average</b>	<b>10.60</b>	<b>2.22</b>	<b>0.36</b>	<b>2.81</b>	<b>0.0007</b>	<b>6.70</b>
SD						0.61

Table 3.45 Determination of permeability coefficient of carboxyfluorescein for time interval 5-140 minutes for cell layer only.

	$PS_{\text{all}}$	$1/PS_{\text{cell}}$	$PS_{\text{cell}}$	$PE_{\text{cell}} [\text{cm}/\text{min}]$	$PE_{\text{cell}} [\mu\text{m}/\text{min}]$
Cell1	2.17	0.46	2.17	0.0005	5.17
Cell2	2.40	0.42	2.40	0.0006	5.71
Cell3	2.09	0.48	2.09	0.0005	4.98
<b>Average</b>	<b>2.22</b>	<b>0.45</b>	<b>2.21</b>	<b>0.0005</b>	<b>5.29</b>
SD					0.38

Table 3.46 Determination of permeability coefficient of carboxyfluorescein for time interval 5-140 minutes for membrane of insert with cells.

In the time interval 0-5 average permeability slope values for carboxyfluorescein were:  $PS_{\text{control}} = 29.95 \mu\text{l}/\text{min}$ ,  $PS_{\text{all}} = 1.85 \mu\text{l}/\text{min}$  and  $PS_{\text{cell}} = 1.97 \mu\text{l}/\text{min}$ .  $PE_{\text{cell}}$  was  $4.71 \pm 1.53 \mu\text{m}/\text{min}$ .  $PE_{\text{all}}$  amounted to  $4.40 \pm 1.35 \mu\text{m}/\text{min}$ . EC reached to 106.61%. All values were calculated using equations from section 2.3.

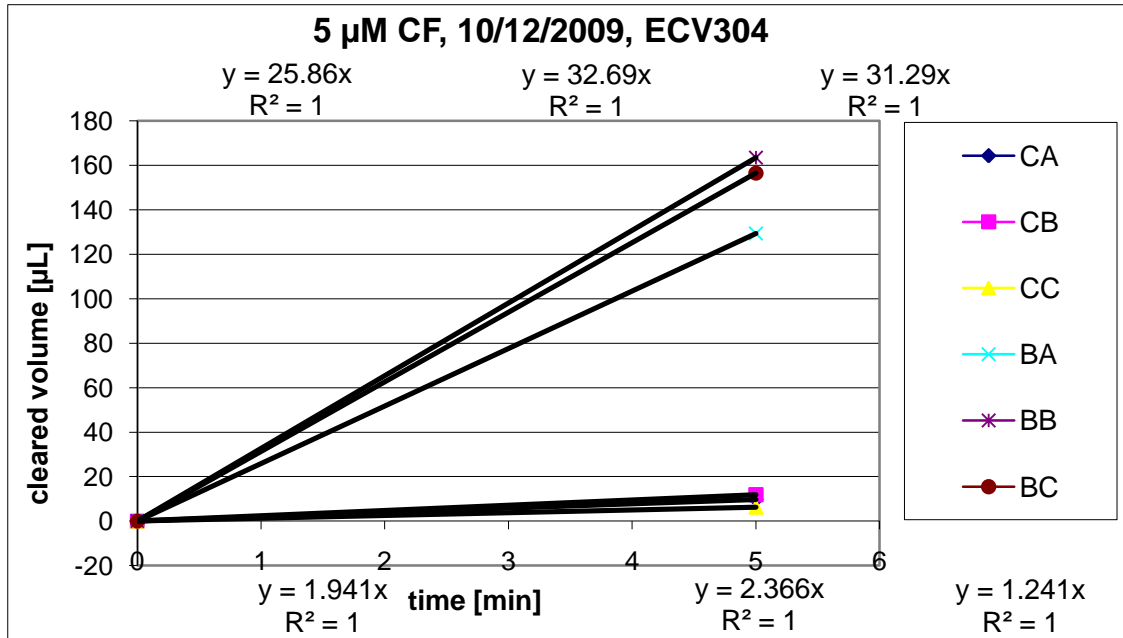


Figure 3.24 Dependence of cleared volume on the time interval 0-5 minutes for internal standard carboxyfluorescein.

	$PS_{\text{Control}}$	$PS_{\text{all}}$	$1/PS_{\text{cell}}$	$PS_{\text{cell}}$	$PE_{\text{cell}}$ [cm/min]	$PE_{\text{cell}}$ [ $\mu\text{m}/\text{min}$ ]
Cell1	29.95	1.94	0.48	2.08	0.0005	4.94
Cell2	29.95	2.37	0.39	2.57	0.0006	6.12
Cell3	29.95	1.24	0.77	1.30	0.0003	3.08
<b>Average</b>	<b>29.95</b>	<b>1.85</b>	<b>0.51</b>	<b>1.97</b>	<b>0.0005</b>	<b>4.71</b>
SD						1.53

Table 3.47 Determination of permeability coefficient of carboxyfluorescein for time interval 0-5 minutes for cell layer only.

	$PS_{\text{all}}$	$1/PS_{\text{cell}}$	$PS_{\text{cell}}$	$PE_{\text{cell}}$ [cm/min]	$PE_{\text{cell}}$ [ $\mu\text{m}/\text{min}$ ]
Cell1	1.94	0.52	1.94	0.0005	4.62
Cell2	2.37	0.42	2.37	0.0006	5.64
Cell3	1.24	0.81	1.24	0.0003	2.96
<b>Average</b>	<b>1.85</b>	<b>0.58</b>	<b>1.72</b>	<b>0.0004</b>	<b>4.40</b>
SD					1.35

Table 3.48 Determination of permeability coefficient of carboxyfluorescein for time interval 0-5 minutes for membrane of insert with cells.

### 3.5 Transport study of memantine – Single study

Transport study of memantine was accomplished across the BBB *in vitro* model based on cell line ECV304. Amounts of permeated substance were quantified by HPLC. In this transport study we fumbled with problem of HPLC analysis of memantine because too small peak areas were found after analysis of samples from first time intervals and the integration of peaks might not be correct. In Table 3.49 results calculating between different time intervals are shown which were used for calculation of permeability coefficient. Finally, the transfer intervals of 30 and 60 minutes were implicated into the results. All values were calculated using equations from section 2.3.

Time intervals	Substance	PE <sub>cell</sub> [μm/min]	PE <sub>all</sub> [μm/min]	EC[%]
5, 10, 15, 20, 30 and 60 minutes	memantine	14.88±1.42	9.15±0.53	162.44±5.95
	diazepam	35.14±4.20	11.98±0.50	292.74±23.06
	carboxyfluorescein	5.47±0.28	4.47±0.18	122.29±1.12
15, 20, 30 and 60 minutes	memantine	15.92±2.88	8.56±0.84	185.08±15.41
	diazepam	42.81±9.50	10.51±0.60	404.80±67.64
	carboxyfluorescein	8.55±0.53	5.76±0.24	148.32±2.99
20, 30 and 60 minutes	memantine	17.78±4.15	8.41±0.97	209.45±25.57
	diazepam	50.40±23.33	9.47±0.87	520.62±194.67
	carboxyfluorescein	9.42±1.07	5.71±0.39	164.59±7.37
30 and 60 minutes	memantine	26.06±11.26	8.50±1.23	298.37±85.72
	diazepam	29.59±11.37	7.31±0.75	398.79±114.80
	carboxyfluorescein	9.80±1.51	5.45±0.48	179.11±12.17

Table 3.49 Comparism PE<sub>cell</sub>, PE<sub>all</sub> and EC values of substances used in transport study of memantine, where different time intervals were used for calculation.

For illustration the total curves (for time interval 5-140 minutes) of memantine, diazepam and carboxyfluorescein are shown in following graphs (Figure 3.25, 3.26 and 3.27) and then the tables with determination of permeability coefficients memantine, diazepam and carboxyfluorescein in transfer intervals 30 and 60 minutes are displayed, too.

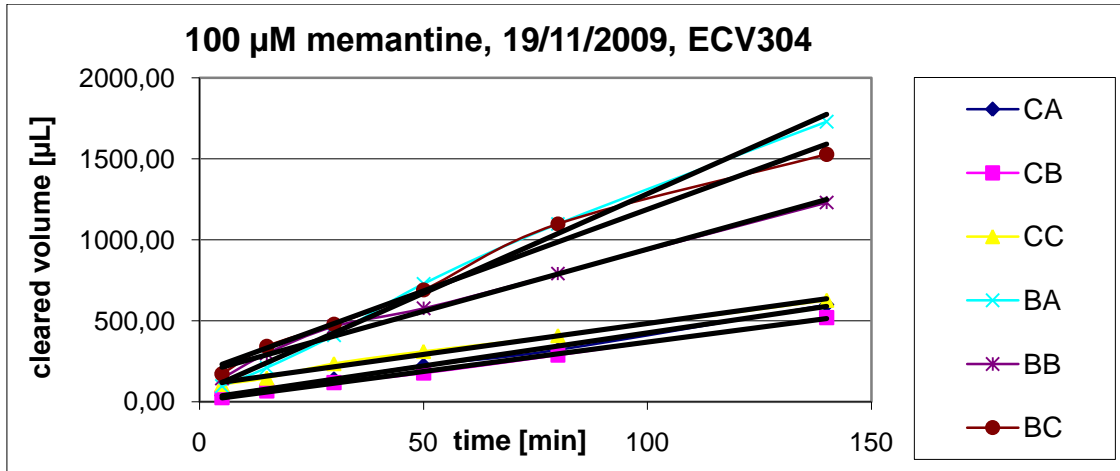


Figure 3.25 Dependence of cleared volume on the time interval 5-140 minutes for phenobarbital.

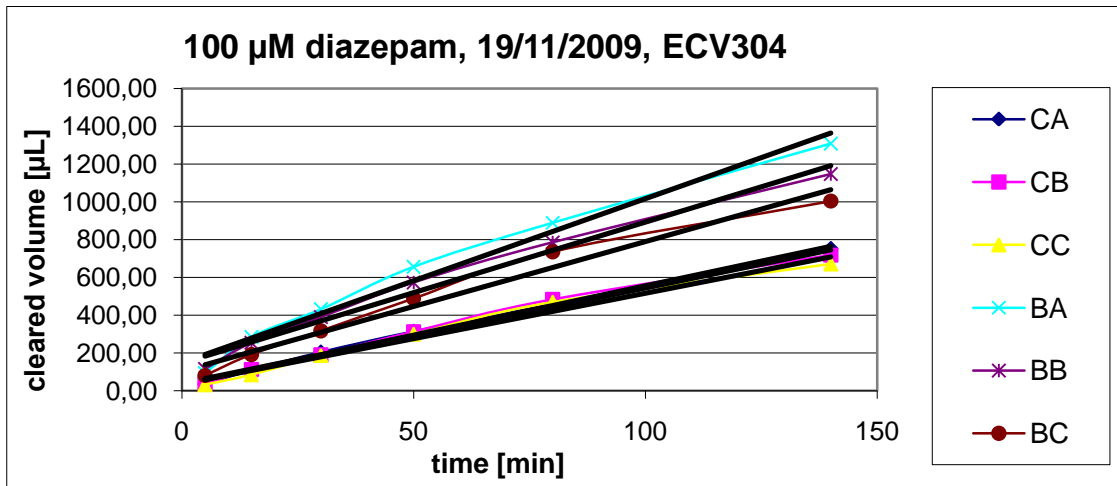


Figure 3.26 Determination of permeability coefficient of diazepam for time interval 5-140 minutes.

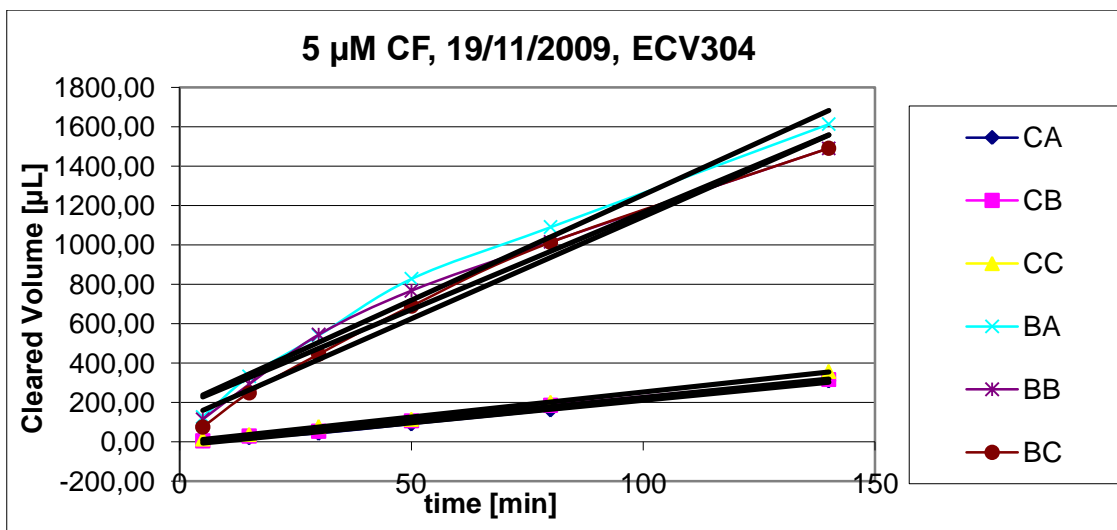


Figure 3.27 Determination of permeability coefficient of carboxyfluorescein for time interval 5-140 minutes.

	PS <sub>Control</sub>	PS <sub>all</sub>	1/PS <sub>cell</sub>	PS <sub>cell</sub>	PE <sub>cell</sub> [cm/min]	PE <sub>cell</sub> [ $\mu$ m/min]
Cell1	5.52	4.12	0.06	16.18	0.0039	38.53
Cell2	5.52	3.51	0.10	9.67	0.0023	23.02
Cell3	5.52	3.08	0.14	6.99	0.0017	16.63
<b>Average</b>	<b>5.52</b>	<b>3.57</b>	<b>0.10</b>	<b>10.12</b>	<b>0.0024</b>	<b>26.06</b>
SD						11.26

Table 3.50 Determination of permeability coefficient of memantine for transfer intervals 30 and 60 minutes for cell layer only.

	PS <sub>all</sub>	1/PS <sub>cell</sub>	PS <sub>cell</sub>	PE <sub>all</sub> [cm/min]	PE <sub>all</sub> [ $\mu$ m/min]	SD
Cell1	4.12	0.24	4.12	0.0010	9.80	
Cell2	3.51	0.28	3.51	0.0008	8.36	
Cell3	3.08	0.32	3.08	0.0007	7.34	
<b>Average</b>	<b>3.57</b>	<b>0.28</b>	<b>3.52</b>	<b>0.0008</b>	<b>8.50</b>	1.23

Table 3.51 Determination of permeability coefficient of memantine for transfer intervals 30 and 60 minutes for membrane of insert with cells.

	PS <sub>Control</sub>	PS <sub>all</sub>	1/PS <sub>cell</sub>	PS <sub>cell</sub>	PE <sub>cell</sub> [cm/min]	PE <sub>cell</sub> [ $\mu$ m/min]
Cell1						
Cell2	4.16	3.29	0.06	15.81	0.0038	37.63
Cell3	4.16	2.85	0.11	9.05	0.0022	21.55
<b>Average</b>	<b>4.16</b>	<b>3.07</b>	<b>0.09</b>	<b>11.74</b>	<b>0.0028</b>	<b>29.59</b>
SD						11.37

Table 3.52 Determination of permeability coefficient of diazepam for transfer intervals 30 and 60 minutes for cell layer only. The first PS<sub>all</sub> value was excluded from calculation.

	PS <sub>all</sub>	1/PS <sub>cell</sub>	PS <sub>cell</sub>	PE <sub>all</sub> [cm/min]	PE <sub>all</sub> [ $\mu$ m/min]	SD
Cell1						
Cell2	3.29	0.30	3.29	0.0008	7.84	
Cell3	2.85	0.35	2.85	0.0007	6.79	
<b>Average</b>	<b>3.07</b>	<b>0.33</b>	<b>3.06</b>	<b>0.0007</b>	<b>7.31</b>	0.75

Table 3.53 Determination of permeability coefficient of diazepam for transfer intervals 30 and 60 minutes for membrane of insert with cells.

	PS <sub>Control</sub>	PS <sub>all</sub>	1/PS <sub>cell</sub>	PS <sub>cell</sub>	PE <sub>cell</sub> [cm/min]	PE <sub>cell</sub> [ $\mu$ m/min]
Cell1	5.20	2.35	0.23	4.28	0.0010	10.19
Cell2	5.20	2.06	0.29	3.42	0.0008	8.13
Cell3	5.20	2.46	0.22	4.65	0.0011	11.07
<b>Average</b>	<b>5.20</b>	<b>2.29</b>	<b>0.24</b>	<b>4.09</b>	<b>0.0010</b>	<b>9.80</b>
SD						1.51

Table 3.54 Determination of permeability coefficient of carboxyfluorescein for transfer interval 30 and 60 minutes for cell layer only.

	PS <sub>all</sub>	1/PS <sub>cell</sub>	PS <sub>cell</sub>	PE <sub>all</sub> [cm/min]	PE <sub>all</sub> [ $\mu$ m/min]	SD
Cell1	2.35	0.43	2.35	0.0006	5.59	
Cell2	2.06	0.48	2.06	0.0005	4.91	
Cell3	2.46	0.41	2.46	0.0006	5.85	
<b>Average</b>	<b>2.29</b>	<b>0.44</b>	<b>2.28</b>	<b>0.0005</b>	<b>5.45</b>	0.48

Table 3.55 Determination of permeability coefficient of carboxyfluorescein for transfer intervals 30 and 60 minutes for membrane of insert with cells.

### 3.6 Transport study of amantadine – Single study

Transport study of amantadine was accomplished across the BBB *in vitro* model based on cell line ECV304. Amounts of permeated substance were quantified by HPLC. In the time interval 5-140 average permeability slope values for amantadine were:  $PS_{\text{control}} = 7.25 \mu\text{l}/\text{min}$ ,  $PS_{\text{all}} = 3.42 \mu\text{l}/\text{min}$  and  $PS_{\text{cell}} = 6.48 \mu\text{l}/\text{min}$ . The average permeability coefficient ( $PE_{\text{cell}}$ ) for cell layer was  $15.49 \pm 1.83 \mu\text{m}/\text{min}$ .  $PE_{\text{all}}$  amounted to  $8.14 \pm 0.53 \mu\text{m}/\text{min}$ . EC reached to 189.73%. All values were calculated using equations from section 2.3.

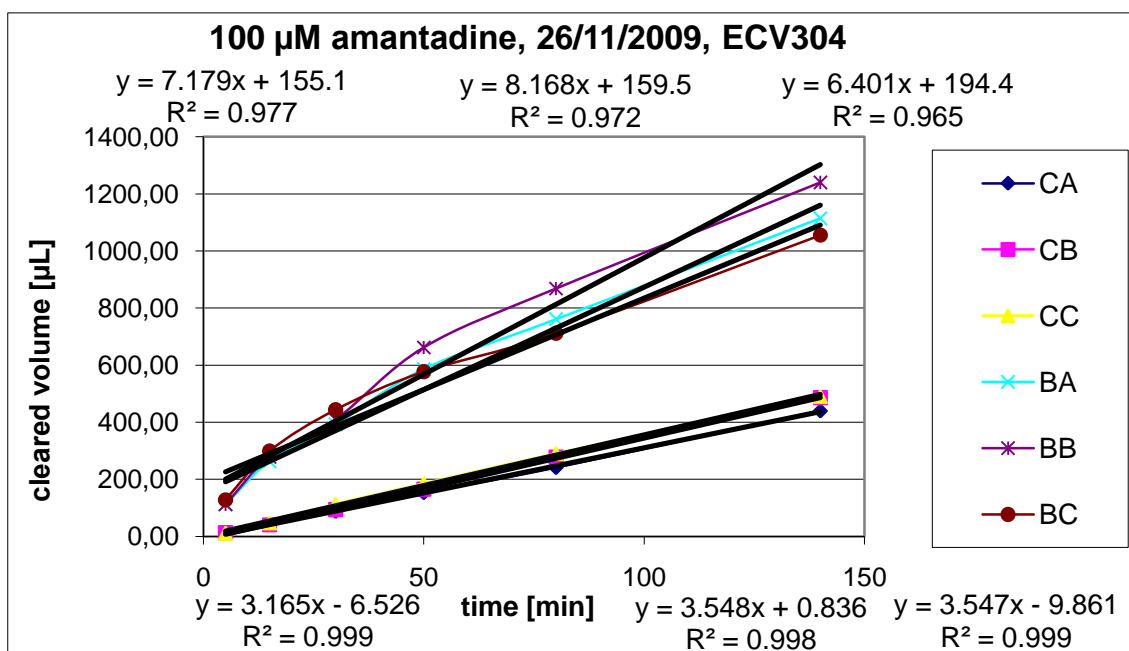


Figure 3.28 Dependence of cleared volume on the time interval 5-140 minutes for amantadine.

	$PS_{\text{Control}}$	$PS_{\text{all}}$	$1/PS_{\text{cell}}$	$PS_{\text{cell}}$	$PE_{\text{cell}} [\text{cm}/\text{min}]$	$PE_{\text{cell}} [\mu\text{m}/\text{min}]$
Cell1	7.25	3.17	0.18	5.62	0.0013	13.38
Cell2	7.25	3.55	0.14	6.95	0.0017	16.54
Cell3	7.25	3.55	0.14	6.95	0.0017	16.55
<b>Average</b>	<b>7.25</b>	<b>3.42</b>	<b>0.15</b>	<b>6.48</b>	<b>0.0015</b>	<b>15.49</b>
SD						1.83

Table 3.56 Determination of permeability coefficient of amantadine for time interval 5-140 minutes for cell layer only.

	$PS_{\text{all}}$	$1/PS_{\text{cell}}$	$PS_{\text{cell}}$	$PE_{\text{all}} [\text{cm}/\text{min}]$	$PE_{\text{all}} [\mu\text{m}/\text{min}]$
Cell1	3.17	0.32	3.17	0.0008	7.54
Cell2	3.55	0.28	3.55	0.0008	8.45
Cell3	3.55	0.28	3.55	0.0008	8.45
<b>Average</b>	<b>3.42</b>	<b>0.29</b>	<b>3.41</b>	<b>0.0008</b>	<b>8.14</b>
SD					0.53

Table 3.57 Determination of permeability coefficient of amantadine for time interval 5-140 minutes for membrane of insert with cells.

In the time interval 0-5 average permeability slope values for amantadine were:  $PS_{\text{control}} = 23.43 \mu\text{l}/\text{min}$ ,  $PS_{\text{all}} = 2.39 \mu\text{l}/\text{min}$  and  $PS_{\text{cell}} = 2.66 \mu\text{l}/\text{min}$ .  $PE_{\text{cell}}$  was  $6.35 \pm 0.53 \mu\text{m}/\text{min}$ .  $PE_{\text{all}}$  amounted to  $5.70 \pm 0.43 \mu\text{m}/\text{min}$ . EC reached to 111.38%. All values were calculated using equations from section 2.3.

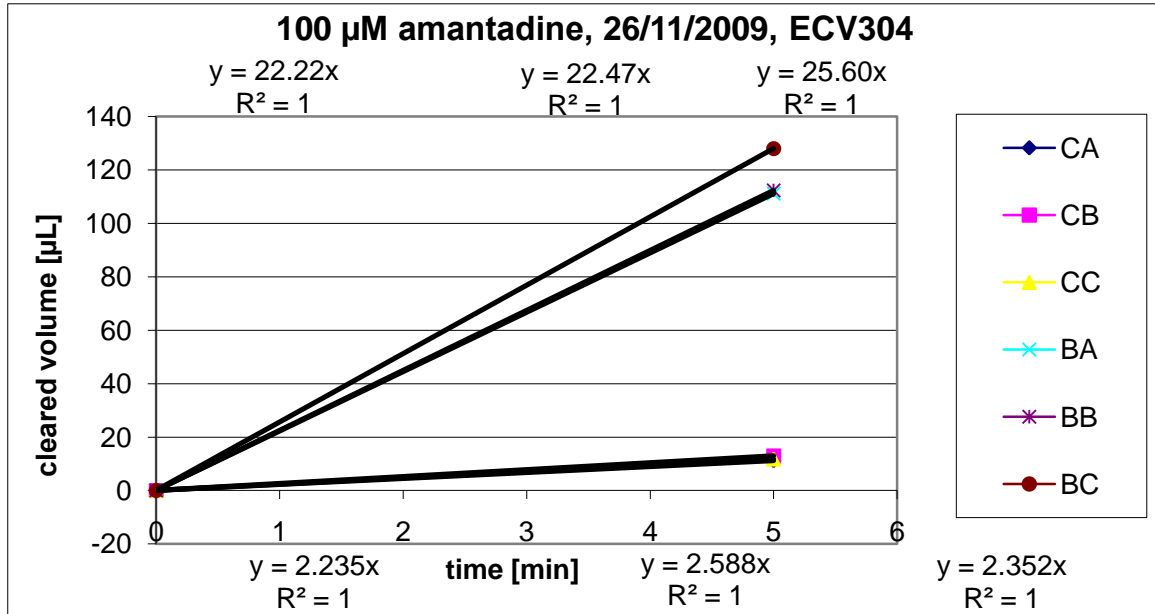


Figure 3.29 Dependence of cleared volume on the time interval 0-5 minutes for amantadine.

	$PS_{\text{Control}}$	$PS_{\text{all}}$	$1/PS_{\text{cell}}$	$PS_{\text{cell}}$	$PE_{\text{cell}} [\text{cm}/\text{min}]$	$PE_{\text{cell}} [\mu\text{m}/\text{min}]$
Cell1	23.43	2.24	0.40	2.47	0.0006	5.89
Cell2	23.43	2.59	0.34	2.91	0.0007	6.93
Cell3	23.43	2.35	0.38	2.61	0.0006	6.22
<b>Average</b>	<b>23.43</b>	<b>2.39</b>	<b>0.38</b>	<b>2.66</b>	<b>0.0006</b>	<b>6.35</b>
SD						0.53

Table 3.58 Determination of permeability coefficient of amantadine for time interval 0-5 minutes for cell layer only.

	$PS_{\text{all}}$	$1/PS_{\text{cell}}$	$PS_{\text{cell}}$	$PE_{\text{all}} [\text{cm}/\text{min}]$	$PE_{\text{all}} [\mu\text{m}/\text{min}]$
Cell1	2.24	0.45	2.24	0.0005	5.33
Cell2	2.59	0.39	2.59	0.0006	6.16
Cell3	2.35	0.43	2.35	0.0006	5.60
<b>Average</b>	<b>2.39</b>	<b>0.42</b>	<b>2.38</b>	<b>0.0006</b>	<b>5.70</b>
SD					0.43

Table 3.59 Determination of permeability coefficient of amantadine for time interval 0-5 minutes for membrane of insert with cells.

## Internal standard diazepam in the transport study of amantadine

The permeability of diazepam as a function of time was determined using the same principles as for amantadine described above.

In the time interval 5-140 average permeability slope values for diazepam were:  $PS_{\text{control}} = 6.01 \mu\text{l}/\text{min}$ ,  $PS_{\text{all}} = 4.27 \mu\text{l}/\text{min}$  and  $PS_{\text{cell}} = 14.72 \mu\text{l}/\text{min}$ .  $PE_{\text{cell}}$  was  $35.43 \pm 5.26 \mu\text{m}/\text{min}$ .  $PE_{\text{all}}$  amounted to  $10.16 \pm 0.45 \mu\text{m}/\text{min}$ . EC reached to 347.68%. All values were calculated using equations from section 2.3.

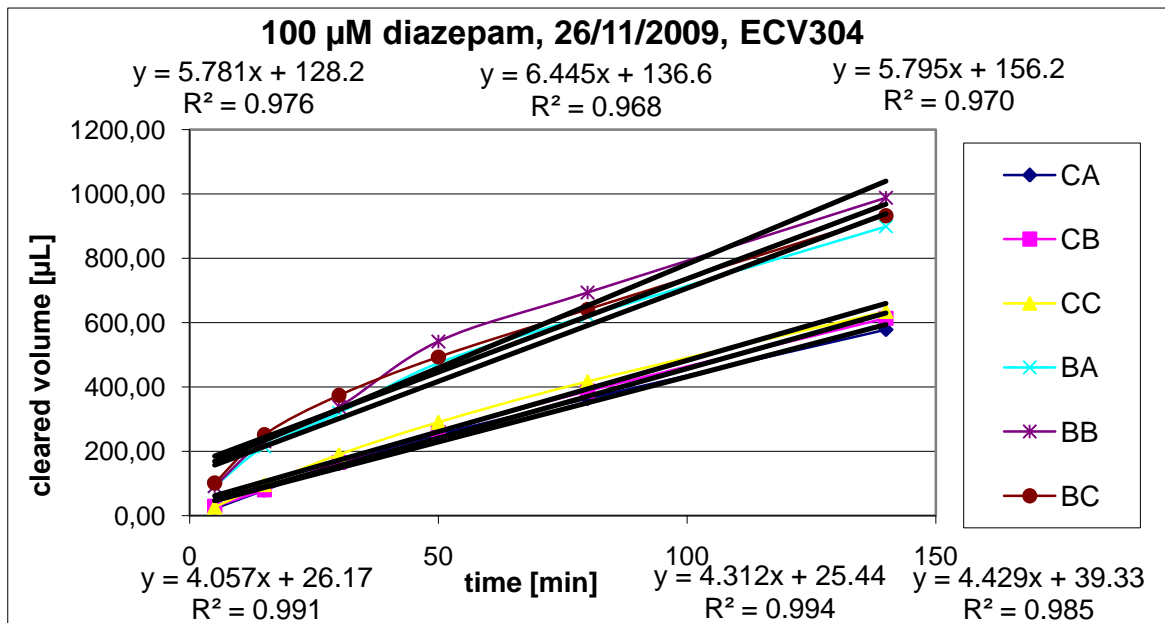


Figure 3.30 Dependence of cleared volume on the time interval 5-140 minutes for internal standard diazepam.

	$PS_{\text{Control}}$	$PS_{\text{all}}$	$1/PS_{\text{cell}}$	$PS_{\text{cell}}$	$PE_{\text{cell}} [\text{cm}/\text{min}]$	$PE_{\text{cell}} [\mu\text{m}/\text{min}]$
Cell1	6.01	4.06	0.08	12.50	0.0030	29.75
Cell2	6.01	4.31	0.07	15.28	0.0036	36.39
Cell3	6.01	4.43	0.06	16.86	0.0040	40.14
<b>Average</b>	<b>6.01</b>	<b>4.27</b>	<b>0.07</b>	<b>14.72</b>	<b>0.0035</b>	<b>35.43</b>
SD						5.26

Table 3.60 Determination of permeability coefficient of diazepam for time interval 5-140 minutes for cell layer only.

	$PS_{\text{all}}$	$1/PS_{\text{cell}}$	$PS_{\text{cell}}$	$PE_{\text{all}} [\text{cm}/\text{min}]$	$PE_{\text{all}} [\mu\text{m}/\text{min}]$
Cell1	4.06	0.25	4.06	0.0010	9.66
Cell2	4.31	0.23	4.31	0.0010	10.27
Cell3	4.43	0.23	4.43	0.0011	10.55
<b>Average</b>	<b>4.27</b>	<b>0.23</b>	<b>4.26</b>	<b>0.0010</b>	<b>10.16</b>
SD					0.45

Table 3.61 Determination of permeability coefficient of diazepam for time interval 5-140 minutes for membrane of insert with cells.

In the time interval 0-5 average permeability slope values for diazepam were:  $PS_{\text{control}} = 18.98 \mu\text{l}/\text{min}$ ,  $PS_{\text{all}} = 5.16 \mu\text{l}/\text{min}$  and  $PS_{\text{cell}} = 7.09 \mu\text{l}/\text{min}$ .  $PE_{\text{cell}}$  was  $16.98 \pm 3.17 \mu\text{m}/\text{min}$ .  $PE_{\text{all}}$  amounted to  $12.28 \pm 1.70 \mu\text{m}/\text{min}$ . EC reached to 137.58%. All values were calculated using equations from section 2.3.

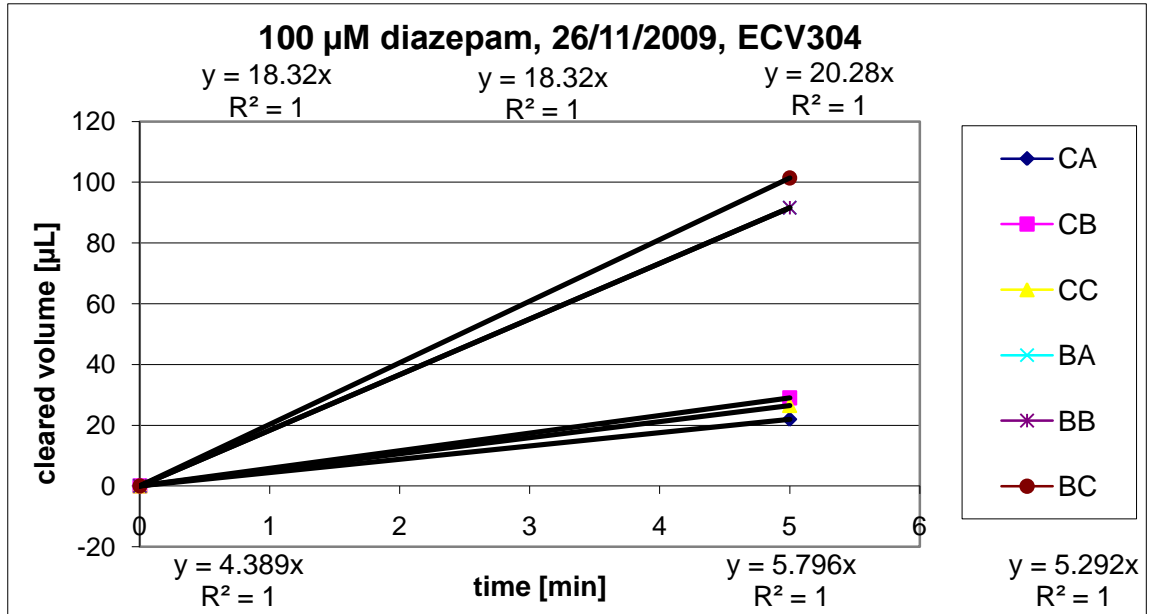


Figure 3.31 Dependence of cleared volume on the time interval 0-5 minutes for internal standard diazepam.

	$PS_{\text{Control}}$	$PS_{\text{all}}$	$1/PS_{\text{cell}}$	$PS_{\text{cell}}$	$PE_{\text{cell}} [\text{cm}/\text{min}]$	$PE_{\text{cell}} [\mu\text{m}/\text{min}]$
Cell1	18.98	4.39	0.18	5.71	0.0014	13.60
Cell2	18.98	5.80	0.12	8.34	0.0020	19.87
Cell3	18.98	5.29	0.14	7.34	0.0017	17.48
<b>Average</b>	<b>18.98</b>	<b>5.16</b>	<b>0.14</b>	<b>7.09</b>	<b>0.0017</b>	<b>16.98</b>
SD						3.17

Table 3.62 Determination of permeability coefficient of diazepam for time interval 0-5 minutes for cell layer only.

	$PS_{\text{all}}$	$1/PS_{\text{cell}}$	$PS_{\text{cell}}$	$PE_{\text{all}} [\text{cm}/\text{min}]$	$PE_{\text{all}} [\mu\text{m}/\text{min}]$
Cell1	4.39	0.23	4.39	0.0010	10.45
Cell2	5.80	0.17	5.80	0.0014	13.80
Cell3	5.29	0.19	5.29	0.0013	12.60
<b>Average</b>	<b>5.16</b>	<b>0.20</b>	<b>5.09</b>	<b>0.0012</b>	<b>12.28</b>
SD					1.70

Table 3.63 Determination of permeability coefficient of diazepam for time interval 0-5 minutes for membrane of insert with cells.

## Internal standard carboxyfluorescein in the transport study of amantadine

The permeability of Carboxyfluorescein as a function of time was determined using the same principles as for Amantadine described above.

In the time interval 5-140 average permeability slope values for carboxyfluorescein were:  $PS_{\text{control}} = 9.52 \mu\text{l}/\text{min}$ ,  $PS_{\text{all}} = 2.60 \mu\text{l}/\text{min}$  and  $PS_{\text{cell}} = 3.58 \mu\text{l}/\text{min}$ .  $PE_{\text{cell}}$  was  $8.52 \pm 0.39 \mu\text{m}/\text{min}$ .  $PE_{\text{all}}$  amounted to  $6.19 \pm 0.21 \mu\text{m}/\text{min}$ . EC reached to 137.60%. All values were calculated using equations from section 2.3.

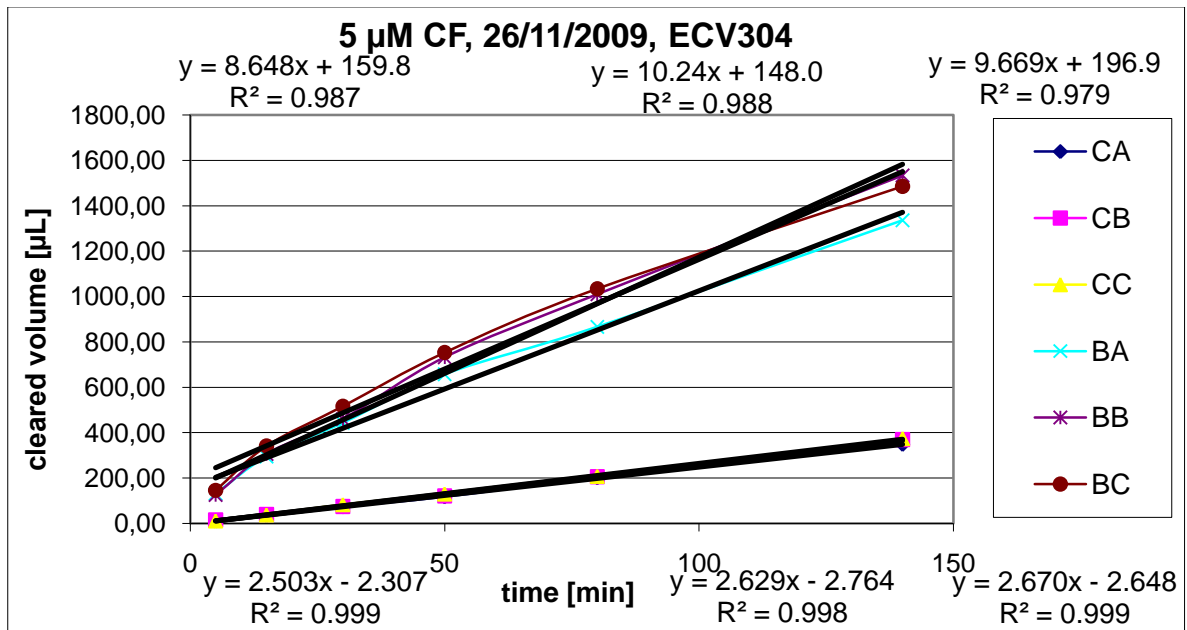


Figure 3.32 Dependence of cleared volume on the time interval 5-140 minutes for internal standard carboxyfluorescein.

	$PS_{\text{Control}}$	$PS_{\text{all}}$	$1/PS_{\text{cell}}$	$PS_{\text{cell}}$	$PE_{\text{cell}} [\text{cm}/\text{min}]$	$PE_{\text{cell}} [\mu\text{m}/\text{min}]$
Cell1	9.52	2.50	0.29	3.40	0.0008	8.09
Cell2	9.52	2.63	0.28	3.63	0.0009	8.65
Cell3	9.52	2.67	0.27	3.71	0.0009	8.84
<b>Average</b>	<b>9.52</b>	<b>2.60</b>	<b>0.28</b>	<b>3.58</b>	<b>0.0009</b>	<b>8.52</b>
SD						0.39

Table 3.64 Determination of permeability coefficient of carboxyfluorescein for time interval 5-140 minutes for cell layer only.

	$PS_{\text{all}}$	$1/PS_{\text{cell}}$	$PS_{\text{cell}}$	$PE_{\text{all}} [\text{cm}/\text{min}]$	$PE_{\text{all}} [\mu\text{m}/\text{min}]$
Cell1	2.50	0.40	2.50	0.0006	5.96
Cell2	2.63	0.38	2.63	0.0006	6.26
Cell3	2.67	0.37	2.67	0.0006	6.36
<b>Average</b>	<b>2.60</b>	<b>0.38</b>	<b>2.60</b>	<b>0.0006</b>	<b>6.19</b>
SD					0.21

Table 3.65 Determination of permeability coefficient of carboxyfluorescein for time interval 5-140 minutes for membrane of insert with cells.

In the time interval 0-5 average permeability slope values for carboxyfluorescein were:  $PS_{\text{control}} = 26.71 \mu\text{l}/\text{min}$ ,  $PS_{\text{all}} = 2.46 \mu\text{l}/\text{min}$  and  $PS_{\text{cell}} = 2.71 \mu\text{l}/\text{min}$ .  $PE_{\text{cell}}$  was  $6.47 \pm 1.50 \mu\text{m}/\text{min}$ .  $PE_{\text{all}}$  amounted to  $5.85 \pm 1.22 \mu\text{m}/\text{min}$ . EC reached to 110.17%. All values were calculated using equations from section 2.3.

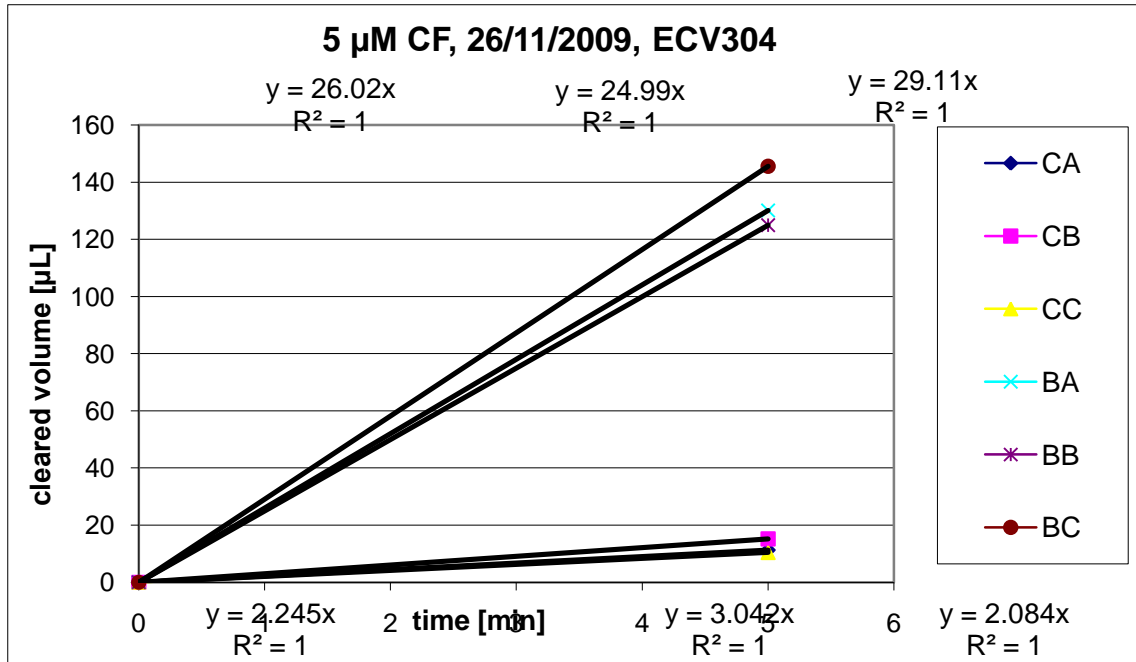


Figure 3.33 Dependence of cleared volume on the time interval 0-5 minutes for internal standard carboxyfluorescein.

	$PS_{\text{Control}}$	$PS_{\text{all}}$	$1/PS_{\text{cell}}$	$PS_{\text{cell}}$	$PE_{\text{cell}} [\text{cm}/\text{min}]$	$PE_{\text{cell}} [\mu\text{m}/\text{min}]$
Cell1	26.71	2.25	0.41	2.45	0.0006	5.84
Cell2	26.71	3.04	0,29	3.43	0.0008	8.17
Cell3	26.71	2.08	0.44	2.26	0.0005	5.38
<b>Average</b>	<b>26.71</b>	<b>2.46</b>	<b>0.37</b>	<b>2.71</b>	<b>0.0006</b>	<b>6.47</b>
SD						1.50

Table 3.66 Determination of permeability coefficient of carboxyfluorescein for time interval 0-5 minutes for cell layer only.

	$PS_{\text{all}}$	$1/PS_{\text{cell}}$	$PS_{\text{cell}}$	$PE_{\text{all}} [\text{cm}/\text{min}]$	$PE_{\text{all}} [\mu\text{m}/\text{min}]$
Cell1	2.25	0.45	2.25	0.0005	5.35
Cell2	3.04	0.33	3.04	0.0007	7.24
Cell3	2.08	0.48	2.08	0.0005	4.96
<b>Average</b>	<b>2.46</b>	<b>0.42</b>	<b>2.39</b>	<b>0.0006</b>	<b>5.85</b>
SD					1.22

Table 3.67 Determination of permeability coefficient of carboxyfluorescein for time interval 0-5 minutes for membrane of insert with cells.

### 3.7 Transport study of diltiazem/phenobarbital - Group study

#### Diltiazem in the transport study of diltiazem/dhenobarbital

Transport study of diltiazem and phenobarbital was accomplished across the BBB in vitro model based on cell line ECV304. Amounts of permeated substances were quantified by HPLC. In the time interval 5-140 average permeability slope values for diltiazem were:  $PS_{control} = 8.46 \mu\text{l}/\text{min}$ ,  $PS_{all} = 4.00 \mu\text{l}/\text{min}$  and  $PS_{cell} = 7.58 \mu\text{l}/\text{min}$ . The average permeability coefficient ( $PE_{cell}$ ) for cell layer was  $18.36 \pm 4.30 \mu\text{m}/\text{min}$ .  $PE_{all}$  amounted to  $9.52 \pm 1.16 \mu\text{m}/\text{min}$ . EC reached to 191,16%. All values were calculated using equations from section 2.3.

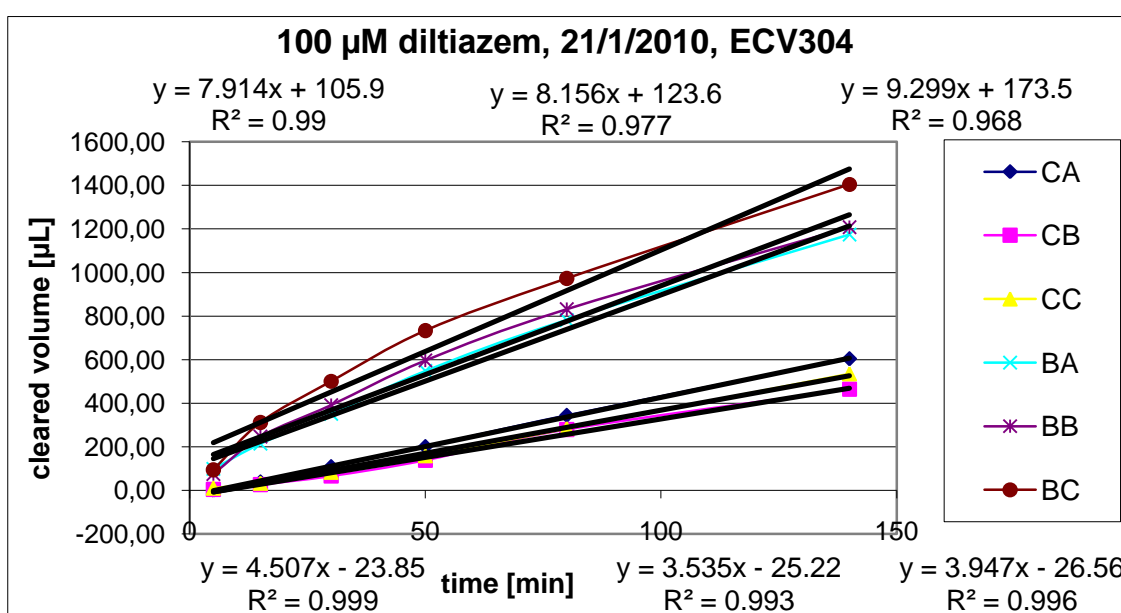


Figure 3.34 Dependence of cleared volume on the time interval 5-140 minutes for diltiazem.

	$PS_{control}$	$PS_{all}$	$1/PS_{cell}$	$PS_{cell}$	$PE_{cell}$ [cm/min]	$PE_{cell}$ [ $\mu\text{m}/\text{min}$ ]
Cell1	8.46	4.51	0.10	9.65	0.0023	22.98
Cell2	8.46	3.54	0.16	6.07	0.0014	14.46
Cell3	8.46	3.95	0.14	7.40	0.0018	17.62
<b>Average</b>	<b>8.46</b>	<b>4.00</b>	<b>0.13</b>	<b>7.58</b>	<b>0.0018</b>	<b>18.36</b>
SD						4.30

Table 3.68 Determination of permeability coefficient of diltiazem for time interval 5-140 minutes for cell layer only.

	$PS_{all}$	$1/PS_{cell}$	$PS_{cell}$	$PE_{all}$ [cm/min]	$PE_{all}$ [ $\mu\text{m}/\text{min}$ ]
Cell1	4.51	0.22	4.51	0.0011	10.73
Cell2	3.54	0.28	3.54	0.0008	8.42
Cell3	3.95	0.25	3.95	0.0009	9.40
<b>Average</b>	<b>4.00</b>	<b>0.25</b>	<b>3.96</b>	<b>0.0009</b>	<b>9.52</b>
SD					1.16

Table 3.69 Determination of permeability coefficient of diltiazem for time interval 5-140 minutes for membrane of insert with cells.

In the time interval 0-5 average permeability slope values for diltiazem were:  $PS_{\text{control}} = 18.24 \mu\text{l}/\text{min}$ ,  $PS_{\text{all}} = 1.10 \mu\text{l}/\text{min}$  and  $PS_{\text{cell}} = 1.17 \mu\text{l}/\text{min}$ .  $PE_{\text{cell}}$  was  $2.88 \pm 2.40 \mu\text{m}/\text{min}$ .  $PE_{\text{all}}$  amounted to  $2.63 \pm 2.07 \mu\text{m}/\text{min}$ . EC reached to 106.63%. All values were calculated using equations from section 2.3.

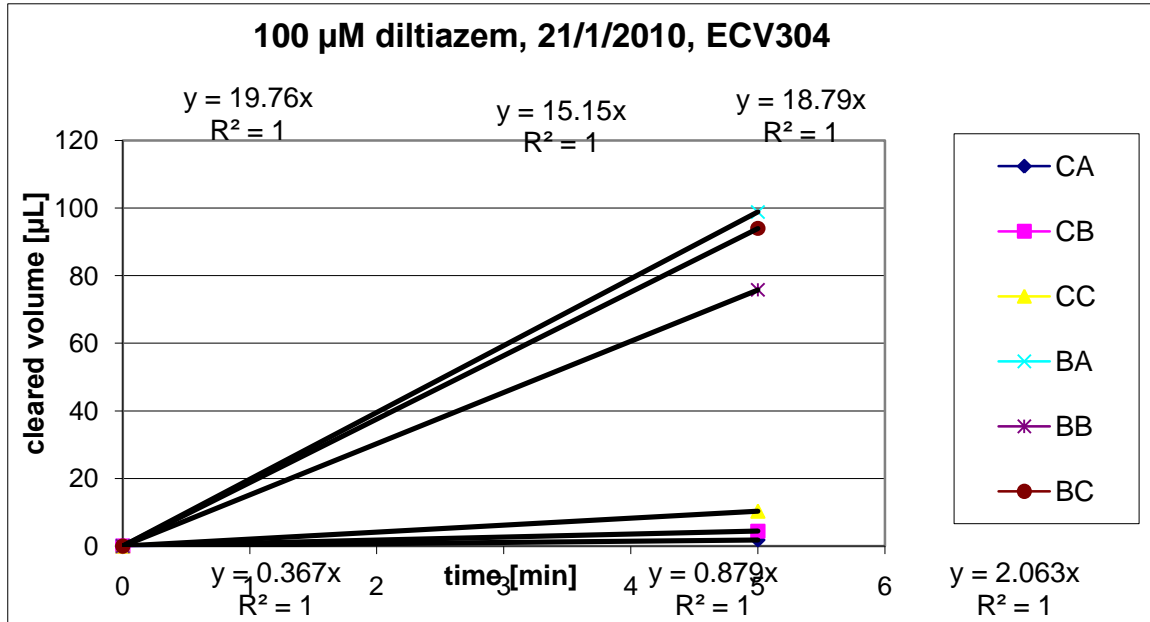


Figure 3.35 Dependence of cleared volume on the time interval 0-5 minutes for diltiazem.

	$PS_{\text{Control}}$	$PS_{\text{all}}$	$1/PS_{\text{cell}}$	$PS_{\text{cell}}$	$PE_{\text{cell}} [\text{cm}/\text{min}]$	$PE_{\text{cell}} [\mu\text{m}/\text{min}]$
Cell1	18.24	0.37	2.67	0.38	0.0001	0.89
Cell2	18.24	0.88	1.08	0.92	0.0002	2.20
Cell3	18.24	2.06	0.43	2.33	0.0006	5.54
<b>Average</b>	<b>18.24</b>	<b>1.10</b>	<b>0.85</b>	<b>1.17</b>	<b>0.0003</b>	<b>2.88</b>
SD						2.40

Table 3.70 Determination of permeability coefficient of diltiazem for time interval 0-5 minutes for cell layer only.

	$PS_{\text{all}}$	$1/PS_{\text{cell}}$	$PS_{\text{cell}}$	$PE_{\text{cell}} [\text{cm}/\text{min}]$	$PE_{\text{cell}} [\mu\text{m}/\text{min}]$
Cell1	0.37	2.72	0.37	0.0001	0.88
Cell2	0.88	1.14	0.88	0.0002	2.10
Cell3	2.06	0.48	2.06	0.0005	4.91
<b>Average</b>	<b>1.10</b>	<b>1.45</b>	<b>0.69</b>	<b>0.0002</b>	<b>2.63</b>
SD					2.07

Table 3.71 Determination of permeability coefficient of diltiazem for time interval 0-5 minutes for membrane of insert with cells.

## Phenobarbital in the transport study of diltiazem/phenobarbital

The permeability of phenobarbital as a function of time was determined using the same principles as for diltiazem described above.

In the time interval 5-140 average permeability slope values for phenobarbital were:  $PS_{\text{control}} = 13.58 \mu\text{l}/\text{min}$ ,  $PS_{\text{all}} = 7.66 \mu\text{l}/\text{min}$  and  $PS_{\text{cell}} = 17.57 \mu\text{l}/\text{min}$ .  $PE_{\text{cell}}$  was  $42.09 \pm 5.33 \mu\text{m}/\text{min}$ .  $PE_{\text{all}}$  amounted to  $18.23 \pm 1.02 \mu\text{m}/\text{min}$ . EC reached to 230.21%. All values were calculated using equations from section 2.3.

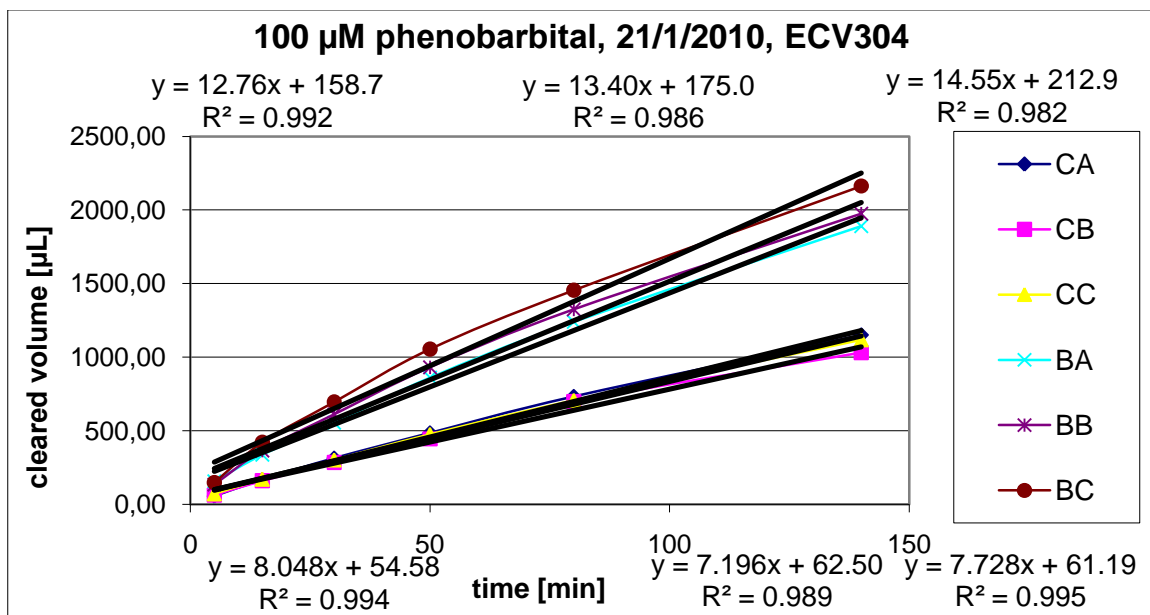


Figure 3.36 Dependence of cleared volume on the time interval 5-140 minutes for phenobarbital.

	$PS_{\text{Control}}$	$PS_{\text{all}}$	$1/PS_{\text{cell}}$	$PS_{\text{cell}}$	$PE_{\text{cell}} [\text{cm}/\text{min}]$	$PE_{\text{cell}} [\mu\text{m}/\text{min}]$
Cell1	13.58	8.05	0.05	19.77	0.0047	47.07
Cell2	13.58	7.20	0.07	15.32	0.0036	36.47
Cell3	13.58	7.73	0.06	17.94	0.0043	42.72
<b>Average</b>	<b>13.58</b>	<b>7.66</b>	<b>0.06</b>	<b>17.57</b>	<b>0.0042</b>	<b>42.09</b>
SD						5.33

Table 3.72 Determination of permeability coefficient of phenobarbital for time interval 5-140 minutes for cell layer only.

	$PS_{\text{all}}$	$1/PS_{\text{cell}}$	$PS_{\text{cell}}$	$PE_{\text{cell}} [\text{cm}/\text{min}]$	$PE_{\text{cell}} [\mu\text{m}/\text{min}]$
Cell1	8.05	0.12	8.05	0.0019	19.16
Cell2	7.20	0.14	7.20	0.0017	17.14
Cell3	7.73	0.13	7.73	0.0018	18.40
<b>Average</b>	<b>7.66</b>	<b>0.13</b>	<b>7.64</b>	<b>0.0018</b>	<b>18.23</b>
SD					1.02

Table 3.73 Determination of permeability coefficient of phenobarbital for time interval 5-140 minutes for membrane of insert with cells.

In the time interval 0-5 average permeability slope values for phenobarbital were:  $PS_{\text{control}} = 29.19 \mu\text{l}/\text{min}$ ,  $PS_{\text{all}} = 12.57 \mu\text{l}/\text{min}$  and  $PS_{\text{cell}} = 22.03 \mu\text{l}/\text{min}$ .  $PE_{\text{cell}}$  was  $53.21 \pm 10.90 \mu\text{m}/\text{min}$ .  $PE_{\text{all}}$  amounted to  $29.93 \pm 3.51 \mu\text{m}/\text{min}$ . EC reached to 176.56%. All values were calculated using equations from section 2.3.

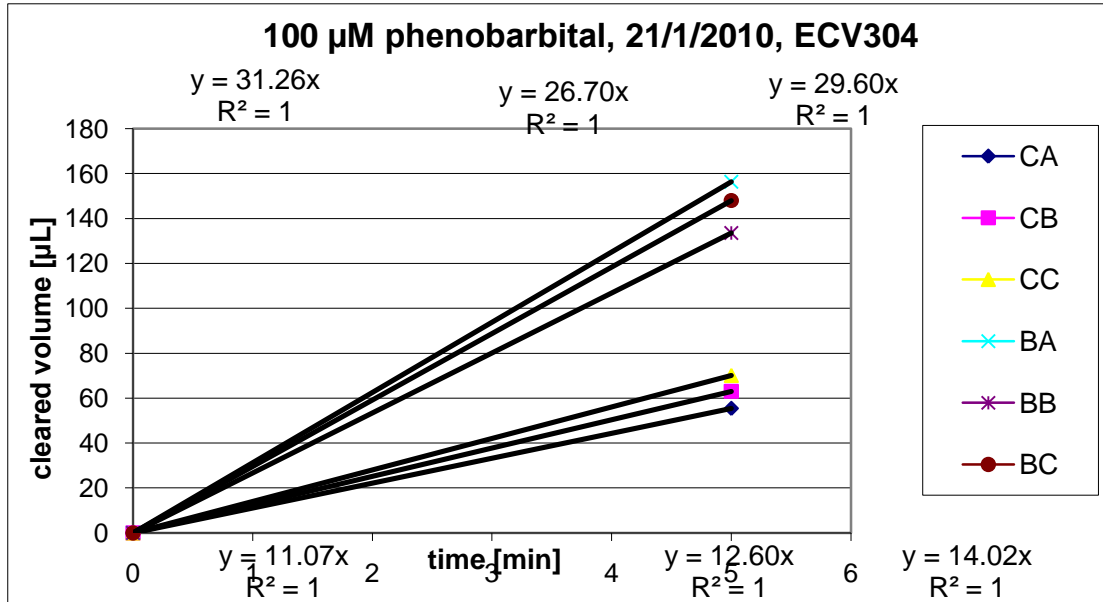


Figure 3.37 Dependence of cleared volume on the time interval 0-5 minutes for phenobarbital.

	$PS_{\text{Control}}$	$PS_{\text{all}}$	$1/PS_{\text{cell}}$	$PS_{\text{cell}}$	$PE_{\text{cell}} [\text{cm}/\text{min}]$	$PE_{\text{cell}} [\mu\text{m}/\text{min}]$
Cell1	29.19	11.08	0.06	17.85	0.0043	42.50
Cell2	29.19	12.61	0.05	22.19	0.0053	52.83
Cell3	29.19	14.03	0.04	27.00	0.0064	64.29
<b>Average</b>	<b>29.19</b>	<b>12.57</b>	<b>0.05</b>	<b>22.08</b>	<b>0.0053</b>	<b>53.21</b>
SD						10.90

Table 3.74 Determination of permeability coefficient of phenobarbital for time interval 0-5 minutes for cell layer only.

	$PS_{\text{all}}$	$1/PS_{\text{cell}}$	$PS_{\text{cell}}$	$PE_{\text{cell}} [\text{cm}/\text{min}]$	$PE_{\text{cell}} [\mu\text{m}/\text{min}]$
Cell1	11.08	0.09	11.08	0.0026	26.37
Cell2	12.61	0.08	12.61	0.0030	30.01
Cell3	14.03	0.07	14.03	0.0033	33.40
<b>Average</b>	<b>12.57</b>	<b>0.08</b>	<b>12.45</b>	<b>0.0030</b>	<b>29.93</b>
SD					3.51

Table 3.75 Determination of permeability coefficient of phenobarbital for time interval 0-5 minutes for membrane of insert with cells.

## Internal standard diazepam in the transport study of diltiazem/phenobarbital

The permeability of diazepam as a function of time was determined using the same principles as for diltiazem described above.

In the time interval 5-140 average permeability slope values for diazepam were:  $PS_{\text{control}} = 9.28 \mu\text{l}/\text{min}$ ,  $PS_{\text{all}} = 6.03 \mu\text{l}/\text{min}$  and  $PS_{\text{cell}} = 17.22 \mu\text{l}/\text{min}$ .  $PE_{\text{cell}}$  was  $41.93 \pm 9.36 \mu\text{m}/\text{min}$ .  $PE_{\text{all}}$  amounted to  $14.36 \pm 1.16 \mu\text{m}/\text{min}$ . EC reached to 289.72%. All values were calculated using equations from section 2.3.

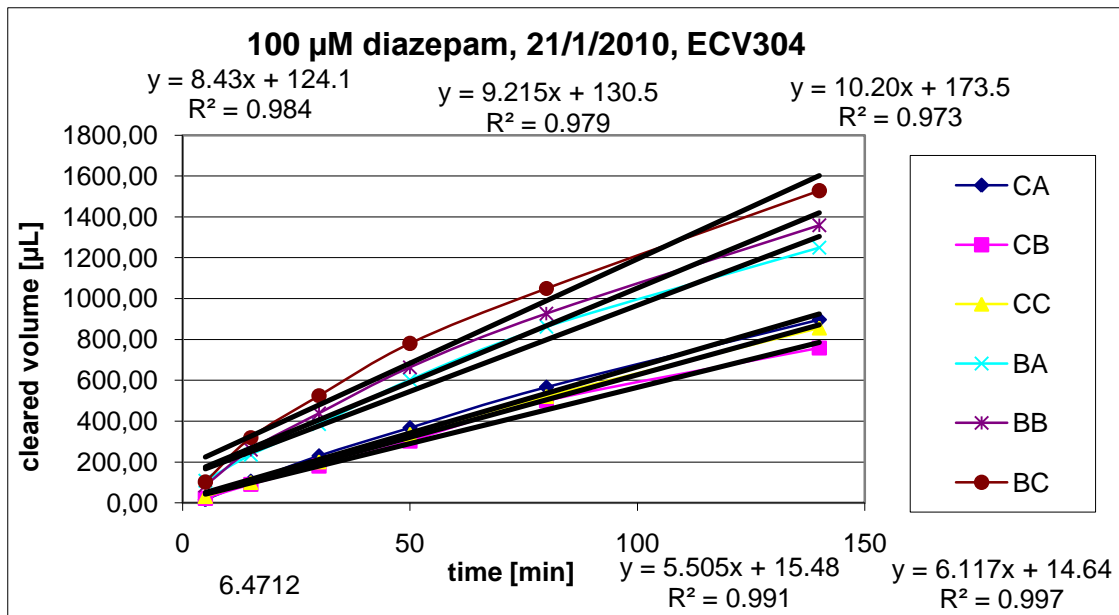


Figure 3.38 Dependence of cleared volume on the time interval 5-140 minutes for internal standard diazepam.

	$PS_{\text{Control}}$	$PS_{\text{all}}$	$1/PS_{\text{cell}}$	$PS_{\text{cell}}$	$PE_{\text{cell}}$ [cm/min]	$PE_{\text{cell}}$ [ $\mu\text{m}/\text{min}$ ]
Cell1	9.28	6.47	0.05	21.36	0.0051	50.87
Cell2	9.28	5.51	0.07	13.53	0.0032	32.21
Cell3	9.28	6.12	0.06	17.94	0.0043	42.72
<b>Average</b>	<b>9.28</b>	<b>6.03</b>	<b>0.06</b>	<b>17.22</b>	<b>0.0041</b>	<b>41.93</b>
SD						9.36

Table 3.76 Determination of permeability coefficient of diazepam for time interval 5-140 minutes for cell layer only.

	$PS_{\text{all}}$	$1/PS_{\text{cell}}$	$PS_{\text{cell}}$	$PE_{\text{cell}}$ [cm/min]	$PE_{\text{cell}}$ [ $\mu\text{m}/\text{min}$ ]
Cell1	6.47	0.15	6.47	0.0015	15.41
Cell2	5.51	0.18	5.51	0.0013	13.11
Cell3	6.12	0.16	6.12	0.0015	14.57
<b>Average</b>	<b>6.03</b>	<b>0.17</b>	<b>6.00</b>	<b>0.0014</b>	<b>14.36</b>
SD					1.16

Table 3.77 Determination of permeability coefficient of diazepam for time interval 5-140 minutes for membrane of insert with cells.

In the time interval 0-5 average permeability slope values for diazepam were:  $PS_{\text{control}} = 19.70 \mu\text{l}/\text{min}$ ,  $PS_{\text{all}} = 4.61 \mu\text{l}/\text{min}$  and  $PS_{\text{cell}} = 6.03 \mu\text{l}/\text{min}$ .  $PE_{\text{cell}}$  was  $14.78 \pm 6.43 \mu\text{m}/\text{min}$ .  $PE_{\text{all}}$  amounted to  $10.99 \pm 3.65 \mu\text{m}/\text{min}$ . EC reached to 131.52%. All values were calculated using equations from section 2.3.

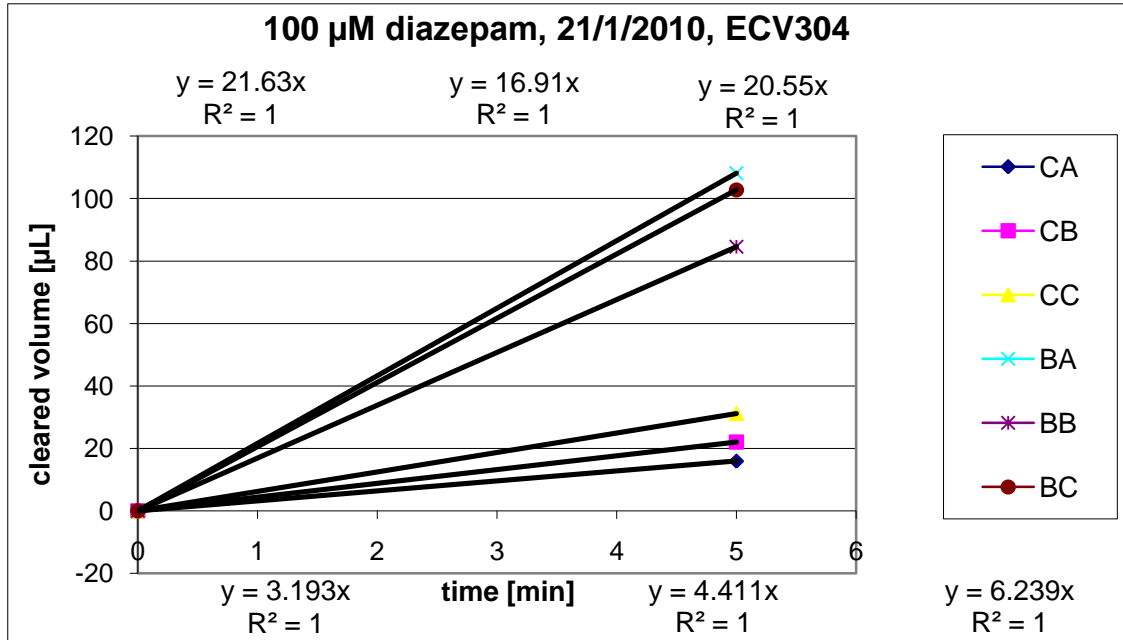


Figure 3.39 Dependence of cleared volume on the time interval 0-5 minutes for internal standard diazepam.

	$PS_{\text{Control}}$	$PS_{\text{all}}$	$1/PS_{\text{cell}}$	$PS_{\text{cell}}$	$PE_{\text{cell}}$ [cm/min]	$PE_{\text{cell}}$ [ $\mu\text{m}/\text{min}$ ]
Cell1	19.70	3.19	0.26	3.81	0.0009	9.07
Cell2	19.70	4.41	0.18	5.69	0.0014	13.54
Cell3	19.70	6.24	0.11	9.13	0.0022	21.74
<b>Average</b>	<b>19.70</b>	<b>4.61</b>	<b>0.17</b>	<b>6.03</b>	<b>0.0014</b>	<b>14.78</b>
SD						6.43

Table 3.78 Determination of permeability coefficient of diazepam for time interval 0-5 minutes for cell layer only.

	$PS_{\text{all}}$	$1/PS_{\text{cell}}$	$PS_{\text{cell}}$	$PE_{\text{cell}}$ [cm/min]	$PE_{\text{cell}}$ [ $\mu\text{m}/\text{min}$ ]
Cell1	3.19	0.31	3.19	0.0008	7.60
Cell2	4.41	0.23	4.41	0.0011	10.50
Cell3	6.24	0.16	6.24	0.0015	14.86
<b>Average</b>	<b>4.61</b>	<b>0.23</b>	<b>4.29</b>	<b>0.0010</b>	<b>10.99</b>
SD					3.65

Table 3.79 Determination of permeability coefficient of diazepam for time interval 0-5 minutes for membrane of insert with cells.

## Internal standard CF in the transport study of diltiazem/phenobarbital

The permeability of carboxyfluorescein as a function of time was determined using the same principles as for diltiazem described above.

In the time interval 5-140 average permeability slope values for carboxyfluorescein were:  $PS_{\text{control}} = 9.80 \mu\text{l}/\text{min}$ ,  $PS_{\text{all}} = 3.28 \mu\text{l}/\text{min}$  and  $PS_{\text{cell}} = 4.94 \mu\text{l}/\text{min}$ .  $PE_{\text{cell}}$  was  $11.79 \pm 1.22 \mu\text{m}/\text{min}$ .  $PE_{\text{all}}$  amounted to  $7.82 \pm 0.55 \mu\text{m}/\text{min}$ . EC reached to 150.54%. All values were calculated using equations from section 2.3.

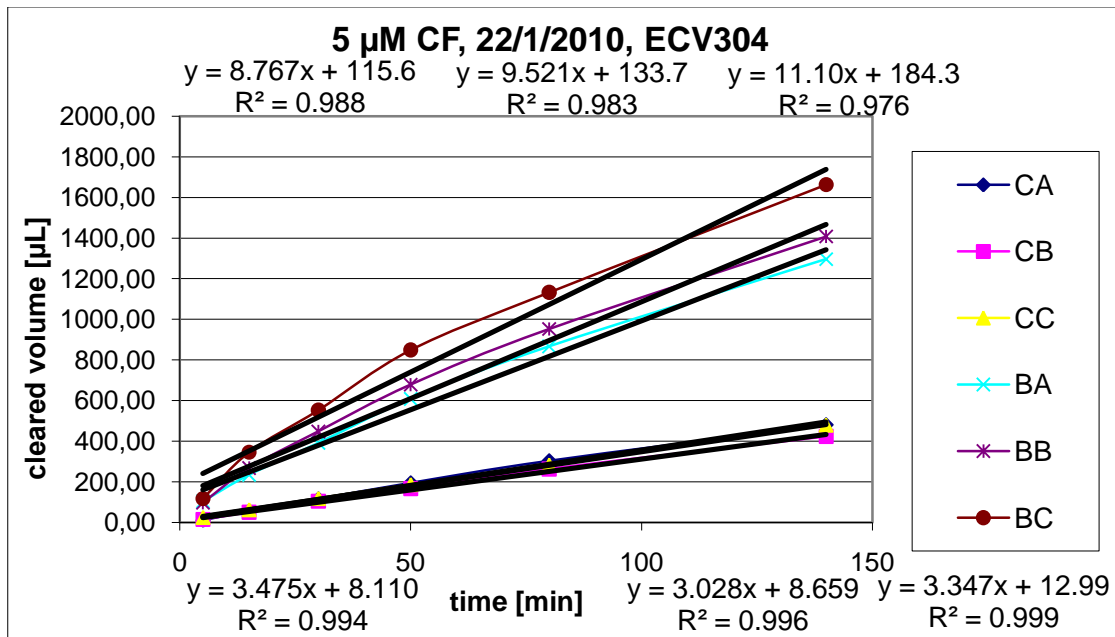


Figure 3.40 Dependence of cleared volume on the time interval 5-140 minutes for internal standard carboxyfluorescein.

	$PS_{\text{Control}}$	$PS_{\text{all}}$	$1/PS_{\text{cell}}$	$PS_{\text{cell}}$	$PE_{\text{cell}} [\text{cm}/\text{min}]$	$PE_{\text{cell}} [\mu\text{m}/\text{min}]$
Cell1	9.80	3.48	0.19	5.39	0.0013	12.82
Cell2	9.80	3.03	0.23	4.38	0.0010	10.44
Cell3	9.80	3.35	0.20	5.09	0.0012	12.11
<b>Average</b>	<b>9.80</b>	<b>3.28</b>	<b>0.20</b>	<b>4.94</b>	<b>0.0012</b>	<b>11.79</b>
SD						1.22

Table 3.80 Determination of permeability coefficient of carboxyfluorescein for time interval 5-140 minutes for cell layer only.

	$PS_{\text{all}}$	$1/PS_{\text{cell}}$	$PS_{\text{cell}}$	$PE_{\text{cell}} [\text{cm}/\text{min}]$	$PE_{\text{cell}} [\mu\text{m}/\text{min}]$
Cell1	3.48	0.29	3.48	0.0008	8.27
Cell2	3.03	0.33	3.03	0.0007	7.21
Cell3	3.35	0.30	3.35	0.0008	7.97
<b>Average</b>	<b>3.28</b>	<b>0.31</b>	<b>3.27</b>	<b>0.0008</b>	<b>7.82</b>
SD					0.55

Table 3.81 Determination of permeability coefficient of carboxyfluorescein for time interval 5-140 minutes for membrane of insert with cells.

In the time interval 0-5 average permeability slope values for carboxyfluorescein were:  $PS_{\text{control}} = 21.12 \mu\text{l}/\text{min}$ ,  $PS_{\text{all}} = 3.27 \mu\text{l}/\text{min}$  and  $PS_{\text{cell}} = 3.87 \mu\text{l}/\text{min}$ .  $PE_{\text{cell}}$  was  $9.45 \pm 4.67 \mu\text{m}/\text{min}$ .  $PE_{\text{all}}$  amounted to  $7.79 \pm 3.22 \mu\text{m}/\text{min}$ . EC reached to 118.79%. All values were calculated using equations from section 2.3.

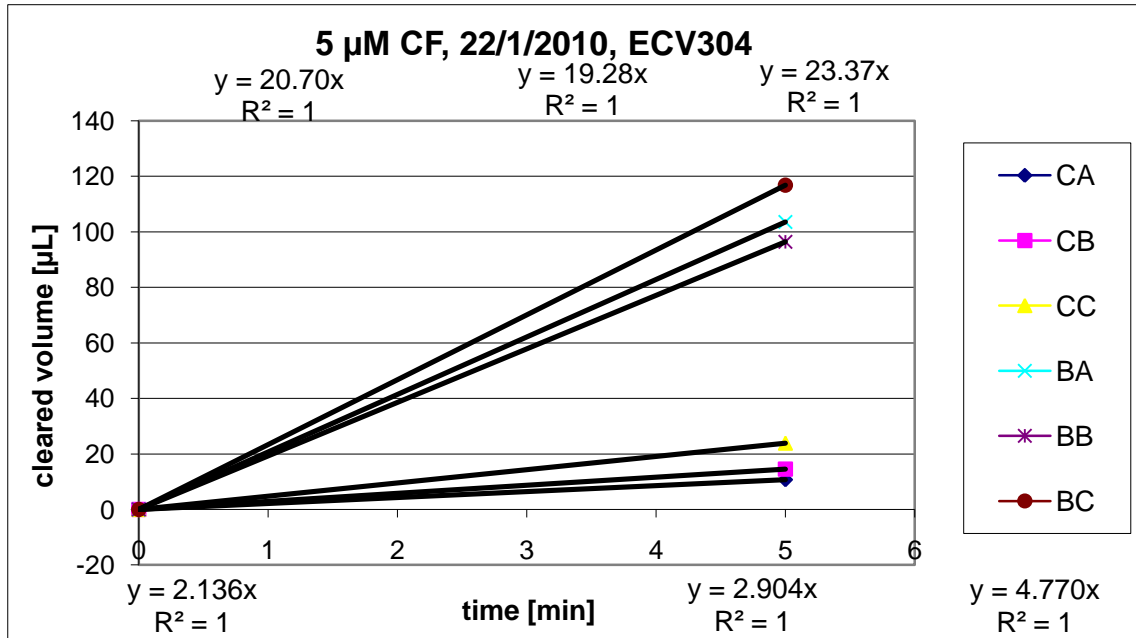


Figure 3.41 Dependence of cleared volume on the time interval 0-5 minutes for internal standard carboxyfluorescein.

	$PS_{\text{Control}}$	$PS_{\text{all}}$	$1/PS_{\text{cell}}$	$PS_{\text{cell}}$	$PE_{\text{cell}} [\text{cm}/\text{min}]$	$PE_{\text{cell}} [\mu\text{m}/\text{min}]$
Cell1	21.12	2.14	0.42	2.38	0.0006	5.66
Cell2	21.12	2.90	0.30	3.37	0.0008	8.02
Cell3	21.12	4.77	0.16	6.16	0.0015	14.67
<b>Average</b>	<b>21.12</b>	<b>3.27</b>	<b>0.26</b>	<b>3.87</b>	<b>0.0009</b>	<b>9.45</b>
SD						4.67

Table 3.82 Determination of permeability coefficient of carboxyfluorescein for time interval 0-5 minutes for cell layer only.

	$PS_{\text{all}}$	$1/PS_{\text{cell}}$	$PS_{\text{cell}}$	$PE_{\text{cell}} [\text{cm}/\text{min}]$	$PE_{\text{cell}} [\mu\text{m}/\text{min}]$
Cell1	2.14	0.47	2.14	0.0005	5.09
Cell2	2.90	0.34	2.90	0.0007	6.92
Cell3	4.77	0.21	4.77	0.0011	11.36
<b>Average</b>	<b>3.27</b>	<b>0.34</b>	<b>2.94</b>	<b>0.0007</b>	<b>7.79</b>
SD					3.22

Table 3.83 Determination of permeability coefficient of carboxyfluorescein for time interval 0-5 minutes for membrane of insert with cells.

### 3.8 Transport study of verapamil/phenobarbital – Group study

#### Verapamil in the transport study of verapamil/phenobarbital

Transport study of verapamil and phenobarbital was accomplished across the BBB in vitro model based on cell line ECV304. Amounts of permeated substance were quantified by HPLC. In the time interval 5-140 average permeability slope values for verapamil were:  $PS_{control} = 8.57 \mu\text{l}/\text{min}$ ,  $PS_{all} = 3.00 \mu\text{l}/\text{min}$  and  $PS_{cell} = 4.62 \mu\text{l}/\text{min}$ . The average permeability coefficient ( $PE_{cell}$ ) for cell layer  $11.02 \pm 0.48 \mu\text{m}/\text{min}$ .  $PE_{all}$  amounted to  $7.15 \pm 0.20 \mu\text{m}/\text{min}$ . EC reached to 153.98%. All values were calculated using equations from section 2.3.

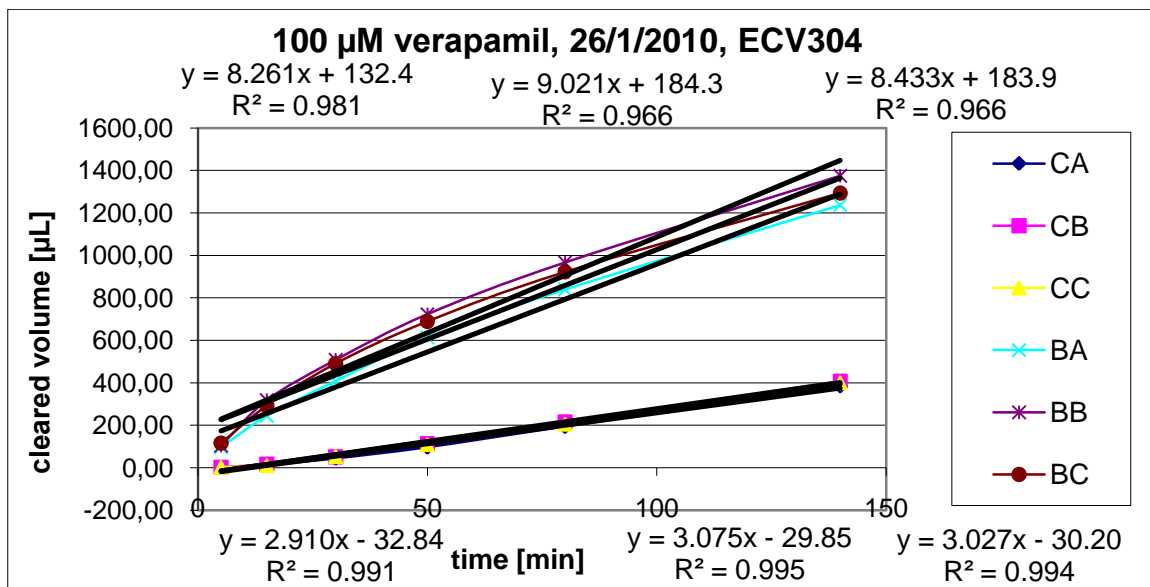


Figure 3.42 Dependence of cleared volume on the time interval 5-140 minutes for verapamil.

	$PS_{Control}$	$PS_{all}$	$1/PS_{cell}$	$PS_{cell}$	$PE_{cell} [\text{cm}/\text{min}]$	$PE_{cell} [\mu\text{m}/\text{min}]$
Cell1	8.57	2.91	0.23	4.41	0.0010	10.49
Cell2	8.57	3.08	0.21	4.80	0.0011	11.42
Cell3	8.57	3.03	0.21	4.68	0.0011	11.14
<b>Average</b>	<b>8.57</b>	<b>3.00</b>	<b>0.22</b>	<b>4.62</b>	<b>0.0011</b>	<b>11.02</b>
SD						0.48

Table 3.84 Determination of permeability coefficient of verapamil for time interval 5-140 minutes for cell layer only.

	$PS_{all}$	$1/PS_{cell}$	$PS_{cell}$	$PE_{cell} [\text{cm}/\text{min}]$	$PE_{cell} [\mu\text{m}/\text{min}]$
Cell1	2.91	0.34	2.91	0.0007	6.93
Cell2	3.08	0.33	3.08	0.0007	7.32
Cell3	3.03	0.33	3.03	0.0007	7.21
<b>Average</b>	<b>3.00</b>	<b>0.33</b>	<b>3.00</b>	<b>0.0007</b>	<b>7.15</b>
SD					0.20

Table 3.85 Determination of permeability coefficient of verapamil for time interval 5-140 minutes for membrane of insert with cells.

In the time interval 0-5 average permeability slope values for verapamil were:  $PS_{\text{control}} = 21.03 \mu\text{l}/\text{min}$ ,  $PS_{\text{all}} = 0.55 \mu\text{l}/\text{min}$  and  $PS_{\text{cell}} = 0.56 \mu\text{l}/\text{min}$ .  $PE_{\text{cell}}$  was  $1.33 \pm 0.28 \mu\text{m}/\text{min}$ .  $PE_{\text{all}}$  amounted to  $1.30 \pm 0.26 \mu\text{m}/\text{min}$ . EC reached to 102.66%. All values were calculated using equations from section 2.3.

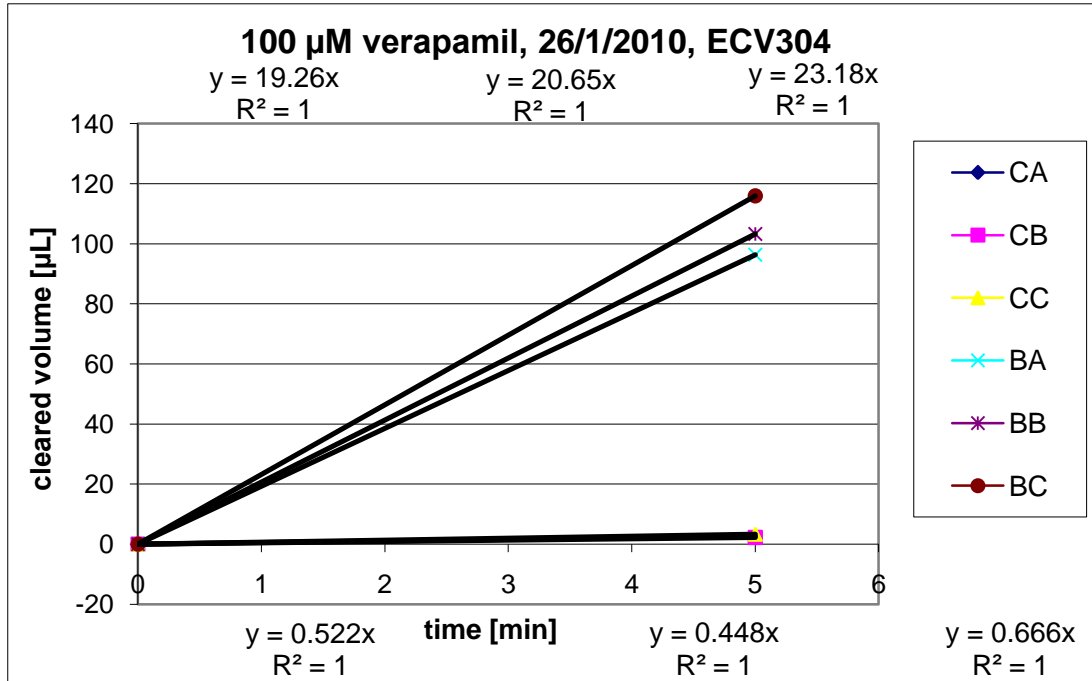


Figure 3.43 Dependence of cleared volume on the time interval 0-5 minutes for verapamil.

	$PS_{\text{Control}}$	$PS_{\text{all}}$	$1/PS_{\text{cell}}$	$PS_{\text{cell}}$	$PE_{\text{cell}} [\text{cm}/\text{min}]$	$PE_{\text{cell}} [\mu\text{m}/\text{min}]$
Cell1	21.03	0.52	1.87	0.54	0.0001	1.27
Cell2	21.03	0.45	2.18	0.46	0.0001	1.09
Cell3	21.03	0.67	1.45	0.69	0.0002	1.64
<b>Average</b>	<b>21.03</b>	<b>0.55</b>	<b>1.79</b>	<b>0.56</b>	<b>0.0001</b>	<b>1.33</b>
SD						0.28

Table 3.86 Determination of permeability coefficient of verapamil for time interval 0-5 minutes for cell layer only.

	$PS_{\text{all}}$	$1/PS_{\text{cell}}$	$PS_{\text{cell}}$	$PE_{\text{cell}} [\text{cm}/\text{min}]$	$PE_{\text{cell}} [\mu\text{m}/\text{min}]$
Cell1	0.52	1.92	0.52	0.0001	1.24
Cell2	0.45	2.23	0.45	0.0001	1.07
Cell3	0.67	1.50	0.67	0.0002	1.59
<b>Average</b>	<b>0.55</b>	<b>1.88</b>	<b>0.53</b>	<b>0.0001</b>	<b>1.30</b>
SD					0.26

Table 3.87 Determination of permeability coefficient of verapamil for time interval 0-5 minutes for membrane of insert with cells.

## Phenobarbital in the transport study of verapamil/phenobarbital

The permeability of phenobarbital as a function of time was determined using the same principles as for verapamil described above.

In the time interval 5-140 average permeability slope values for phenobarbital were:  $PS_{\text{control}} = 17.98 \mu\text{l}/\text{min}$ ,  $PS_{\text{all}} = 8.59 \mu\text{l}/\text{min}$  and  $PS_{\text{cell}} = 16.45 \mu\text{l}/\text{min}$ .  $PE_{\text{cell}}$  was  $39.17 \pm 1.31 \mu\text{m}/\text{min}$ .  $PE_{\text{all}}$  amounted to  $20.45 \pm 0.36 \mu\text{m}/\text{min}$ . EC reached to 191.50%. All values were calculated using equations from section 2.3.

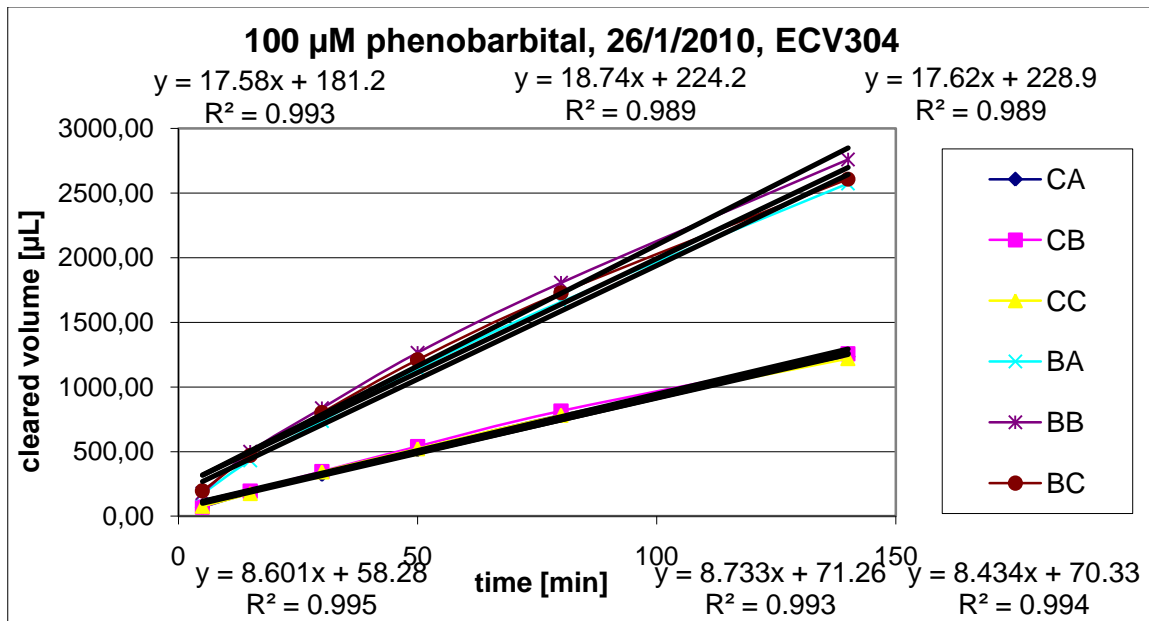


Figure 3.44 Dependence of cleared volume on the time interval 5-140 minutes for phenobarbital.

	$PS_{\text{Control}}$	$PS_{\text{all}}$	$1/PS_{\text{cell}}$	$PS_{\text{cell}}$	$PE_{\text{cell}}$ [cm/min]	$PE_{\text{cell}}$ [ $\mu\text{m}/\text{min}$ ]
Cell1	17.98	8.60	0.06	16.49	0.0039	39.26
Cell2	17.98	8.73	0.06	16.98	0.0040	40.43
Cell3	17.98	8.43	0.06	15.89	0.0038	37.82
<b>Average</b>	<b>17.98</b>	<b>8.59</b>	<b>0.06</b>	<b>16.45</b>	<b>0.0039</b>	<b>39.17</b>
SD						1.31

Table 3.88 Determination of permeability coefficient of phenobarbital for time interval 5-140 minutes for cell layer only.

	$PS_{\text{all}}$	$1/PS_{\text{cell}}$	$PS_{\text{cell}}$	$PE_{\text{cell}}$ [cm/min]	$PE_{\text{cell}}$ [ $\mu\text{m}/\text{min}$ ]
Cell1	8.60	0.12	8.60	0.0020	20.48
Cell2	8.73	0.11	8.73	0.0021	20.79
Cell3	8.43	0.12	8.43	0.0020	20.08
<b>Average</b>	<b>8.59</b>	<b>0.12</b>	<b>8.59</b>	<b>0.0020</b>	<b>20.45</b>
SD					0.36

Table 3.89 Determination of permeability coefficient of phenobarbital for time interval 5-140 minutes for membrane of insert with cells.

In the time interval 0-5 average permeability slope values for phenobarbital were:  $PS_{\text{control}} = 36.67 \mu\text{l}/\text{min}$ ,  $PS_{\text{all}} = 14.57 \mu\text{l}/\text{min}$  and  $PS_{\text{cell}} = 24.18 \mu\text{l}/\text{min}$ .  $PE_{\text{cell}}$  was  $57.76 \pm 6.65 \mu\text{m}/\text{min}$ .  $PE_{\text{all}}$  amounted to  $34.69 \pm 2.35 \mu\text{m}/\text{min}$ . EC reached to 166.15%. All values were calculated using equations from section 2.3.

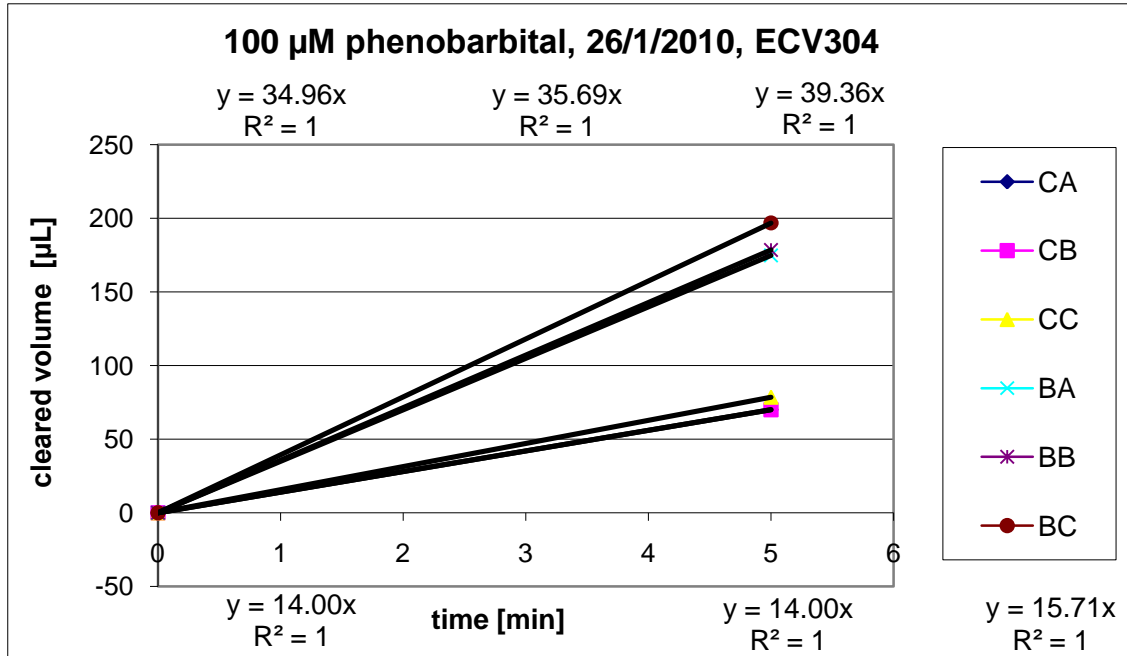


Figure 3.45 Dependence of cleared volume on the time interval 0-5 minutes for phenobarbital.

	$PS_{\text{Control}}$	$PS_{\text{all}}$	$1/PS_{\text{cell}}$	$PS_{\text{cell}}$	$PE_{\text{cell}} [\text{cm}/\text{min}]$	$PE_{\text{cell}} [\mu\text{m}/\text{min}]$
Cell1	36.67	14.00	0.04	22.65	0.0054	53.92
Cell2	36.67	14.00	0.04	22.65	0.0054	53.92
Cell3	36.67	15,71	0.04	27.49	0.0065	65.44
<b>Average</b>	<b>36.67</b>	<b>14.57</b>	<b>0,04</b>	<b>24.18</b>	<b>0.0058</b>	<b>57.76</b>
SD						6.65

Table 3.90 Determination of permeability coefficient of phenobarbital for time interval 0-5 minutes for cell layer only.

	$PS_{\text{all}}$	$1/PS_{\text{cell}}$	$PS_{\text{cell}}$	$PE_{\text{cell}} [\text{cm}/\text{min}]$	$PE_{\text{cell}} [\mu\text{m}/\text{min}]$
Cell1	14.00	0.07	14.00	0.0033	33.33
Cell2	14.00	0.07	14.00	0.0033	33.33
Cell3	15.71	0.06	15.71	0.0037	37.40
<b>Average</b>	<b>14.57</b>	<b>0.07</b>	<b>14.53</b>	<b>0.0035</b>	<b>34.69</b>
SD					2.35

Table 3.91 Determination of permeability coefficient of phenobarbital for time interval 0-5 minutes for membrane of insert with cells.

## Internal standard diazepam in the transport study of verapamil/phenobarbital

The permeability of diazepam as a function of time was determined using the same principles as for verapamil described above.

In the time interval 5-140 average permeability slope values for diazepam were:  $PS_{\text{control}} = 10.81 \mu\text{l}/\text{min}$ ,  $PS_{\text{all}} = 5.96 \mu\text{l}/\text{min}$  and  $PS_{\text{cell}} = 13.27 \mu\text{l}/\text{min}$ .  $PE_{\text{cell}}$  was  $31.61 \pm 0.23 \mu\text{m}/\text{min}$ .  $PE_{\text{all}}$  amounted to  $14.19 \pm 0.05 \mu\text{m}/\text{min}$ . EC reached to 222, . %. All values were calculated using equations from section 2.3.

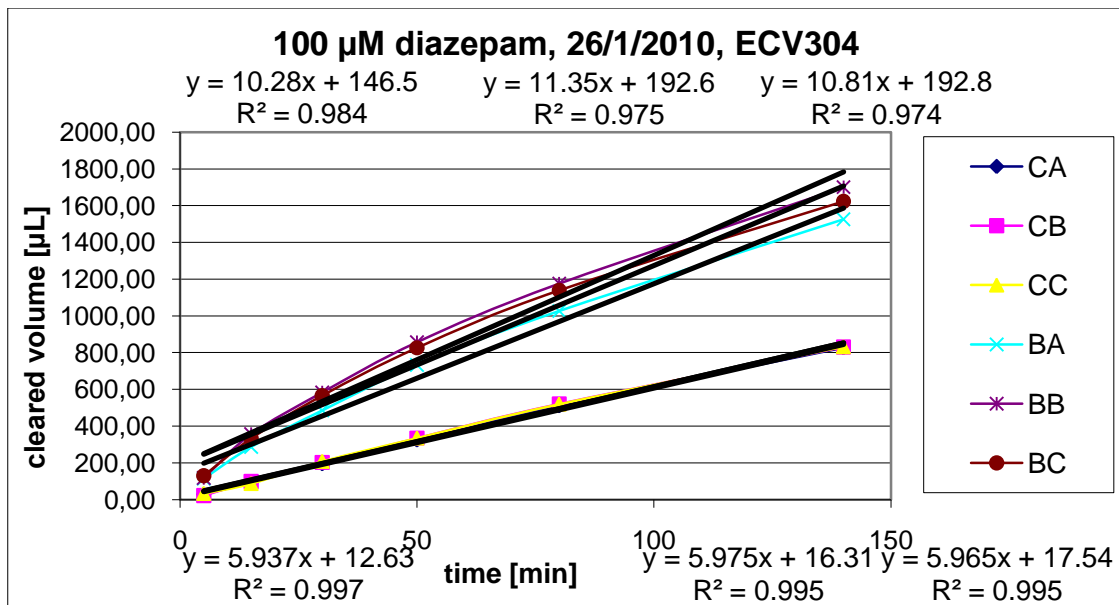


Figure 3.46 Dependence of cleared volume on the time interval 5-140 minutes for internal standard diazepam.

	$PS_{\text{Control}}$	$PS_{\text{all}}$	$1/PS_{\text{cell}}$	$PS_{\text{cell}}$	$PE_{\text{cell}}$ [cm/min]	$PE_{\text{cell}}$ [ $\mu\text{m}/\text{min}$ ]
Cell1	10.81	5.94	0.08	13.17	0.0031	31.35
Cell2	10.81	5.98	0.07	13.35	0.0032	31.79
Cell3	10.81	5.97	0.08	13.30	0.0032	31.68
<b>Average</b>	<b>10.81</b>	<b>5.96</b>	<b>0.08</b>	<b>13.27</b>	<b>0.0032</b>	<b>31.61</b>
SD						0.23

Table 3.92 Determination of permeability coefficient of diazepam for time interval 5-140 minutes for cell layer only.

	$PS_{\text{all}}$	$1/PS_{\text{cell}}$	$PS_{\text{cell}}$	$PE_{\text{cell}}$ [cm/min]	$PE_{\text{cell}}$ [ $\mu\text{m}/\text{min}$ ]
Cell1	5.94	0.17	5.94	0.0014	14.14
Cell2	5.98	0.17	5.98	0.0014	14.23
Cell3	5.97	0.17	5.97	0.0014	14.20
<b>Average</b>	<b>5.96</b>	<b>0.17</b>	<b>5.96</b>	<b>0.0014</b>	<b>14.19</b>
SD					0.05

Table 3.93 Determination of permeability coefficient of diazepam for time interval 5-140 minutes for membrane of insert with cells.

In the time interval 0-5 average permeability slope values for diazepam were:  $PS_{\text{control}} = 24.10 \mu\text{l}/\text{min}$ ,  $PS_{\text{all}} = 5.59 \mu\text{l}/\text{min}$  and  $PS_{\text{cell}} = 7.29 \mu\text{l}/\text{min}$ .  $PE_{\text{cell}}$  was  $17.51 \pm 4.30 \mu\text{m}/\text{min}$ .  $PE_{\text{all}}$  amounted to  $13.32 \pm 2.54 \mu\text{m}/\text{min}$ . EC reached to 130.52%. All values were calculated using equations from section 2.3.

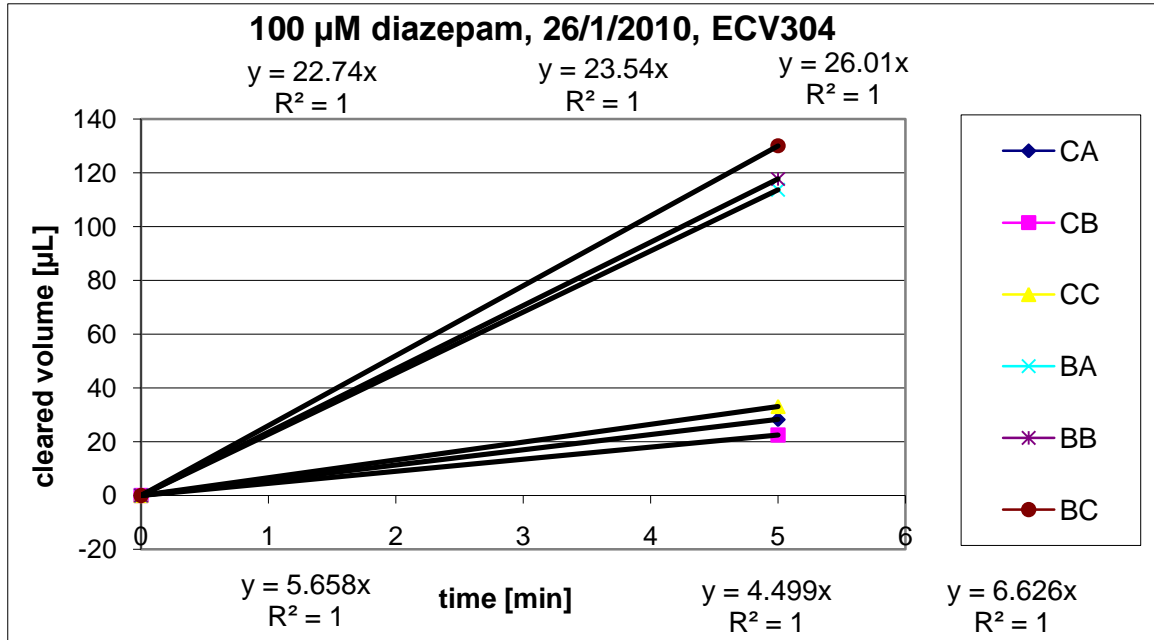


Figure 3.47 Dependence of cleared volume on the time interval 0-5 minutes for internal standard diazepam.

	$PS_{\text{Control}}$	$PS_{\text{all}}$	$1/PS_{\text{cell}}$	$PS_{\text{cell}}$	$PE_{\text{cell}} [\text{cm}/\text{min}]$	$PE_{\text{cell}} [\mu\text{m}/\text{min}]$
Cell1	24.10	5.66	0.14	7.39	0.0018	17.61
Cell2	24.10	4.50	0.18	5.53	0.0013	13.17
Cell3	24.10	6.63	0.11	9.14	0.0022	21.76
<b>Average</b>	<b>24.10</b>	<b>5.59</b>	<b>0.14</b>	<b>7.29</b>	<b>0.0017</b>	<b>17.51</b>
SD						4.30

Table 3.94 Determination of permeability coefficient of diazepam for time interval 0-5 minutes for cell layer only.

	$PS_{\text{all}}$	$1/PS_{\text{cell}}$	$PS_{\text{cell}}$	$PE_{\text{cell}} [\text{cm}/\text{min}]$	$PE_{\text{cell}} [\mu\text{m}/\text{min}]$
Cell1	5.66	0.18	5.66	0.0013	13.47
Cell2	4.50	0.22	4.50	0.0011	10.71
Cell3	6.63	0.15	6.63	0.0016	15.78
<b>Average</b>	<b>5.59</b>	<b>0.18</b>	<b>5.46</b>	<b>0.0013</b>	<b>13.32</b>
SD					2.54

Table 3.95 Determination of permeability coefficient of diazepam for time interval 0-5 minutes for membrane of insert with cells.

## Internal standard CF in the transport study of verapamil/phenobarbital

The permeability of carboxyfluorescein as a function of time was determined using the same principles as for verapamil described above.

In the time interval 5-140 average permeability slope values for carboxyfluorescein were:  $PS_{\text{control}} = 13.15 \mu\text{l}/\text{min}$ ,  $PS_{\text{all}} = 3.10 \mu\text{l}/\text{min}$  and  $PS_{\text{cell}} = 4.06 \mu\text{l}/\text{min}$ .  $PE_{\text{cell}}$  was  $9.67 \pm 0.617 \mu\text{m}/\text{min}$ .  $PE_{\text{all}}$  amounted to  $7.38 \pm 0.36 \mu\text{m}/\text{min}$ . EC reached to 130.88%. All values were calculated using equations from section 2.3.

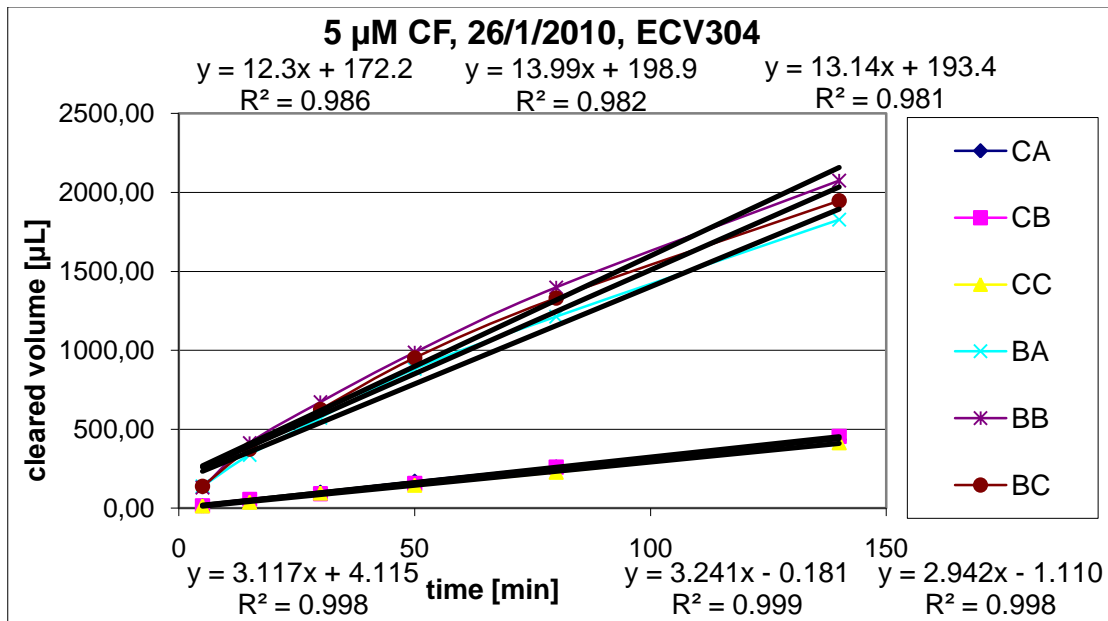


Figure 3.48 Dependence of cleared volume on the time interval 5-140 minutes for internal standard carboxyfluorescein.

	$PS_{\text{Control}}$	$PS_{\text{all}}$	$1/PS_{\text{cell}}$	$PS_{\text{cell}}$	$PE_{\text{cell}} [\text{cm}/\text{min}]$	$PE_{\text{cell}} [\mu\text{m}/\text{min}]$
Cell1	13.15	3.12	0.24	4.09	0.0010	9.73
Cell2	13.15	3.24	0.23	4.30	0.0010	10.24
Cell3	13.15	2.94	0.26	3.79	0.0009	9.02
<b>Average</b>	<b>13.15</b>	<b>3.10</b>	<b>0.25</b>	<b>4.06</b>	<b>0.0010</b>	<b>9.67</b>
SD						0.61

Table 3.96 Determination of permeability coefficient of carboxyfluorescein for time interval 5-140 minutes for cell layer only.

	$PS_{\text{all}}$	$1/PS_{\text{cell}}$	$PS_{\text{cell}}$	$PE_{\text{cell}} [\text{cm}/\text{min}]$	$PE_{\text{cell}} [\mu\text{m}/\text{min}]$
Cell1	3.12	0.32	3.12	0.0007	7.42
Cell2	3.24	0.31	3.24	0.0008	7.72
Cell3	2.94	0.34	2.94	0.0007	7.01
<b>Average</b>	<b>3.10</b>	<b>0.32</b>	<b>3.10</b>	<b>0.0007</b>	<b>7.38</b>
SD					0.36

Table 3.97 Determination of permeability coefficient of carboxyfluorescein for time interval 5-140 minutes for membrane of insert with cells.

In the time interval 0-5 average permeability slope values for carboxyfluorescein were:  $PS_{\text{control}} = 27.10 \mu\text{l}/\text{min}$ ,  $PS_{\text{all}} = 2.91 \mu\text{l}/\text{min}$  and  $PS_{\text{cell}} = 3.26 \mu\text{l}/\text{min}$ .  $PE_{\text{cell}}$  was  $7.78 \pm 0.74 \mu\text{m}/\text{min}$ .  $PE_{\text{all}}$  amounted to  $6.94 \pm 0.59 \mu\text{m}/\text{min}$ . EC reached to 112.05%. All values were calculated using equations from section 2.3.

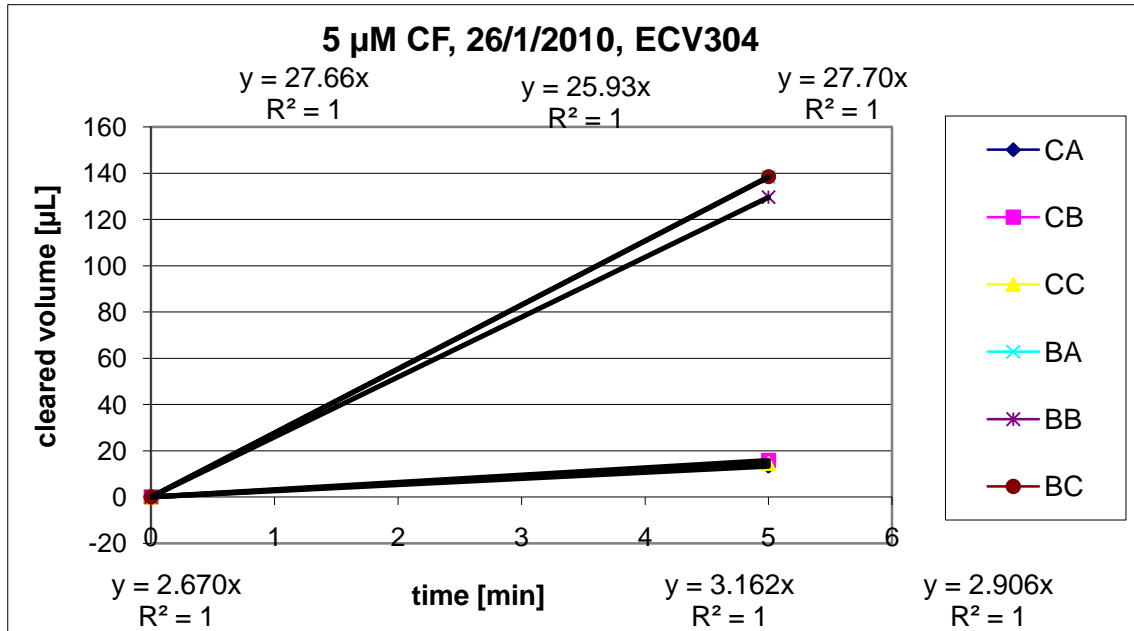


Figure 3.49 Dependence of cleared volume on the time interval 0-5 minutes for internal standard carboxyfluorescein.

	$PS_{\text{Control}}$	$PS_{\text{all}}$	$1/PS_{\text{cell}}$	$PS_{\text{cell}}$	$PE_{\text{cell}} [\text{cm}/\text{min}]$	$PE_{\text{cell}} [\mu\text{m}/\text{min}]$
Cell1	27.10	2.67	0.34	2.96	0.0007	7.05
Cell2	27.10	3.16	0.28	3.58	0.0009	8.52
Cell3	27.10	2.91	0.31	3.26	0.0008	7.75
<b>Average</b>	<b>27.10</b>	<b>2.91</b>	<b>0.31</b>	<b>3.26</b>	<b>0.0008</b>	<b>7.78</b>
SD						0.74

Table 3.98 Determination of permeability coefficient of carboxyfluorescein for time interval 0-5 minutes for cell layer only.

	$PS_{\text{all}}$	$1/PS_{\text{cell}}$	$PS_{\text{cell}}$	$PE_{\text{cell}} [\text{cm}/\text{min}]$	$PE_{\text{cell}} [\mu\text{m}/\text{min}]$
Cell1	2.67	0.37	2.67	0.0006	6.36
Cell2	3.16	0.32	3.16	0.0008	7.53
Cell3	2.91	0.34	2.91	0.0007	6.92
<b>Average</b>	<b>2.91</b>	<b>0.34</b>	<b>2.90</b>	<b>0.0007</b>	<b>6.94</b>
SD					0.59

Table 3.99 Determination of permeability coefficient of carboxyfluorescein for time interval 0-5 minutes for membrane of insert with cells.

## 3.9 Summary of transport study results

### 3.9.1 Single studies

Substance	PS <sub>control</sub> [μl/min]	PS <sub>all</sub> [μl/min]	PS <sub>cell</sub> [μl/min]	PE <sub>all</sub> [μm/min]	PE <sub>cell</sub> [μm/min]	EC [%]
verapamil* diazepam CF	7.25±0.61	3.36±0.28	6.27±0.99	8.01±0.66	15.05±3.36	187.18±13.70
	9.94±0.70	6.01±0.19	15.21±1.24	14.31±0.46	36.31±2.94	253.40±12.43
	12.28±0.59	2.20±0.30	3.80±0.52	6.91±0.71	9.07±1.23	131.03±4.23
diltiazem diazepam CF	8.93±1.34	3.61±0.21	6.06±0.60	8.59±0.50	14.46±1.43	168.02±6.75
	11.01±1.17	6.03±0.22	13.33±1.05	14.36±0.52	31.80±2.49	221.28±9.49
	11.97±2.14	2.77±0.49	3.61±0.84	6.60±1.16	8.65±1.99	130.36±6.99
nifedipine diazepam CF	46.05±12.23	11.76±0.35	15.79±0.64	27.99±0.84	37.60±1.52	134.30±1.38
	9.36±0.63	5.12±0.17	11.63±0.86	12.34±0.40	27.75±2.04	224.56±9.17
	9.98±0.69	2.37±0.05	3.10±0.08	5.63±0.11	7.38±0.19	131.04±0.78
phenobarbital diazepam CF	11.34±0.51	4.74±0.14	8.13±0.41	11.28±0.34	19.38±3.98	171.76±43.64
	10.58±0.44	5.81±0.38	12.92±1.94	13.84±0.91	31.00±4.62	223.12±18.34
	10.66±0.40	2.22±0.16	2.81±0.26	5.29±0.38	6.70±0.61	126.52±2.42
memantine** diazepam CF	5.52±1.04	3.57±0.52	10.12±4.73	8.50±1.23	26.06±11.26	298.37±85.72
	4.16±0.72	3.07±0.31	11.74±4.78	7.31±0.75	29.59±11.37	398.79±114.8
	5.20±0.15	2.29±0.20	4.09±0.63	5.45±0.48	9.80±1.51	179.11±12.17
amantadine diazepam CF	7.25±0.89	3.42±0.22	6.48±0.77	8.14±0.53	15.49±1.83	189.73±10.58
	6.01±0.38	4.27±0.19	14.72±2.21	10.16±0.45	35.42±5.26	347.65±36.77
	9.52±0.81	2.60±0.09	3.58±0.16	6.19±0.21	8.52±0.39	137.60±1.72

Table 3.100 The fastness of the used calcium channels blockers and internal standards within every single transport study in the time interval 5-140 minutes.

\* The interval 8-140 minutes was used for calculation.

\*\* Only values from time points 30 and 60 minutes were included to calculation.

Substance	PS <sup>control</sup> [μl/min]	PS <sup>all</sup> [μl/min]	PS <sup>cell</sup> [μl/min]	PF <sup>all</sup> [μm/min]	PF <sup>cell</sup> [μm/min]	EC [%]
verapamil*	28.28±1.33	3.36±0.68	3.81±0.88	8.00±1.62	9.12±2.09	113.55±3.11
diazepam	33.37±1.08	8.95±2.33	12.22±4.15	21.30±5.55	29.73±9.89	137.41±12.45
CF	23.65±2.47	2.15±0.63	2.36±0.75	5.10±1.49	5.65±1.78	110.04±3.16
diltiazem	19.25±5.42	1.19±0.23	1.27±0.26	2.83±0.55	3.02±0.62	106.59±1.35
diazepam	22.84±5.38	4.89±1.09	6.21±1.82	11.63±2.60	14.97±4.33	127.54±7.96
CF	23.37±6.15	2.66±0.89	3.00±1.11	6.33±2.13	7.22±2.65	112.96±4.76
nifedipine	50.54±11.28	5.09±0.35	5.67±1.18	12.13±2.29	13.53±2.81	111.24±2.34
diazepam	24.64±4.18	4.96±0.78	6.20±1.25	11.80±1.86	14.85±2.98	125.31±5.08
CF	26.05±5.72	2.89±0.20	3.24±0.25	6.87±0.47	7.73±0.48	112.46±0.96
phenobarbital	30.43±3.41	3.56±0.61	4.03±0.77	8.47±1.45	9.62±1.84	113.27±2.54
diazepam	28.73±3.49	4.86±0.49	5.85±0.71	11.57±1.16	13.95±1.70	120.40±2.48
CF	29.95±3.61	1.85±0.57	1.97±0.64	4.40±1.35	4.71±1.53	106.61±2.15
memantine diazepam CF	-	-	-	-	-	-
amantadine diazepam CF	23.43±1.88 18.98±1.13 26.71±2.14	2.39±0.18 5.16±0.71 2.46±0.51	2.66±0.22 7.09±1.33 2.71±0.63	5.70±0.43 12.28±1.70 5.85±1.22	6.35±0.53 16.98±3.17 6.47±1.50	111.38±0.95 137.58±7.01 110.17±2.36

Table 3.101 The fastness of the used calcium channels blockers and internal standards within every single transport study in the time interval 0-5 minutes.

\*The interval 8-140 minutes was used for calculation.

Substance	Ratio PE <sub>cell</sub> /CF	Ratio PE <sub>al</sub> /CF	Ratio PE <sub>cell</sub> /Diaz.	Ratio PE <sub>al</sub> /Diaz.	Ratio PE <sub>cell</sub> Diaz/C F	Ratio PE <sub>al</sub> Diaz/ CF
verapamil*	1.66±0.14	1.16±0.07	0.42±0.07	0.56±0.05	4.04±0.49	2.08±0.19
diltiazem	1.70±0.21	1.32±0.15	0.45±0.02	0.60±0.02	3.76±0.67	2.21±0.30
nifedipine	5.09±0.24	4.97±0.18	1.36±0.05	2.27±0.01	3.77±0.26	2.20±0.07
phenobarbital	2.91±0.28	2.14±0.16	0.63±0.07	0.82±0.04	4.67±0.99	2.63±0.31
mementine**	2.70±1.14	2.57±0.27	0.69±0.11	1.05±0.05	3.28±1.89	1.51±0.31
amantadine	1.81±0.14	1.31±0.04	0.44±0.02	0.80±0.02	4.14±0.44	1.64±0.02

Substance	Ratio PE <sub>cell</sub> /CF	Ratio PE <sub>al</sub> /CF	Ratio PE <sub>cell</sub> /Diaz.	Ratio PE <sub>al</sub> /Diaz.	Ratio PE <sub>cell</sub> Diaz/ CF	Ratio PE <sub>al</sub> Diaz/ CF
verapamil*	1.75±0.70	1.68±0.62	0.33±0.14	0.39±0.13	5.25±0.60	4.20±0.37
diltiazem	0.45±0.12	0.47±0.11	0.21±0.05	0.25±0.05	2.29±0.98	2.00±0.78
nifedipine	1.77±0.47	1.78±0.43	0.91±0.11	1.03±0.11	3.93±3.10	3.37±2.57
phenobarbital	2.11±0.32	1.99±0.31	0.69±0.12	0.73±0.11	3.17±0.97	2.79±0.83
mementine	-	-	-	-	-	-
amantadine	1.00±0.15	0.99±0.14	0.38±0.05	0.47±0.04	2.67±0.50	2.13±0.35

Table 3.102 Different ratios between substance, diazepam and carboxyfluorescein in time interval 5-140 minutes (left) and 0-5 minute (right).

\*The intervals 8-140 and 0-8 minutes were used for calculation.

\*\* Only values from time points 30 and 60 minutes were included to calculation.

### 3.9.2 Group studies

Substance	PS <sub>control</sub> [μl/min]	PS <sub>all</sub> [μl/min]	PS <sub>cell</sub> [μl/min]	PE <sub>all</sub> [μm/min]	PE <sub>cell</sub> [μm/min]	EC [%]
verapamil	8.57±0.40	3.00±0.08	4.62±0.20	7.15±0.20	11.02±0.48	153.98±2.33
phenobarbital	17.98±0.66	8.59±0.15	16.44±0.55	20.45±0.36	39.17±1.31	191.50±3.05
diazepam	10.81±0.54	5.96±0.02	13.27±0.10	14.19±0.05	31.61±0.23	222.76±0.90
CF	13.15±0.85	3.10±0.15	4.06±0.26	7.38±0.36	9.67±0.61	130.88±1.95
diltiazem	8.46±0.74	4.00±0.49	7.58±1.81	9.52±1.16	18.36±4.30	191.16±21.38
phenobarbital	13.58±0.91	7.66±0.43	17.57±2.24	18.23±1.02	42.09±5.33	230.21±16.49
diazepam	9.29±0.89	6.03±0.49	17.22±3.93	14.36±1.16	41.93±9.36	289.72±42.33
CF	9.80±1.19	3.28±0.23	4.94±0.51	7.82±0.55	11.79±1.22	150.54±5.25

Substance	PS <sub>control</sub> [μl/min]	PS <sub>all</sub> [μl/min]	PS <sub>cell</sub> [μl/min]	PE <sub>all</sub> [μm/min]	PE <sub>cell</sub> [μm/min]	EC [%]
verapamil	21.03±1.99	0.55±0.11	0.56±0.12	1.30±0.26	1.33±0.28	102.66±0.56
phenobarbital	34.67±2.36	14.57±0.99	24.18±2.79	34.69±2.35	57.76±6.65	166.15±7.62
diazepam	24.10±1.70	5.59±1.06	7.29±1.80	13.32±3.54	17.51±4.30	130.52±7.49
CF	27.10±1.01	2.91±0.25	3.26±0.31	6.94±0.59	7.78±0.74	112.05±1.14
diltiazem	18.24±2.67	1.10±0.87	1.17±1.01	2.63±2.07	2.88±2.40	106.63±5.52
phenobarbital	29.19±2.31	12.57±1.48	22.08±4.58	29.93±3.51	53.21±10.90	176.56±15.68
diazepam	19.70±2.47	2.61±1.53	6.03±2.70	10.99±3.65	14.78±6.43	131.52±13.70
CF	21.12±2.08	3.27±1.35	3.87±1.96	7.79±3.22	9.45±4.67	118.79±9.29

Table 3.103 The fastness of the used calcium channels blockers and internal standards within every group transport study in the time intervals 5-140 minutes (left) and 0-5 minutes (right).

Substance	Ratio PE <sub>cell</sub> /CF	Ratio PE <sub>all</sub> /CF	Ratio PE <sub>cell</sub> /Diaz	Ratio PE <sub>all</sub> /Diaz	Ratio PE <sub>cell</sub> Diaz/CF	Ratio PE <sub>all</sub> Diaz/CF
verapamil phenobarbital	1.14±0.08 4.05±0.12	0.99±0.04 2.83±0.12	0.35±0.01 1.24±0.04	0.50±0.01 1.44±0.02	3.28±0.21	1.93±0.09
diltiazem phenobarbital	1.54±0.22 3.56±0.09	1.21±0.07 2.33±0.12	0.44±0.02 1.02±0.10	0.50±0.01 1.44±0.02	3.53±0.44	1.84±0.02

Substance	Ratio PE <sub>cell</sub> /CF	Ratio PE <sub>all</sub> /CF	Ratio PE <sub>cell</sub> /Diaz.	Ratio PE <sub>all</sub> /Diaz	Ratio PE <sub>cell</sub> Diaz/CF	Ratio PE <sub>all</sub> Diaz/CF
verapamil phenobarbital	0.17±0.04 7.47±1.07	0.19±0.04 5.03±0.52	0.08±0.01 3.39±0.61	0.10±0.00 2.65±0.40	2.28±0.66	1.94±0.46
diltiazem phenobarbital	0.27±0.11 6.16±1.61	0.30±0.13 4.16±1.13	0.17±0.08 3.85±0.87	0.22±0.11 2.86±0.61	1.59±0.10	1.44±0.12

Table 3.104 Different ratios between substance, diazepam and carboxyfluorescein in time interval 5-140 minutes (left) and 0-5 minutes (right).

### 3.9.3 Ranking of substances according to the fastness (RatioPE<sub>cell</sub>/Diaz)

#### 3.9.3.1 Single studies

The following Table 3.105 and Figures 3.50 and 3.51 displays that nifedipine permeated faster than diazepam in time interval 5-140 minutes but in time interval 0-5 minutes nifedipine was slower than diazepam. Furthermore we can compare fastness of all tested substances.

5-140 minutes		0-5 minutes	
Substance	PE <sub>cell</sub> /Diaz	Substance	PE <sub>cell</sub> /Diaz
nifedipine	1.36±0.05	diazepam	1
diazepam	1	nifedipine	0.91±0.11
memantine	0.69±0.11	phenobarbital	0.69±0.12
phenobarbital	0.63±0.07	amantadine	0.38±0.05
diltiazem	0.45±0.02	verapamil	0.33±0.14
amantadine	0.44±0.02	diltiazem	0.21±0.05
verapamil	0.42±0.07	memantine	-

Table 3.105 The substances used in each single transport study are ordered according to the PE<sub>cell</sub>/Diaz in the time intervals 0-5 and 5-140 minutes. Here, it is demonstrated which substances are faster or slower

\*The intervals 8-140 and 0-8 minutes were used for calculation.

\*\* Only values from transfer intervals 30 and 60 minutes were included to calculation.

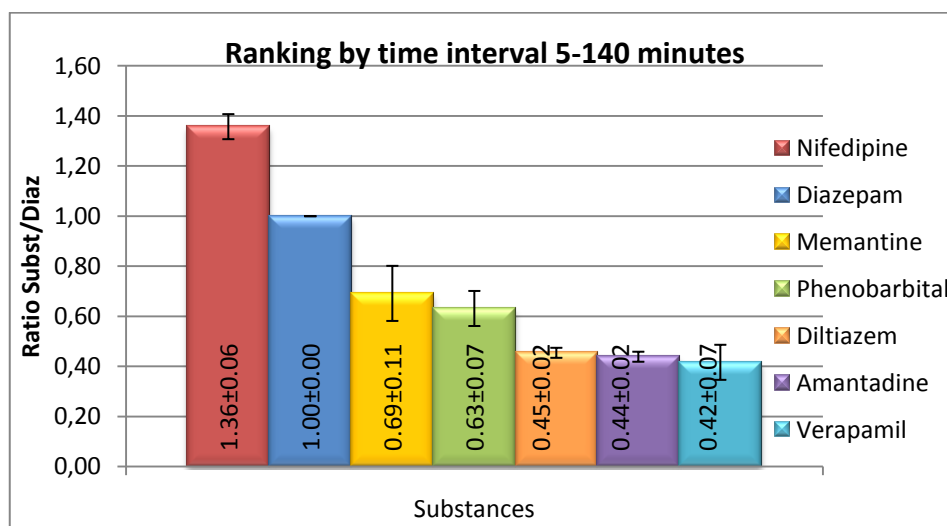


Figure 3.50 shows ranking of used substances against fastness (ratio PE<sub>cell</sub>/Diaz) in the time interval 5-140 minutes.

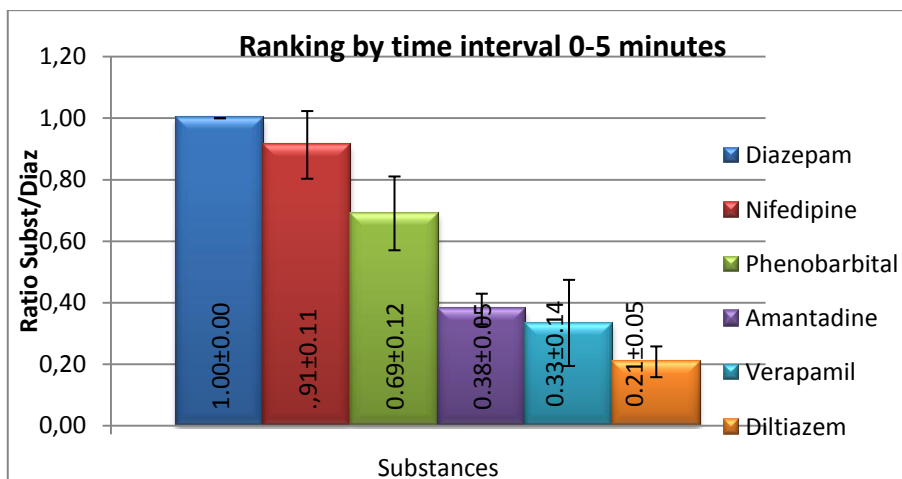


Figure 3.51 shows ranking of used substances against fastness (ratio  $PE_{cell}/Diaz$ ) in the time interval 0-5 minutes.

### 3.9.3.2 Group studies

The following Table 3.106 displays that phenobarbital permeated faster than internal standard diazepam when its transport abilities were tested together with verapamil or diltiazem. The figures 3.52 and 3.53 demonstrate the faster permeation of phenobarbital in group studies, it means when transported together with diltiazem or verapamil, than in single studies.

5-140 minutes		0-5 minutes	
Substance	$PE_{cell}/Diaz$	Substance	$PE_{cell}/Diaz$
diltiazem	0.44±0.02	diltiazem	0.17±0.08
phenobarbital	1.02±0.10	phenobarbital	3.85±0.87
diazepam	1	diazepam	1
CF	0.29±0.04	CF	0.63±0.04
verapamil	0.35±0.01	verapamil	0.08±0.01
phenobarbital	1.24±0.04	phenobarbital	3.39±0.61
diazepam	1	diazepam	1
CF	0.31±0.02	CF	0.47±0,16

Table 3.106 the substances used in each single transport study are ordered according to the ratio  $PE_{cell}/Diaz$  in the time intervals 0-5 and 5-140 minutes.

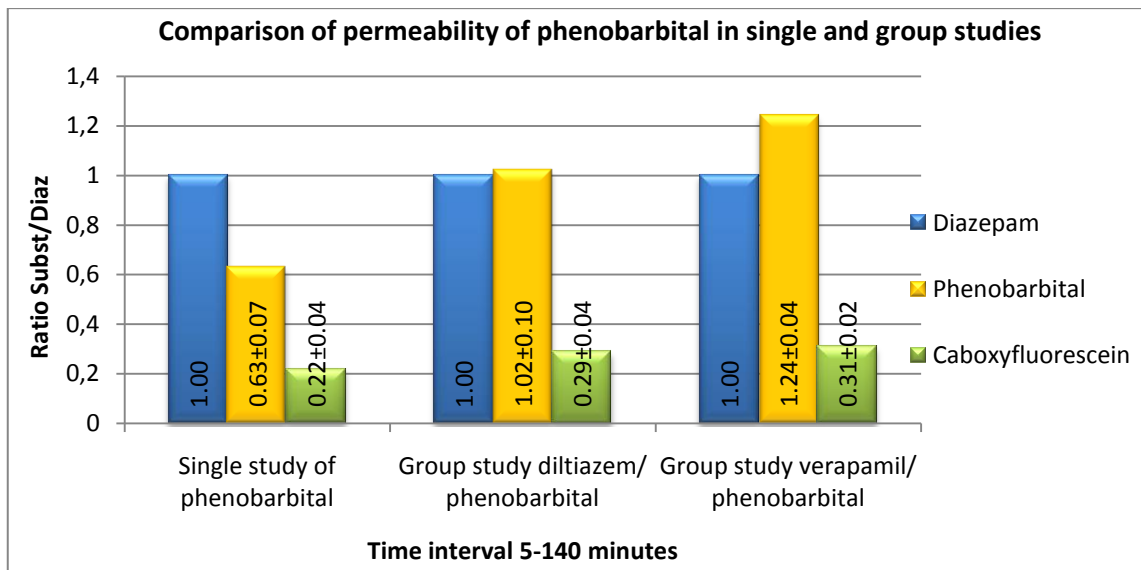


Figure 3.52 this graph for time interval 5-140 minutes shows how is permeability of phenobarbital influenced by verapamil or diltiazem in group studies in comparison to single study.

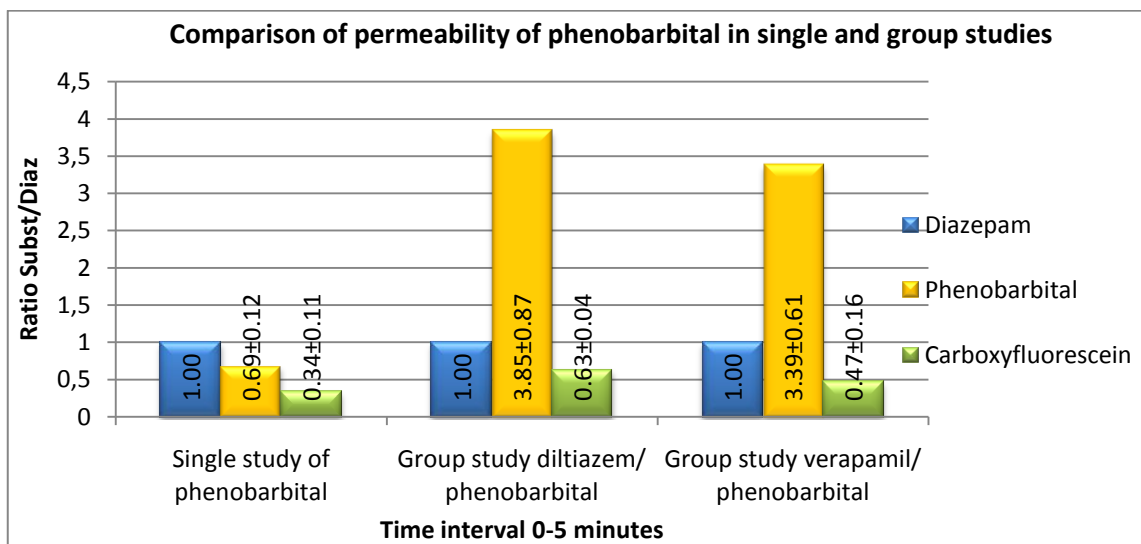


Figure 3.53 this graph for time interval 0-5 minutes shows how is permeability of phenobarbital influenced by verapamil or diltiazem in group studies in comparison to single study.

### 3.9.4 Measurement of the TEER during transport studies

TEER values for control inserts and inserts with cells were measured in medium and in HBSS solution before and after each transport study. From the obtained data TEER values for each cell layer were calculated (Table 3.107 and Table 3.108) using equation from section 2.3, this values reflects integrity of the cell layer therefore they should not significantly change during transport study.

Single studies	TEER [ $\Omega\text{cm}^2$ ]			
	Cells before transport study in medium (room temp.)	Cells before transport study in HBSS (37°C)	Cells immediately after transport study in HBSS (37°C)	Cells 1 hour after transport study in medium (room temp.)
verapamil	127.40±4.20	44.80±8.70	44.80±2.42	138.60±2.42
diltiazem	109.20±4.20	50.40±6.42	46.20±2.42	98.00±8.40
nifedipine	128.80±2.42	60.20±6.42	63.00±2.42	128.80±2.42
phenobarbital	114.80±6.42	82.60±6.42	81.20±4.85	134.40±7.27
memantine	127.40±8.74	74.20±4.20	75.60±11.11	123.20±6.42
amantadine	103.60±4.20	63.00±6.42	70.00±6.42	117.60±2.42

Table 3.107 TEER values for each cell layer measured before and after each single transport study.

Group studies	TEER [ $\Omega\text{cm}^2$ ]			
	Cells before transport study in medium (room temp.)	Cells before transport study in HBSS (37°C)	Cells immediately after transport study in HBSS (37°C)	Cells 1 hour after transport study in medium (room temp.)
verapamil/ phenobarbital	107.80±2.42	44.80±2.42	42.00±4.20	127.40±8.40
diltiazem/ phenobarbital	98.00±8.74	44.80±6.42	47.60±8.40	121.80±2.42

Table 3.108 TEER values for each cell layer measured before and after each group transport study.

## 4 DISCUSSION AND CONCLUSIONS

On the one hand this thesis was aimed at investigating and comparing the abilities of chosen ion channel blockers to overcome the BBB. The results were obtained from 6 single studies where the transport of verapamil, diltiazem, nifedipine, phenobarbital, memantine and amantadine were studied. On the other hand we wanted to find out the interference between chosen ion channel antagonists. For this purpose an antiepileptic agent phenobarbital was chosen as a representative drug used in therapy, because of its acting within the CNS, and two group studies were made to see if the fastness of phenobarbital to cross the BBB is influenced by verapamil or diltiazem, which represent the drugs acting in periphery (with effect on heart and blood vessels). The substances were chosen according to their ability to influence the level of calcium, and the adverse effects within CNS were important deciding factor, too, because they show that the substance is able to pass the brain. Therefore transport rates across the BBB and concentration of drugs in the CNS are important factors determining central effects of drugs (Vaněček, 2007).

The required data for each substance used in single and group studies were determined using the Transwell BBB in vitro model based on EVC304 cell line, where fluorescence measurement and RP-HPLC were used for quantification of amounts of permeated substances. The permeability slope (PS) values were determined by linear regression analysis using Microsoft Excel program and used for calculation of permeability coefficient (PE). Then the permeability coefficients of tested substances were compared with two internal standards in two time intervals (0-5 and 5-140 minutes). The internal standard diazepam was chosen because it is transported by passive diffusion and thus it could be used as general standard for substances permeability of which is independent from an active transport system (Neuhaus et al., 2006). On the other hand, the internal standard carboxyfluorescein was used as representative of the paracellular transport route. Therefore, both these substances were suitable comparative standards for tested substances.

TEER values for control inserts and inserts with cells were measured in medium and in HBSS solution before and after each transport study. TEER values for each cell layer were calculated from obtained values (using equation

from section 2.3) this values reflects integrity of the cell layer. Our TEER values were not significantly changed during transport study.

Ranking according to the  $PE_{cell}$  values for time interval 5-140 minutes was revealed after evaluation of data from single transport studies:

**nifedipine → diazepam → memantine → phenobarbital → amantadine → verapamil → diltiazem → carboxyfluorescein**

Unexpectedly, nifedipine was the fastest substance followed by diazepam, memantine, phenobarbital, amantadine, verapamil, diltiazem and carboxyfluorescein. With these results two hypotheses arose. Either it can correlate with higher lipophilicity of nifedipine in comparism to diazepam or nifedipine may be a substrate of an active transporter presented in cell layer of the Transwell model. For comparison of the substances used in single transport studies, the ratios  $PE_{cell}/PE_{cellDiaz.}$ , where the  $PE_{cell}$  values of each substance were normalized to the appropriate  $PE_{cell}$  values of diazepam, were established. This resulted in a quite similar ranking:

**nifedipine → diazepam → memantine → phenobarbital → diltiazem → amantadine → verapamil**

In the Table 4.1 the substance used in each single transport study are ranked according to the  $PE_{cell}$  values normalized to diazepam and their sites of acting are compared. Here is demonstrate that nifedipine as drug acting in periphery pass the BBB faster than internal standard diazepam and much more faster than other ion channel blockers acting in periphery, too. In clinical practice it can mean that nifedipine used for concrete clinical problem can have more CNS adverse effects in comparison to verapamil or diltiazem.

Time interval 5-140 minutes		
Substance	PE <sub>cell</sub> /Diaz	Site of acting
nifedipine	1.36±0.05	Periphery
diazepam	1	CNS
memantine	0.69±0.11	CNS
phenobarbital	0.63±0.07	CNS
diltiazem	0.45±0.02	Periphery
amantadine	0.44±0.02	CNS
verapamil	0.42±0.07	Periphery

Table 4.1 The substances used in each single transport study are ordered according to the PE<sub>cell</sub>/Diaz in the time interval 5-140 minutes. This table shows site of action in comparison to their PE<sub>cell</sub>/Diaz.

For completeness' sake, after normalization to the internal standard carboxyfluorescein a ranking was observed:

**nifedipine → phenobarbital → memantine → amantadine → diltiazem → verapamil → carboxyfluorescein**

Ranking according to the PE<sub>cell</sub> values for time interval 0-5 minutes was established, too:

**diazepam → nifedipine → phenobarbital → verapamil → amantadine → carboxyfluorescein → diltiazem**

In comparison to time interval 5-140 minutes, two interesting things were found. On the one hand, nifedipine was not faster than diazepam, and on the other hand, diltiazem was slower than carboxyfluorescein. This can point out that diltiazem could be restricted by an efflux system.

Ranking according to ratios PE<sub>cell</sub>/PE<sub>cell</sub> CF for this time interval was quite similar to ranking in time interval 5-140 minutes:

**nifedipine → phenobarbital → amantadine → verapamil → carboxyfluorescein → diltiazem**

Finally, ranking according to ratios PE<sub>cell</sub>/PE<sub>cell</sub>Diaz.:

**diazepam → nifedipine → phenobarbital → amantadine → verapamil → diltiazem**

Additionally, it must be mentioned that in transport study of verapamil some mistake occurred, and therefore the time intervals 0-8 and 8-140 minutes were used. Next, in transport study of memantine only values from transfer intervals

30 and 60 minutes were included to calculation and therefore the fastness of memantine to cross the BBB in time interval 0-5 could not be compared with other substances. It is also important to intimate that in transport study of nifedipine we had problems with analysis, because molecule of nifedipine is unstable and therefore we found lots of peaks. At first only peaks of nifedipine and then all peaks of disintegrated nifedipine were integrated and permeability coefficients were calculated. When we compared both permeability coefficients, they were quite similar and therefore we decided to choose only peaks of nifedipine for further calculation.

In the next step we tried to find about if the permeability properties of chosen ion channel blockers could correlate with  $\log P$  or  $\log D$  (for pH=7 and pH=8) values of each substance. The values are listed in the Table 4.2. Therefore the  $PE_{cell}$  values from time interval 5-140 minutes normalized to diazepam ( $PE_{cell}/Diaz$ ) or their logarithms ( $\log PE_{cell}/Diaz$ ) were entered to the graphs in dependence to  $\log P$  or  $\log D$  (for pH=7 and pH=8) and after linear regression analysis the correlation coefficients ( $R^2$ ) were obtained for the time interval 5-140 minutes. The  $R^2$  values are presented in the Table 4.3).

Substance	Log $P$	Log $D$ , pH=7	Log $D$ , pH=8
verapamil	3.899±0.51	1.96	2.89
diltiazem	3.634±0.94	1.72	1.72
nifedipine	2.966±0.58	2.97	2.97
phenobarbital	1.668±0.26	1.62	1.62
memantine	3.177±0.27	0.16	0.56
amantadine	2.218±0.24	-0.79	-0.38
diazepam	2.964±0.58	2.96	2.96
carboxyfluorescein	-	-	-

Table 4.2 An overview of  $\log P$  and  $\log D$  values of used ion channel blockers. The values were adopted from <http://scifinder.cas.org>, accessed on 18<sup>th</sup> of February 2010.

Linear correlation	Correlation coefficient (R <sup>2</sup> )		
	All substances	Without memantine and amantadine	Without memantine, amantadine and phenobarbital
PE <sub>cell</sub> /Diaz vs. log <i>P</i>	0.007	0.066	0.852
logPE <sub>cell</sub> /Diaz vs. Log <i>P</i>	0.023	0.136	0.931
PE <sub>cell</sub> /Diaz vs. Log <i>D</i> (pH=7)	0.388	0.779	0.871
logPE <sub>cell</sub> /Diaz vs. Log <i>D</i> (pH=7)	0.357	0.753	0.919
PE <sub>cell</sub> /Diaz vs. Log <i>D</i> (pH=8)	0.178	0.104	0.496
logPE <sub>cell</sub> /Diaz vs. Log <i>D</i> (pH=8)	0.138	0.056	0.503

Table 4.3 lists the R<sup>2</sup> values after linear regression analysis of ratio PE<sub>cell</sub>/Diaz and logPE<sub>cell</sub>/Diaz to log *P*, log *D* (pH=7) and log *D* (pH=8) values. The PE<sub>cell</sub> values were obtained from the single studies in time interval 5-140 and were normalized to the according values of diazepam.

For example, the following graph (Figure 4.1) shows linear correlation between log *P* and log PE<sub>cell</sub>/Diaz values for all substances used in single studies (time interval 5-140 minutes).

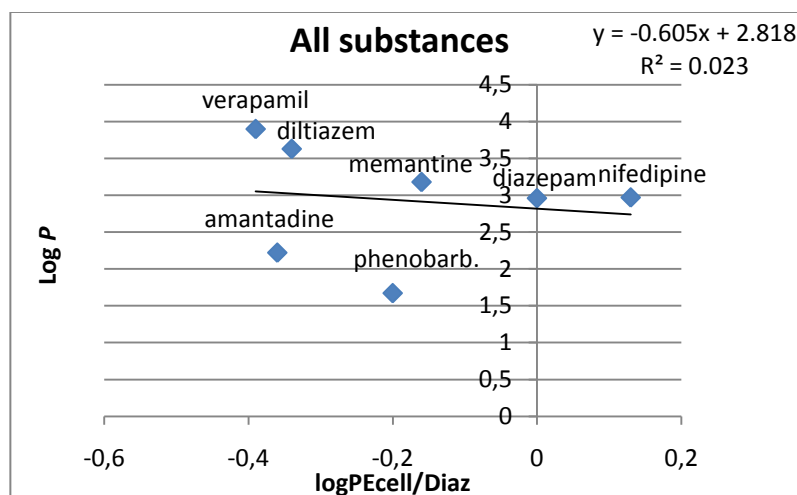


Figure 4.1 shows linear regression analysis of logPE<sub>cell</sub>/Diaz to log *P*, where all substances used in single transport studies are included.

In the next graph (Figure 4.2) the memantine and amantadine values were excluded, because of problems with HPLC analysis (as it was mentioned before), when too small peaks were found and their integration was complicated.

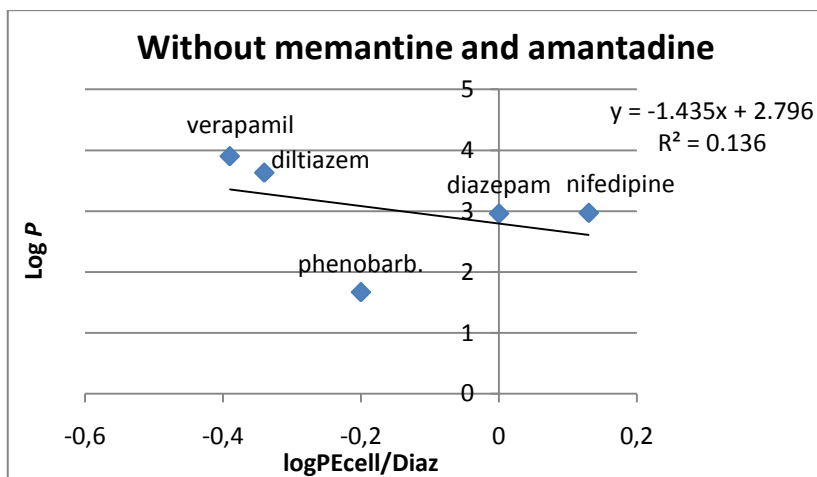


Figure 4.2 shows linear regression analysis of  $\log PE_{\text{cell}}/\text{Diaz}$  to  $\log P$ , where memantine and amantadine were excluded from the determination of correlation coefficient ( $R^2$ ).

The last graph (Figure 4.3) demonstrates linear correlation, where memantine, amantadine and phenobarbital were not used for determination of correlation coefficient. After excluding phenobarbital the high correlation coefficient ( $R^2 \geq 0,9$ ) was found, which demonstrates that verapamil, diltiazem, nifedipine and diazepam permeate through the BBB according to their lipohlicity in contrast to phenobarbital, which must be actively transported. This fact is support by the results from group studies, where it was found that the permeation of phenobarbital was significantly increased after co-administration with verapamil and diltiazem. Consequently, we have confirmed the concept that phenobarbital can be substrate of P-gP, which functionality is influenced by verapamil and diltiazem.

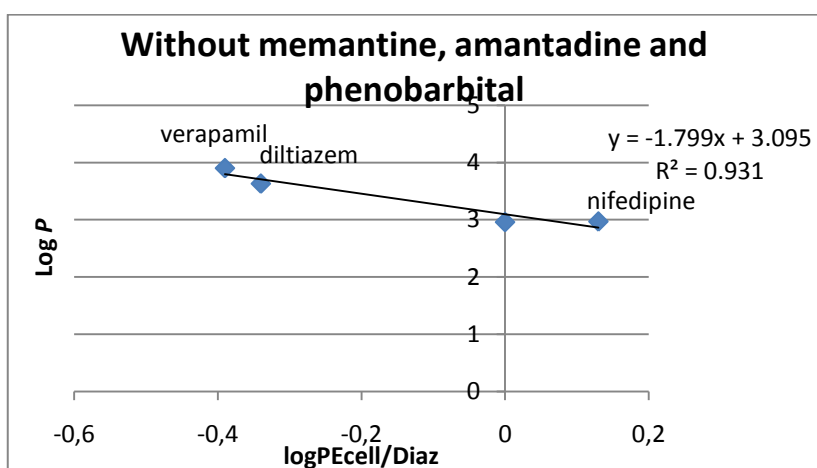


Figure 4.3 shows linear regression analysis of  $\log PE_{\text{cell}}/\text{Diaz}$  to  $\log P$ , where memantine, amantadine and fenobarbital were excluded from the determination of correlation coefficient ( $R^2$ ).

Two group transport studies were made: Transport study of diltiazem/phenobarbital and Transport study of verapamil/phenobarbital. In both these studies we have found that permeation of phenobarbital through the BBB is significantly increased by used calcium channel blockers (verapamil and diltiazem). This is evidenced in Figure 4.1 and 4.2. The permeation of phenobarbital increased about the factor 1.62 after co-administration of diltiazem in time interval 5-140 minutes and about the factor 5.58 in time interval 0-5 minutes. After co-administration of verapamil the permeation of phenobarbital increased about the factor 1.97 in time interval 5-140 minutes and about the factor 4.90 in time interval 0-5 minutes.

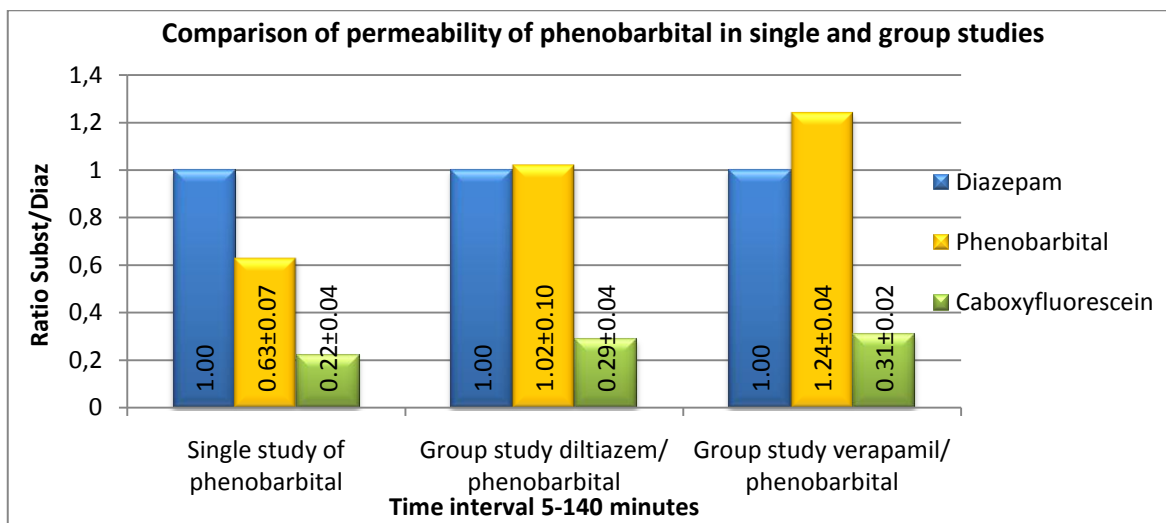


Figure 4.1 This graph for time interval 5-140 minutes shows how is permeability of phenobarbital influenced by verapamil or diltiazem in groups studies in comparison to single study.

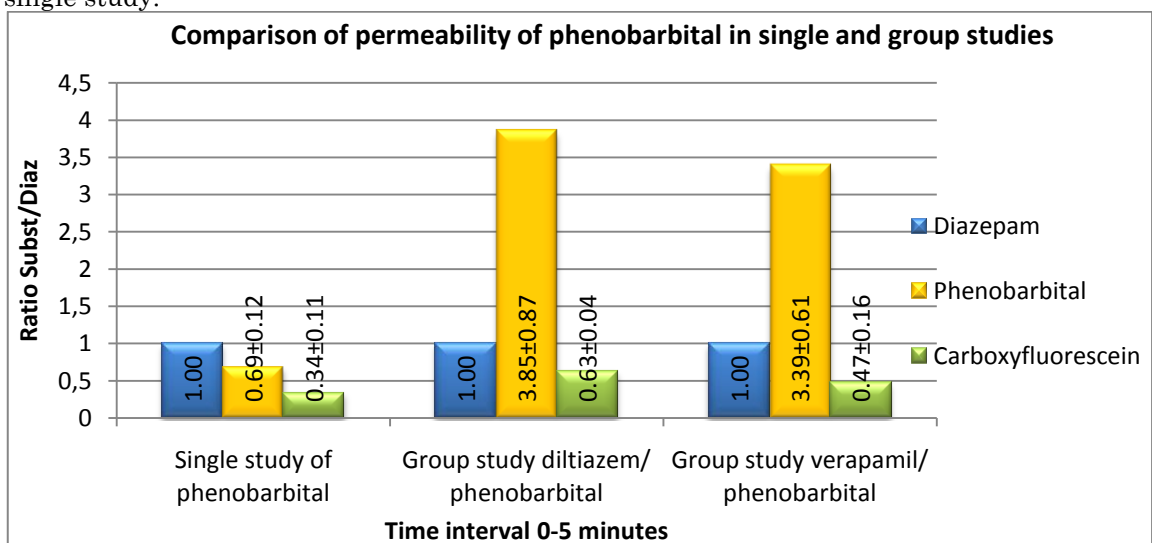


Figure 4.2 This graph for time interval 0-5 minutes shows how is permeability of phenobarbital influenced by verapamil or diltiazem in groups studies in comparison to single study.

Several different explanation could exist for the fact that permeability of increased after co-administration with verapamil and diltiazem. One of them is that P-glycoprotein (P-gP) functionality could be influenced by verapamil and diltiazem. It has been shown for several times that phenobarbital is a substrate of P-gP and verapamil can inhibit P-gP functionality which would explain the found results. However, low P-gP expression was reported for cell line ECV304. Thus, further studies have to be carried out in order elucidate the role of P-gP in ECV304 in the experimental setting used. Since it is also known that verapamil can also induce P-gP functionality, this should be verified before the direct link between the increase of phenobarbital permeability and P-gP functionality in this model is drawn. Interestingly, few papers refer to diltiazem and its P-gP modulatory properties. Consequently, it could be possible that we have shown as one of few that diltiazem is a P-gP modulator or that other transporter systems are involved in our ECV304 model with the transport of Phenobarbital. Not only P-gP, but OATP Transporters (Organic Anion Transporter Peptides) may be also influenced by verapamil and diltiazem. In this context, Elkiweri et al. (2009) have reported that verapamil interfered with OATP and OCT transporters (Zolk et al., 2009). As third possibility it has to be mentioned that it was also reported that verapamil was able to decrease TEER of some BBB *in vitro* models by modulating probable the homeostasis of intracellular calcium which may lead to relocation and consequently loss of tight junction proteins. This loss of BBB integrity may then increase the amount of paracellularly permeated phenobarbital. All our speculation can be topics for next experiments and e.g. other calcium channel blockers can be tested or experimental conditions can be changed. However, regardless the responsible and not resolved mechanism it was able to show that the permeability of the CNS drug phenobarbital was significantly increased by co-administration of peripherally acting Ca<sup>2+</sup>-channel blockers verapamil and diltiazem.

## 5 SOUHRN

Hematoencefalická bariéra (HEB) odděluje centrální nervový systém od krevního řečiště, umožňuje selektivní transport živin a odstranění potenciálně škodlivých látek a díky své enzymatické aktivitě inaktivuje spoustu neuroaktivních a toxických sloučenin. HEB je tvořena kapilárními endoteliálními buňkami, jejichž propustnost je regulována komplexem těsných spojů (tight junctions) (Engelhardt and Sorokin, 2009).

Pro účel této diplomové práce bylo vybráno šest různých blokátorů iontových kanálů běžně používaných v klinické praxi (verapamil, diltiazem, nifedipin, fenobarbital, memantin a amantadin). Je dobře známo, že během terapie těmito látkami se mohou vyskytnout nežádoucí účinky v centrálním nervovém systému. Proto byly provedeny jak jednotlivé, tak i skupinové transportní studie, aby bylo možno porovnat u zvolených blokátorů iontových kanálů jejich schopnost transportu přes hematoencefalickou bariéru (HEB), popřípadě zhodnotit interakce mezi nimi.

Získaná data o každé látce použité v jednotlivých a skupinových studiích byla stanovena za použití Transwell *in vitro* modelu hematoencefalické bariéry tvořeného humánní buněčnou linií ECV304, každý vzorek z transportní studie byl 3x analyzován pomocí RP-HPLC a průměrné hodnoty ploch „píků“ byly použity pro výpočet cleared volume (CV). Závislost CV na čase byla vynesena do grafu a hodnoty permeabilitní křivky byly získány lineární regresí za pomoci programu Microsoft Excell a použity k výpočtu koeficientu permeability (PE). Pro minimalizaci variabilit byly koeficienty permeability normalizovány k vnitřním standardům diazepam a karboxyfluoresceinu.

Látky použité v jednotlivých transportních studiích byly seřazeny podle koeficientu permeability normalizovaného na diazepam ( $PE_{\text{cell/Diaz}}$ ) a porovnány vzhledem k místu jejich terapeutického účinku. Bylo prokázáno, že nifedipin, jakožto látka účinkující na periférii, prostupoval přes HEB rychleji než vnitřní standard diazepam (působící v CNS) a mnohem rychleji než ostatní blokátory iontových kanálů, jež účinkují též na periférii. V klinické praxi to může znamenat, že nifedipin použitý při léčbě konkrétního klinického problému může mít v porovnání s verapamilem nebo diltiazemem víc centrálních nežádoucích účinků. Abychom zjistili, zda prostupnost jednotlivých blokátorů kalciových kanálů přes HEB koreluje s jejich lipofilitou, byla do grafu vynesena závislost

mezi  $\log PE_{\text{cell/Diaz}}$  a  $\log P$ , čímž jsme prokázali, že verapamil, diltiazem, nifedipin a diazepam pronikají do mozku podle lipofility, tedy rozdílně než fenobarbital, který je pravděpodobně aktivně transportován. Tento fakt je podporován výsledky ze skupinových studií, kde bylo nalezeno, že permeabilita fenobarbitalu, jakožto látky účinkující v CNS, podstatně vzrostla při transportu společně s periferně účinkujícím verapamilem a diltiazemem. Následně je zde potvrzeno, že fenobarbital je substrátem P-glykoproteinu a jeho funkce je ovlivněna verapamilem a diltiazemem.

## 6 REFERENCES

- Abbott, N.J., Rönnebeck, L. et al. (2006) Astrocyte-endothelial interactions at the blood-brain barrier. *Nat Rev Neurosci.* 7:41-53
- Abbott, N.J. et al. (2010) Structure and function of the blood-brain barrier. *Neurobiol. Dis.* 37:13-25
- Ballabh, P., Braun, A., Nedergaard, M. (2003) The blood-brain barrier: an overview. Structure, Regulation, and clinical implications. *Neurol. Dis.* 16:1-13
- Begley, D.J. (2004) Delivery of therapeutic agents to the central nervous system: the problems and the possibilities. *Pharmacol. Ther.* 104:29-45
- Bezprozvanny, I., Mattson, M.P. (2008) Neuronal calcium mishandling and the pathogenesis of Alzheimer's disease. *Trends Neurosci.* 31:454-63
- Bootman, M.D., Lipp, P., Berridge, M.J. (2001a) The organisation and functions of local Ca(2+) signals. *J. Cell. Sci.* 114:2213-22
- Bootman, M.D. et al. (2001b) Calcium signalling-an overview. *Semin. Cell Dev. Biol.* 12:3-10
- Bradbury, M.W. (2006) The blood-brain barrier. *Exp. Physiol.* 78:453-72
- Carvey, P.M., Hendey, B., Monahan, A.J. (2009) The blood-brain barrier in neurodegenerative disease: a rhetorical perspective." *J. Neurochem.* 111:291-314
- Chen, G.L, Lee, F.Y. (1996) Validation of bioanalytical method fo verapamil by Highperformance Liquid Chromatography. *J. Med. Sci.* 17:16-23
- Chen, H.S.V. and Lipton, S.A. (2006) The chemical biology of clinically tolerated NMDA receptor antagonists. *J. Neurochem.* 96: 1611-1626
- Correale, J., Villa, A. (2009) Cellular Elements of the Blood-Brain Barrier. *Neurochem. Res.*
- Cucullo, L., Aumayr, B., Rapp, E., Janigro, D. (2005) Drug delivery and *in vitro* models of the blood-brain barrier. *Curr. Opin. Drug. Discov Devel.* 8:89-99
- De Boer, A.G., Gaillard, P.J. (2007) Drug targeting to the brain. *Annu. Rev. Pharmacol. Toxicol.* 47:323-55
- Deli, M.A., Abrahám, C.S., Kataoka, Y., Niwa, M. (2005) Permeability studies on *in vitro* blood-brain-barrier models: physiology, pathology, and pharmacology. *Cell. Mol. Neurobiol.* 25:59-127
- Elkiweri, I.A., Tissot van Patot, M.C., Zhang Y.L., Christians, U., Henthorn, T.K. (2009) The Effect of Loperamide and Fentanyl on the Distribution Kinetics of Verapamil in the Lung and Brain in Sprague Dawley Rats. *World Academy of Science, Engineering and Technology* 55

- Engelhardt, B, Sorokin, L. (2005) The blood-brain and the blood-cerebrospinal fluid barriers: function and dysfunction. *Semin. Immunopathol.* 31:497-511
- Fanning, A.S., Jameson, B.J., Jesaitis, L.A., Anderson, J.M. (1998) The tight junction protein ZO-1 establishes a link between the transmembrane protein occludin and the actin cytoskeleton. *J. Biol. Chem.* 273:29745-53
- Franeta, J.T, Agbaba, D., Eric, S., Pavkov, S., Aleksic, M., Vladimirov, S. (2002) HPLC assay of acetylsalicylic acid, paracetamol, caffeine and phenobarbital in tablets. *Farmaco.* 57:709-13
- Grossman, E., Messerli, F.H. (2004) Calcium Antagonists. *Prog. Cardiovasc. Dis.* 47:34-57
- Hawkins, B.T., Davis, T.P. (2005) The blood-Brain Barrier/Neurovascular Unit in Health and Disease. *Pharmacol. Rev.* 57:173-85
- Higashi, Y., Fujii, Y. (2005) Simultaneous determination of the binding of amantadine and its analogues to synthetic melanin by liquid chromatography after precolumn derivatization with dansyl chloride. *J Chromatogr Sci.* 43:213-7
- Huber, J.D., Egleton, R.D., Davis, T.P. (2001a) Molecular physiology and pathophysiology of tight junctions in the blood-brain barrier. *Trends Neurosci.* 24:719-25
- Huber, J.D., Witt, K.A., Hom, S., Egleton, R.D., Mark, K.S., Davis, T.P. (2001b). Inflammatory pain alters blood-brain barrier permeability and tight junctional protein expression. *Am. J. Physiol. Heart Circ. Physiol.* 280:H1241-8
- Johnson, W.J. and Kotermanski, S.E. (2006) Mechanism of action of memantine. *Curr. Opin. Pharmacol.* 6:61-67
- Kwan, P. and Brodie, M.J. (2004) Phenobarbital for the Treatment of Epilepsy in the 21st Century: A Critical Review. *Epilepsia.* 45(9): 1141-1149
- Li, K., Zhang, X., Zhao, F. (2003) HPLC determination of diltiazem in human plasma and its application to pharmacokinetics in humans. *Biomed. Chromatogr.* 17:522-525
- Liao, P., Zhang, H.Y., Soong, T.W. (2009) Alternative splicing of voltage-gated calcium channels: from molecular biology to disease. *Pflugers. Arch.* 458:481-7
- Lim, E. (2005) A walk through the management of Parkinson's Disease. *Ann. Acad. Med.Singapore.* 34:188-95
- Lincová, D., Farghali, H. et al. (2007) *Základní a aplikovaná farmakologie.* Praha, Galén. ISBN:978-80-7262-373-0
- Lo, E.H., Singhal, A.B., Torchilin, V.P., Abbott, N.J. (2001) Drug delivery to damaged brain. *Brain. Res. Rev.* 38(1-2):140-8

- Lüllmann, H., Ziegler, A., Mohr, K., Bieger, D. (2000) Color Atlas of Pharmacology. New York, Thieme Stuttgart. ISBN: 3-13-781702-1
- Marambaud, P., Dreses-Werringloer, U., Vingtdeux, V. (2009) Calcium signalling in neurodegeneration. *Mol. Neurodegener.* 4:20
- Moody, D.M. (2006) The blood-brain barrier and blood-cerebral spinal fluid barrier. *Semin. Cardiothorac. Vasc. Anesth.* 10:1 28-31
- Neuhaus, W., Lauer, R., Oelzant, S., Fringeli, U.P., Ecker, G.F., Noe, C.R. (2006) A novel based jollow-fiber blood-brain barrier in vitro model with immortalised cell line PBMEC/C1-2. *J. Biotechnol.* 125:127-41
- Novakova, I. (2009) Transport of NSAIDs across the blood-brain barrier *in vitro*. Diploma thesis. Department of Pharmacology and Toxicology, Charles University in Prague, Faculty of Pharmacy in Hradec Králové.
- Ribatti, D., Nico, B., Crivellato, E., Artico, M. (2006) Development of the blood-brain barrier: a historical point of view. *Anat. Rec. B. New. Anat.* 289:3-8
- Shuangjin, C., Fang, F., Han, L., Ming, M. (2007) New method for high-performance liquid chromatographic determination of amantadine and its analogues in rat plasma. *J. Pharm. Biomed. Anal.* 44:1100-5
- Stamatovic, S.M., Keep, R.F., Andjelkovic, A.V. (2008) Brain endothelial cell-cell junctions: how to “open” the blood brain barrier. *Curr. Neuropharmacol.* 6:179-92
- Takahashi, K., Sawasaki, Y., Hata, J., Mukai, K., Goto, T. (1990) Spontaneous transformation and immortalization of human endothelial cells. *In Vitro Cell Dev. Biol.* 26:265-74
- Van Itallie, C.M., Fanning, A.S., Bridges, A., Anderson, J.M. (2009) ZO-1 stabilizes the tight junction solute barrier through coupling to the perijunctional cytoskeleton. *Mol. Biol. Cell.* 20:3930-40
- Vaněček, V. (2007) The effects of Glycopyrronium Bromide and Tiotropium Bromide on tight junctional proteins of blood-brain barrier mimicking cells and their transport across a blood-brain barrier *in vitro* model. Diploma thesis. Department of Pharmacology and Toxicology, Charles University in Prague, Faculty of Pharmacy in Hradec Králové.
- Verkman, A.S. (2002) Aquaporin water channels and endothelial cell function. *J. Anat.* 200:617-27
- Vorbrodt, A.W., Dobrogowska, D.H. (2003) Molecular anatomy of intercellular junctions in brain endothelial and epithelial barriers: electron microscopist's view. *Brain. Res. Rev.* 42:221-42
- Wolburg, H., Lippoldt, A. (2002) Tight junctions of the blood-brain barrier: development, composition and regulation. *Vascul. Pharmacol.* 38:323-37

Yu, J.T., Chang, R.C., Tan, L. (2009) Calcium dysregulation in Alzheimer's disease: From mechanisms to therapeutic opportunities. *Prog. Neurobiol.* 89:240-255

Zendelovska, D. et al. (2006) Development of an HPLC method for the determination of nifedipine in human plasma by solid-phase extraction. *J. Chromatogr. B. Analyt. Technol. Biomed. Life. Sci.* 839:85-8

Zolk O., Solbach, T.F., König, J., Fromm, M.F. (2009) Functional characterization of human organic cation transporter 2 variant p.270Ala>Ser.“ *Drug Metab. Dispos.* 37:1312-8